INTERNATIONAL JOURNAL OF CHEMICAL REACTOR ENGINEERING

Volume 7 2009 *Review* R1

Literature Review on Heat Transfer in Two- and Three-Phase Bubble Columns

Craig Hulet[*] Patrice Clement[†] Patrice Tochon[‡]
Daniel Schweich[**] Nicolas Dromard[††] Jerome Anfray[‡‡]

[*]CEA, cahulet@hotmail.com
[†]CEA, Patrice.Clement@cea.fr
[‡]CEA, Patrice.Tochon@CEA.fr
[**]LGPC, dsw@lgpc.cpe.fr
[††]TOTAL, nicolas.dromard@total.com
[‡‡]TOTAL, jerome.anfray@total.com
ISSN 1542-6580

Literature Review on Heat Transfer in Two- and Three-Phase Bubble Columns

Craig Hulet, Patrice Clement, Patrice Tochon, Daniel Schweich, Nicolas Dromard, and Jerome Anfray

Abstract

Fischer-Tropsch synthesis (FTS), an exothermic reaction where hydrogen and carbon monoxide synthesis gas are converted to hydrocarbon products, has been under development since the 1930's. The interest in FTS depends on current and perceived future prices of crude oil but is increasingly viewed as an option for exploiting stranded natural gas. Other advantages of FTS hydrocarbons include the absence of sulphur, nitrogen, heavy metal contaminants, low aromatic content and the ability to produce high value middle distillates/fuels. Current interest is directed towards slurry bubble processes – comprising gas, liquid, and solid phases. Industrial slurry phase FTS reactors may range in size from 6 – 10 m in diameter and upwards of 30 m in height and include multiple internal heat transfer tubes. Such systems offer numerous advantages including high heat transfer rates, good mixing, and ease of online catalyst addition and withdrawal. However, one disadvantage is the complex hydrodynamics associated with slurry bubble columns, which make scale-up difficult. A literature review on heat transfer studies and correlations has been completed focusing on previous experimental setups, the synthesis of the key findings/parameters, and the identification of the necessary criteria required for reactor design and scale-up.

The parameters having the most pronounced impact on heat transfer in slurry bubble columns and three-phase fluidized beds are the superficial gas velocity and liquid properties such as viscosity and surface tension, which significantly alter the bubble properties and the column hydrodynamics. The effect of particles is poorly understood and is a complex function of particle diameter and concentration. The experimental results and correlations reported here from the majority of studies are dependent upon the equipment and properties of the three phases studied – resulting in very limited applicability to other systems or for scale-up. Other concerns include the use of relatively low gas velocities, ambient temperature and pressure, relatively large particles, and relatively small columns employed in most

studies, which are not relevant to industrial operating conditions. Furthermore, studies involving multiple internals were relatively few. Most columns were only equipped with a single tube or small heat flux probe thereby measuring only the local heat transfer and not taking into account the effect on column hydrodynamics of multiple internals. Of these studies only a few tubes were equipped with heaters (that did not run the entire tube length) and heat flux probes while the remaining probes were inactive.

KEYWORDS: Fischer-Tropsch synthesis, gas-liquid-solid fluidization, heat transfer, hydrodynamics, slurry bubble column

1 Introduction

Three-phase reactor systems, including slurry bubble columns and gas-liquid-solid fluidized beds, are commonly used in the chemical and petrochemical industries where large liquid phase hold-up is suitable for slow chemical reactions. Such applications included: absorption, hydrogenation, oxidation, desulphurization, coal liquefaction, polymerization, and Fischer-Tropsch synthesis (Saxena and Chen, 1994). Proper design of the heat removal surfaces is crucial in order to maintain catalyst activity, reaction integrity, and product quality given that a large number of such processes are highly exothermic. For example, the Fischer-Tropsch process has a heat of reaction of the order of -172 kJ/mol of converted CO (Maretto and Krishna, 1999). Operating temperatures and pressures reported in the literature depend on the selected catalyst and reactor configuration ranging anywhere from 200 – 350°C and pressures of 10 – 50 bars (Krishna, 2000; Schluter et al., 1995; Stynberg and Dry, 2004). Heat transfer may be in fact be the most important aspect in defining reactor performance in gas-liquid-solid fluidized bed systems (Kim and Laurent, 1991). Therefore, it is important to understand and quantify heat transfer for optimum operation and to minimize capital costs. Unfortunately, up-to-date knowledge of pressurized and high temperature three-phase systems (i.e. fluidized beds) is slight. Table 1 presents some typical heat transfer coefficients of various reactor systems.

Table 1. Maximum heat transfer coefficients in various systems (after Nigam and Schumpe, 1996).

System	Phases	Maximum h (W/m^2K)	Author (as cited in Nigam and Schumpe, 1996)
bubble column	air-water	5500	Kölbel et al. (1958)
slurry bubble column	air-water-sand	7500	Kölbel et al. (1960)
liquid-solid fluidized bed	water-glass beads	6500	Muroyama et al., (1984)
three phase fluidized bed	air water-glass beads	8000	Muroyama et al., (1984)
gas-liquid packed bed	air-water-glass beads	4300	Weekman and Meyer (1965)
gas-solid fluidized bed	gas-glass beads	870	Bashakov (1968)

The primary objective of this review is to summarize and analyze the relevance of current experimental and theoretical knowledge concerning heat transfer in bubble columns to Fischer-Tropsch synthesis. Existing works have been extensively referenced including several major reviews published by Kim and Laurent (1991), Schluter et al. (1995), Pandit and Joshi (1986), Kim and Kang (1997), Kantarci et al. (2005a), Saxena and Chen (Saxena and Chen, 1994), and Saxena (1995). In particular, the experimental data in the literature has been

examined in order to assess the effect of particle properties and liquid properties, operating pressure and temperature, and the presence of internal heat transfer surfaces on heat transfer. The empirical models and correlations currently available for estimating the heat transfer coefficients are examined and compared to the experimental results and their applicability to high temperature and high pressure are appraised. A discussion of the hydrodynamics (gas phase holdup, bubble dynamics, flow pattern) and phase interaction (slurry viscosity, particle concentration) are discussed in terms of their effects on the heat transfer. Finally, recommendations for future research are presented.

1.1 Slurry Bubble Columns and Three-Phase Fluidized Beds

The solid particles employed in slurry bubble columns and three-phase (gas-liquid-solid) fluidized beds may range in size from a few microns up to a few millimeters. When the particles are relatively small (typically less than 60 μm) the liquid-solid mixture is referred to as a slurry. These relatively small particles tend to follow the liquid flow patterns quite closely. However, at relatively higher solids loading (> 20 – 30 wt. %) and larger particle diameters this may no longer be the case and these systems are generally referred to as three-phase fluidized beds.

A typical slurry bubble column operating in continuous mode with the liquid phase flowing co-currently relative to the gas phase is illustrated in Figure 1. In continuous operation the liquid flow is sustained and the liquid is actively circulated through the column as opposed to batch mode where the gas flow is sustained and continuous, but the liquid is not actively circulated. Generally, the gas phase is introduced at the bottom of the cylindrical vertical column by a multiple orifice sparger. The bubbles that form constitute the discontinuous phase while the surrounding liquid is the continuous phase. The liquid flow may also be counter-current to the gas flow. The solid particles are suspended and dispersed by the liquid movement induced by the bubble motion. Scale-up of such systems is considered difficult due to the resulting complex flow patterns. The presence of internal heat transfer surfaces such as heat exchanger tubes will further modify the flow patterns. Columns with internals are sometimes referred to baffled columns in the literature (Saxena and Chen, 1994).

There are three main flow regimes in upflow co-current gas-liquid and gas-liquid-solid columns: bubble or homogeneous flow, churn-turbulent or heterogeneous flow, or slug flow, which are illustrated in Figure 2. The latter is exist for superficial gas velocities of less than 0.05 m/s. There is no bubble coalescence or break-up and the gas hold-up increases linearly with increasing U_g. generally only observed for relatively small diameter columns. The homogeneous bubbling regime is characterized by uniformly sized and distributed bubbles

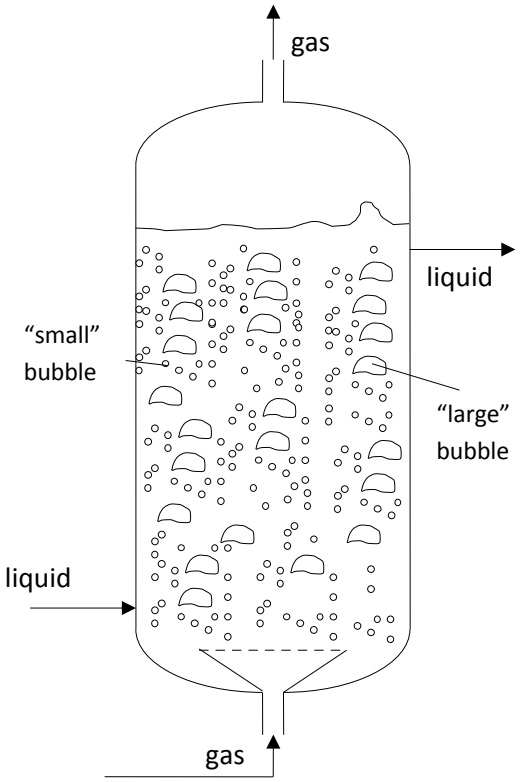

Figure 1. Typical three-phase (gas-liquid-solid) bubble column.

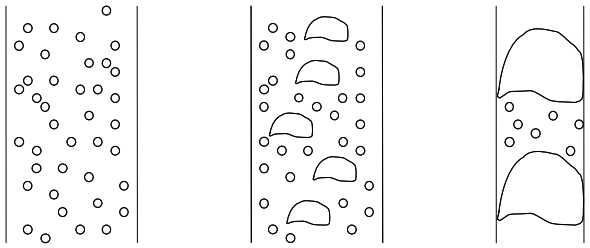

Figure 2. Illustration of the three primary flow regimes encountered in gas-liquid-solid bubble columns.

(depending upon the sparger design and the column operating conditions) which By comparison, the churn-turbulent flow regime exhibits a wide bubble size distribution with continuous bubble coalescence and break-up. Some processes operate in the bubbly flow regime; however, current industrial interest is in the churn-turbulent flow regime ($10 < U_g < 30 – 50$ cm/s) because it allows for higher gas throughputs and a more homogeneous catalyst suspension (Dudukovic et al., 2002).

A major advantage of slurry bubble columns is the excellent level of mixing compared to agitated reactors and the absence of any internal moving parts. This results in relatively high heat and mass transfer rates and nearly isothermal conditions. Continuous operation in terms of online catalyst addition and withdrawal is another advantage. Generally, capital and operating costs associated with bubble columns are smaller given the high catalyst durability, relative compact size of the reactors, and plug-free operation (Dudukovic et al., 2002; Kantarci et al., 2005a; Li and Prakash, 2001). High overall reaction rates are favoured by the use of relatively small particles (< 100 μm) since the intraparticle resistance and liquid-solid mass transfer resistance is minimized. However, the use of small particles may lead to problems with liquid-solid separation (Li et al., 2003). Another potential disadvantage includes the significant back-mixing (i.e. axial dispersion) that could result in a relatively low conversion per pass for a given reactor volume (Dudukovic et al., 2002). All equations reported utilize SI units (unless noted otherwise).

1.2 Definition of Select Key Variables

The gas superficial (U_g) velocity is a key variable in nearly all literature studies concerning heat transfer in three-phase systems discussed below. It is defined at column conditions by Equation (1):

$$U_g = \frac{Q_g}{\frac{\pi}{4} D_c^2} \tag{1}$$

where Q_g is the volumetric flow rate of gas to the column and the denominator represents the empty cross-sectional area of the column. The liquid superficial velocity (U_l) is defined in a similar manner.

Another key parameter in defining two- and three-phase bubble column operations are the phase hold-ups, which by definition, must sum to one. The local gas phase hold-up may be obtained using Equation (2):

$$\varepsilon_g = 1 \quad \frac{\Delta P}{\left(\rho_l \varepsilon_l + \rho_s \varepsilon_s\right) g \Delta z} \tag{2}$$

where ΔP is the pressure drop measured between two given pressure taps and Δz is the distance between the same two pressure taps. The mean ε_g value is given by Equation (3):

$$\varepsilon_g = 1 - H_0/H_e \tag{3}$$

where H_e is the expanded bed height for a given U_g and U_l, and H_0 is the initial static bed height with no gas or liquid flow. The solids hold-up may be estimated using Equation (4) provided the solids do not leave the column:

$$\varepsilon_s = \frac{m_s}{H_e A_c \rho_s} \tag{4}$$

where m_s is the mass (kg) of solids in the column. The solids hold-up may also be obtained using the so-called Wenge method (Wenge et al., 1995 as cited in Dhaouadi et al., 2006).

$$\varepsilon_s = \frac{\rho_l}{\rho_l - \rho_s}\left(1 - P/P_0\right) - \Delta \quad \Delta \tag{5}$$

where ΔP and ΔP_0 are the steady state pressures drops without and with fluidization and the corresponding gas hold-up is given by

$$\varepsilon_g = 1 - R/R_0 - \varepsilon_s\left(\rho_s - \rho_l\right)/\rho_l \tag{6}$$

Finally, the bed porosity is defined as:

$$\varepsilon = \varepsilon_g + \varepsilon_l = 1 - \varepsilon_s \tag{7}$$

The addition of solid particles alters the viscosity and density of the slurry. Two commonly used correlations for predicting the slurry viscosity are by Thomas [Equation (8)] and Barnea and Mizrahi [Equation (9)] (as cited in Li and Prakash, 1997):

$$\mu_{sl} = \mu_l\left[1 + 2.5\varepsilon_s + 10\varepsilon_s^2 + 0.00273\exp\left(16.6\varepsilon_s\right)\right] \tag{8}$$

$$\mu_{sl} = \mu_l \exp\left[\frac{5\varepsilon_s}{3\left(1-\varepsilon_s\right)}\right] \tag{9}$$

The slurry density is typically estimated using Equation (10):

$$\rho_{sl} = \varepsilon_s\rho_s + \varepsilon_l\rho_l \tag{10}$$

The heat capacity is defined in a similar manner using the mass fraction of solids

$$C_{p,sl} = \Theta_s C_{ps} + \left(1 - \Theta_s\right) C_{pl} \tag{11}$$

Finally, the thermal conductivity of the slurry may be estimated by using a correlation such as Equation (12) from Tareef (1940) (as cited in Li et al., 2003):

$$k_{sl} = k_l \frac{2k_l + k_s - 2\varepsilon_s\left(k_l - k_s\right)}{2k_l + k_s - \varepsilon_s\left(k_l - k_s\right)} \tag{12}$$

Lastly, the particle diameter appears in many heat transfer and gas hold-up equations. Typically, the particle diameter is taken as the Sauter mean diameter but in the case of a cylindrical particle the equivalent particle diameter is used:

$$d_{pe} = \left(1.5 d_p^2 L_p\right)^{1/3} \tag{13}$$

Some correlations presented may also include the particle shape factor Φ, which indicates the sphericity of a particle and is obtained from Equation (14):

$$\Phi = \frac{d_{eq}^2}{d_p\left(L_p + 0.5 d_p\right)} \tag{14}$$

2 Detailed Literature Analysis

2.1 Experimental Investigations in Columns without Internals

2.1.1 Hikita and coworkers

Hikita et al. (1981) studied heat transfer from the wall of two columns of 0.10 and 0.19 m i.d. and using a single nozzle sparger in a gas-liquid column. Various water/sucrose or water/alcohol solutions were utilized for the liquid phase while air served for the gas phase. Twelve thermocouples were embedded in the wall to measure the surface temperature. The authors report that the liquid velocity, nozzle diameter, column diameter, or axial location of the heater had a negligible effect on the heat transfer coefficient. Based on their analysis of the reported findings and the literature they state that even the type of heater (i.e. wall or tube) may be negligible. The heat transfer coefficient was found to increase with

increasing gas velocity while it decreased with increasing sucrose concentration (this was attributed to the corresponding increasing in liquid viscosity). The measured heat transfer coefficient decreased in the following order: air-water, air-methanol, and air-1-butanol (attributed to the combined effect of surface tension, viscosity, and thermal conductivity). Equation (15) gives the correlation developed by Hikita et al. (1981) for calculating h_w. While the authors report an average deviation of 3.9 % (maximum deviation 13.9%) Saxena (1995) reported that the computed values obtained are consistently much greater than those measured experimentally; the reason for this was attributed to the relatively small size of the heater (2 cm high).

$$\frac{h_w}{\rho_l C_{pl} U_g}\left(\frac{C_{pl}\mu_l}{k_l}\right)^{2/3} = 0.411\left(\frac{U_g \mu_l}{\sigma_l}\right)^{-0.851}\left(\frac{\mu_l^4 g}{\rho_l \sigma_l^3}\right)^{0.308} \tag{15}$$

2.1.2 Kato and coworkers

Kato et al. (1981; 1982) measured wall heat transfer coefficients in 0.052 and 0.12 m i.d and 1.5 m high. Various concentrations of carboxy-methyl cellulose (CMC) were used to study the effect of liquid viscosity (0.001 to 0.052 Pa·s) on the heat transfer coefficient for liquid velocities of 0.003 to 0.15 m/s. Air was used for the gas phase ($0.03 < U_g < 0.15$ m/s) while the solid phase consisted of glass beads (d_p = 0.42 – 2.2 mm) and porous alumina spheres (d_p = 3.3 mm). The solid concentrations are not specified. The location of the electric heating surface (0.03 and 0.10 m high for the 0.052 and 0.12 m columns, respectively) was varied between 0.1 and 0.25 m above the grid surface. Nine thermocouples were installed to measure the wall surface temperature and 6 were placed within the bed. A temperature difference between the bed and wall of ~3 K was maintained during all experiments. Liquid hold-up was measured using electrical conductivity probes.

In general, h_w was found to increase with U_g (the effect of U_g is decreased for large U_t) and decrease with increasing μ_l (the effect of U_l on h_w was minimal in the gas-liquid system). The heat transfer coefficient was higher in the larger column due to the increased internal circulating liquid velocity, which increases with increasing D_c (h_w became independent of D_c when $D_c > 0.12$ m as the flow becomes fully developed). In the gas-liquid-solid system as U_l was increased h_w initially increased, reached a local maximum, and then decreased to a local minimum, then again rapidly increased before finally reaching asymptotic value. This value of U_l, initially increased with d_p for smaller particles but is not affected by relatively large particles). Furthermore, the minimum was only seen in the smaller column and at lowest μ_l. Similarly, in a liquid-solid system while

increasing U_l the heat transfer coefficient exhibits a local maximum followed by a local minimum before reaching the value found for single phase (liquid) system. The effect of U_l and d_p are not pronounced at fully fluidized conditions. Kato et al. (1981) proposed the following correlation for their experimental findings:

$$\mathrm{Nu}' = 0.044\left(\mathrm{Re}'\,\mathrm{Pr}\right)^{0.78} + 2.0\mathrm{Fr}_g^{0.17} \tag{16}$$

where $\mathrm{Nu}' = \dfrac{h_w d_p \varepsilon_l}{k_l\left(1-\varepsilon_l\right)}$, $\mathrm{Re}' = \dfrac{\rho_l d_p U_l}{\mu_l\left(1-\varepsilon_l\right)}$, $\mathrm{Pr} = \dfrac{\mu_l C_{pl}}{k_l}$, and $\mathrm{Fr_g} = \dfrac{U_g^2}{g d_p}$. The agreement with experimental data is relatively poor (+/- 30% agreement with experimental values). Furthermore, even though viscosity was one of the key variables studied, it is not taken into account explicitly in the equation. It should be noted that the during the study of Kato et al. (1981) k_l and C_{pl} were not varied and their correlation is based on the correlation from Garside and Al-Dibouni (1977) (as cited in Saberian-Broudjenni et al., 1985) which has 15 empirical coefficients and does not take into account liquid properties and is not applicable at low U_l.

2.1.3 Chiu and Ziegler

Chiu and Ziegler (1983; 1985) performed studies using a 0.051 m i.d. (1.52 m high) column equipped with an electric wall heater 0.28 m high at ambient pressure and temperature equipped with a 0.30 m high calming section. The three-phase system consisted of air, water, and either glass beads (d_p = 0.05 – 3 mm) and γ-alumina particles (d_{pe} = 3.5 – 5.3 mm). The gas and liquid velocity ranges were 0 – 0.14 m/s and 0.063 – 0.15 m/s, respectively. The concentration of particles used in the study is not specified. The wall temperatures, inlet and outlet temperatures, and room temperature were measured by a total of 16 copper-constantan thermocouples, while the radial temperature profile was measured using a sheathed thermocouple. To avoid any thermal entrance length effects, the ΔT between the wall and bed was used rather than an integrated or logarithmic mean temperature difference. In all cases, the heat transfer coefficient was found to increase with increasing U_g (the rate of initial dependent on U_l and d_p) reaching an asymptotic value at high U_g. In contrast, for increasing U_l, the heat transfer coefficient exhibits a maximum value. This maximum value was found to increase with increasing d_p suggesting that heat transfer via particle carrier is not the main path for heat transfer. Generally, the heat transfer coefficient increased with increasing d_p (except at high U_g and low d_p, where it passed through a minimum). The radial temperature profile was found to flatten with increasing U_g (although the effect is less pronounced at relatively high U_g). Chiu and Ziegler

(1985) proposed the following correlation for calculation of the wall-to-bed heat transfer coefficient:

$$\frac{h_w d_p}{k_l} = 0.762\left(\frac{\rho_l U_l\left(\varepsilon_g+\varepsilon_l\right)}{S_p\left(1-\varepsilon_g-\varepsilon_l\right)\varepsilon_{l3}\mu_l}\right)^{0.646}\left(\frac{C_{pl}\mu_l}{k_l}\right)^{0.638} U_R^{0.266}\Phi_s^{-1}\left(\frac{1-\varepsilon_2}{\varepsilon_{l3}}\right) \qquad (17)$$

where ε_{l2} and ε_{l3} are the liquid phase holdups in the 2 phase and 3 systems, S_p is the particle surface area per unit volume, Φ is the particle shape factor, and U_R is the ratio of the minimum fluidization velocity and particle terminal velocity (U_t).

2.1.4 Hatate and coworkers

Hatate et al. (1987) studied wall heat transfer in an up-flowing three-phase system using air, water, and glass beads (d_p = 29 – 96 μm) in a relatively small column (D_c = 1.5 to 2.7 cm) (see Figure 3). The Teflon coated wire heater was insulated with 10 cm of glass-wool to prevent heat transfer to the exterior. The presence of gas and solids (< 40 wt. %) was found to increase the heat transfer, which also increased with increasing U_g and U_l. The heat transfer coefficient exhibited a maximum at a concentration of approximately 20 to 30 wt. %. In this study, no effect of particle diameter on the heat transfer coefficient was found. The correlation derived by Hatate et al. (1987) is presented in Equation (18) and is reported as being accurate to plus or minus 30%.

$$\frac{\left(\frac{h_w D_c}{k_l}\right)\left(\frac{C_{pl}\mu_l}{k_l}\right)^{-0.33}\left(\frac{\mu_l}{\mu_w}\right)^{-0.14}}{\left(\frac{D_c U_g \rho_g}{\mu_g}\right)^{0.055}\left(\frac{D_c U_l \rho_l}{\mu_l}\right)^{0.2}} = 10.5\exp\left\{\ 0.00031\Theta\left(\ _s\ \ 22\right)\Theta^2\right\} - \qquad (18)$$

where μ_l and μ_w are the fluid (or slurry) viscosities at the average bulk and wall temperatures, respectively. (Note: Θ_s in this case must *not* be expressed as a fraction).

2.1.5 Hart

Hart (1976) studied heat transfer in bubble column (9.91 cm i.d. by 107 cm high) using air and either water or ethylene glycol solutions. The column was heated using an electric wall heater. Nine thermocouples measured the wall temperature while 5 thermocouples – located within a copper tube submerged in the column –

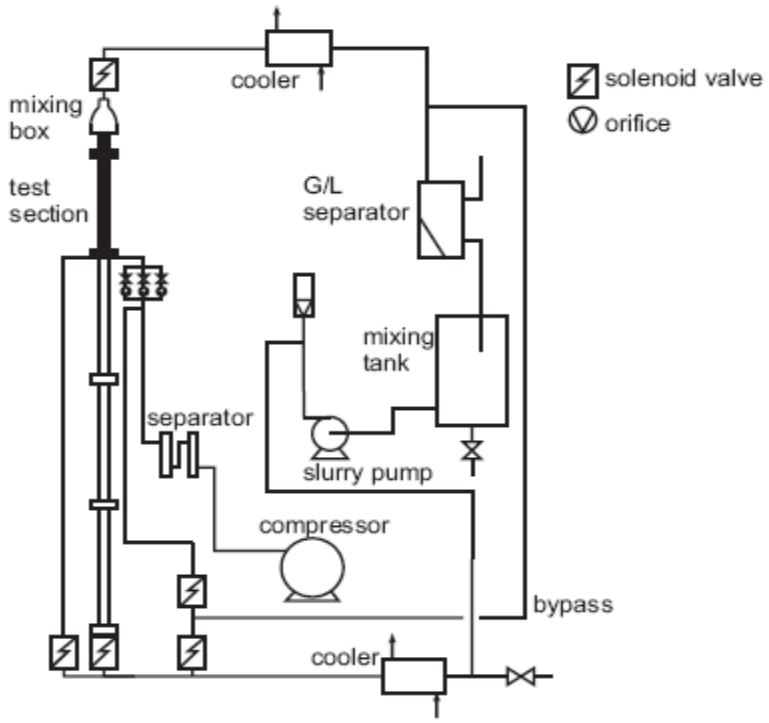

Figure 3. Experimental apparatus of Hatate and coworkers (after Hatate et al., 1987).

measured the bulk temperature. Gas injection was via a single nozzle (6.4 mm i.d.) at relatively low gas flow rates (0.0003 – 0.02 m/s). The heat transfer coefficient was determined at the midpoint of the column. It was determined that power dissipation per unit volume is a function of U_g, gravity, and ρ_l: similar dependencies were reported for h, with the addition of liquid viscosity. The author proposed the following correlation for the wall heat transfer coefficient:

$$\left(\frac{h_w}{C_{pl}U_g\rho_l}\right)\left(\frac{\mu_l C_{pl}}{k_l}\right)^{0.6} = 0.125\left(\frac{U_g^3\rho_l}{\mu_l g}\right)^{-0.25} \tag{19}$$

2.1.6 Shaykhutdinov and coworkers

Shaykhutdinov et al. (1971) studied heating and cooling of air and water/glycerine solutions (0, 25, 50 wt. %) in 4.8 cm i.d. and 40 cm high column. The gas velocities were varied from 0.002 to 1.0 m/s while U_l was set to 0.0036, 0.0105, or 0.0163 m/s. It was observed that h_w increased in the inlet region over the entire range of liquid and gas flow rates regardless of the heat flux direction. Furthermore, the heat transfer coefficient tended to decrease with the axial

distance above the distributor for heating: however, the opposite trend was observed for cooling. This was attributed to changes in liquid viscosity and back-mixing. Equation (20) and Equation (21) presents their derived correlations for bubble-flow and foaming conditions, respectively:

$$h_w = A\left(\frac{0.184 k_l^{0.56} C_{pl}^{0.44} \rho_l^{0.78} U_g^{0.33}}{\mu_l^{0.34}}\right) \tag{20}$$

$$h_w = A\left(\frac{0.310 k_l^{0.73} C_{pl}^{0.27} \rho_l^{0.71} U_g^{0.13}}{\mu_l^{0.44}}\right) \tag{21}$$

where A = 1 for z = 1 to 4 m and 1.25 for z < 1 m.

2.1.7 Joshi and coworkers

Joshi and coworkers have completed numerous studies on heat transfer in bubble columns using both experimental and CFD modeling methods. Pandit and Joshi (1984; 1986) review three-phase sparged reactors including example calculations for determining the average liquid circulation velocity (V_c) and h_w (Pandit and Joshi, 1984). An extensive literature review of CFD modeling of bubble columns including discussion of model development and previous experimental work has been completed by (Joshi, 2001). Other CFD studies have concentrated on modeling of the velocity and hold-up profiles and heat transfer near the vessel wall (Dhotre et al., 2005; Vitankar et al., 2002). Dhotre and Joshi (2004) also studied flow patterns, eddy diffusivity, pressure drop, and heat transfer concerning air and water/ethanol/CMC solutions.

Kulkarni and Joshi (2006) completed an experimental study using an air-water system in a 0.385 m i.d. (2.8 m high) column while varying U_g from 0.028 to 0.25 m/s. Using a data acquisition rate of up to 20 kHz the pressure signals were examined using cross-correlation analysis to quantify bubble coalescence, break-up, and liquid eddies, surface renewal rate and average liquid circulation velocity (V_c). The surface renewal time was observed to decrease with increasing U_g. CFD modeling was conducted using a Reynolds number k-ε model for predicting V_c. Kulkarni and Joshi (2006) report the presence of multiple circulation cells at the column wall while liquid primarily rises in the centre of the column (refer to Figure 4). Estimations of the heat transfer coefficient were obtained using the surface renewal time (θ_c) derived from the pressure fluctuation signals according to Equations (22) and (23):

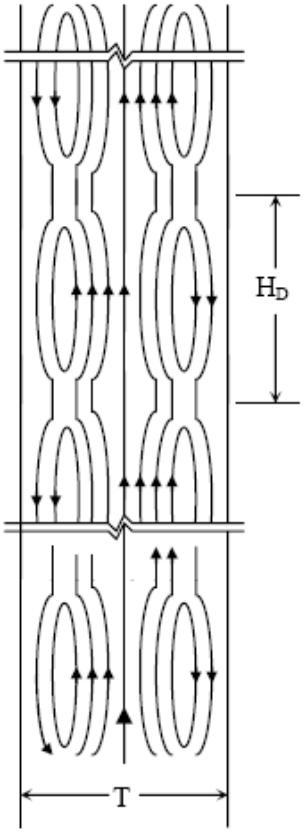

Figure 4. Circulation cells as described by Joshi et al. (2006).

$$\theta_c = \frac{\sum n_i \Delta t_i}{\sum n_i} \tag{22}$$

$$h_w = \left(\frac{\rho_l C_{pl} k_l}{\theta_c} \right)^{0.5} \tag{23}$$

The heat transfer coefficient was also determined using the eddy diffusivity and velocity profiles obtained via the CFD simulations and substituting them into Equation (24), which was then solved using a control volume as described by Dhotre and Joshi (2004):

$$\frac{1}{r}\frac{\partial}{\partial r}\left(r\varepsilon_l \rho_l \nu_l T\right) + \frac{\partial}{\partial z}\left(\varepsilon_l \rho_l V_a T\right) = \frac{1}{r}\frac{\partial}{\partial r}\left[r\varepsilon_l \left(\frac{\nu_l + \nu_T}{\mathrm{Pr}} \right) \frac{\partial T}{\partial r} \right] \quad \frac{\partial}{\partial z}\left[\varepsilon_l \left(\frac{\nu_l + \nu_T}{\mathrm{Pr}} \right) \frac{\partial T}{\partial z} \right] \tag{24}$$

The heat transfer predictions based on ΔP measurements show proper trend with respect to U_g but consistently underpredicted the results of Burkel (as cited in Kulkarni and Joshi, 2006) by approximately 15 to 20% and Verma (1989) by about 5%.

2.1.8 Holcombe and coworkers

Nitrogen and water cooled by means of an external water jacket were used in the wall heat transfer study by Holcombe et al. (1983) in a 7.8 cm i.d. and 1.8 m high column. Six multiple thermocouple probes were evenly spaced every 0.305 m along the column axis (see Figure 5). The heat transfer coefficient was determined by measuring the bulk and cooling water temperature profiles. The gas and liquid superficial velocities were varied from 0 to 0.06 and 0.02 m/s, respectively, while three different pressures (0.30, 0.51, and 0.71 MPa) were studied. Constant radial temperature profiles indicated that there was good radial mixing while the axial temperature profile was well described using the axial thermal dispersion model as given by Equation (25):

$$D_h = 1.26 D_c^{4/3} U_g^{0.46} \tag{25}$$

It was reported that pressure had no effect on h_w for the system under study. Based on their experimental finding, Holcombe et al. (1983) derived the following correlation:

$$\frac{h_w}{\rho_l C_{pl} U_g} = 0.1 \left[\left(\frac{d_b F_g}{\mu_g} \right) \left(\frac{U_g^2}{g d_b} \right) \left(\frac{C_{pl} \mu_l}{k_l} \right)^2 \right]^{-0.26} \exp\left[0.00024 \left(\frac{D_c F_l}{\mu_l} \right) \right] \tag{26}$$

where the units for μ_l and μ_g are kg/m·s and F_l and F_g are the liquid and gas mass flow rates (kg/m^{2}s), respectively.

2.2 Experimental Investigations in Columns with Single Internal

2.2.1 Kölbel and coworkers

Pioneering studies by Kölbel and coworkers concerned heat transfer in bubble columns 2 m in height and 0.092, 0.192 or 0.292 m i.d. The heat transfer tubes measured 30 mm o.d. by 0.10 m long. Power supplied to the heater inside the tube ranged from 50 – 460 W providing a ΔT between the surface and bed or between 10 and 15 K. The distance between the measurement section and the

porous distributor was varied from 0.20 to 1.20 m. Sugar cane and potassium ethyl Xanthate solutions were studied in order to understand the effect of viscosity (up to 100 cSt) and surface tension (30 dynes/cm), respectively, on the heat transfer coefficient (Kölbel et al., 1958b). The air velocity through the column ranged from 0.01 to 0.35 m/s. Radial temperature measurements revealed a constant temperature profile throughout the column with a rapid reduction at the wall. This was attributed to boundary layer formation at the wall where heat transfer would occur only by conduction. The heat transfer measurements had to be performed quickly before bed temperature changed too much and it was ensured that the probe surface was wiped clean between runs to remove any stationary bubbles adhered to the surface. It was determined that h increased with increasing U_g and this was attributed to thinning of the boundary layer. The bubble size was found to have practically no influence on h (however, it should be noted that these tests were conducted at relatively low U_g). Increased surface tension corresponded to a slight increase in h at lower U_g (but not at high U_g). The liquid viscosity was found to have a significant effect on h (more so at low viscosities and U_g < 8 cm/s) – h decreased with increasing μ_l. Measurements showed that h was independent of D_c if D_c/d_b > 20. Kölbel et al. (1958b) proposed the following correlation for heat transfer in a bubble column:

$$\frac{h d_{tube}}{k_l} = c\left(\frac{\rho_l U_g d_{tube}}{\mu_l}\right)^m \tag{27}$$

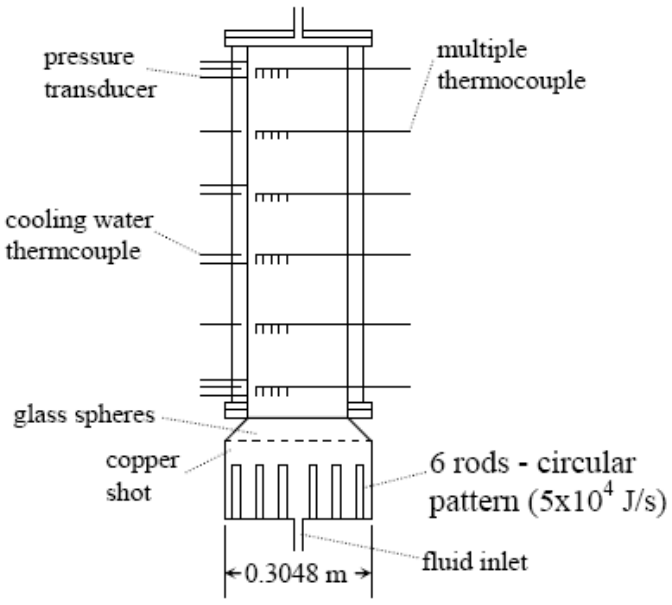

Figure 5. Experimental apparatus of Holcombe et al. (after Holcombe et al., 1983).

where c and m are 43.7 and 0.22, respectively for Re > 150 and 22.4 and 0.355, respectively, for Re < 150. This correlation is not recommended for heating surfaces with different diameters and would at best provide rough first approximations. Furthermore, Saxena et al. (Saxena et al., 1990m) also found it to be inadequate and unrealistic due to the occurrence of d_{tube} in the equation.

Other studies by Kölbel and coworkers (Kölbel et al., 1958a; 1960; Kölbel and Langemann, 1964) utilized sand particles with diameters ranging from 0.04 to 0.20 mm and concentrations of 0 to 40 wt. %. The liquid phase consisted of either water, machine oil, spindle oil, water-glycerine, or sugar water solutions, with air for the gas phase at temperatures of 20 to 80°C and pressure of 0.1 to 1.6 MPa. The liquid phase was stationary while the superficial gas velocity was varied from 1 to 12 cm/s. It was reported that pressure had little effect on the heat transfer coefficient, while h increased with increasing Θ_s and d_p. The heat transfer coefficient was observed to increase with increasing temperature and superficial gas velocity (reaching an asymptotic value above 10 cm/s). Equations (28) and (29) were proposed for determining h in the presence of suspended particles under laminar and turbulent conditions, respectively:

$$Nu = 222.8\,\mathrm{Re}^{0.16}\left(\frac{d_p}{d_{p,\min}}\right)^{0.05} \tag{28}$$

$$Nu = 350.8\,\mathrm{Re}^{0.108}\left(\frac{d_p}{d_{p,\min}}\right)^{0.05} \tag{29}$$

where $d_{p,min}$ is the smallest particle size present in the column ($d_{p,min}$ = 0.04 mm). The above two equations are applicable for $1 < (d_p/d_{p,min})$. The Nusselt and Reynolds numbers are given below as cited in Saxena and Chen (1994):

$$Nu = \frac{h d_p}{k_l} \quad \text{and} \quad \mathrm{Re} = \frac{U_g \rho_g d_p}{\mu_g}$$

For viscous solutions the following two correlations were proposed for laminar and turbulent flow, respectively:

$$Nu = 227.5\left(\frac{\rho_{H_2O}\mu_l}{\rho_l \mu_{H_2O}}\right)^{0.1} \mathrm{Re}^{0.161}\,\mathrm{Pr}^{-0.038} \tag{30}$$

$$Nu = 454.0\left(\frac{\rho_{H_2O}\mu_l}{\rho_l\mu_{H_2O}}\right)^{0.1} \mathrm{Re}^{0.113}\,\mathrm{Pr}^{-0.135} \tag{31}$$

2.2.2 Baker and coworkers

Baker et al. (1978) studied heat transfer from an immersed probe in a cylindrical column (0.24 m i.d. by 2.75 m high) for air-water, water-glass beads, and air-water-glass bead systems. The average particle diameters ranged from 0.50 – 5.0 mm, while the gas and liquid velocities were varied in the range of 0 – 0.24 m/s and 0.006 – 0.13 m/s, respectively. The heat transfer surface (0.064 m o.d. by 0.25 m long) consisted of four 1500 W (240 V) heating elements with three embedded constantan thermocouples soldered flush with the heater surface. The conical tip of the probe was roughened using sand paper in order to promote the development of a fully developed boundary layer and the probe held in place with three spring loaded rods. Generally, the heat transfer coefficient was found to increase with increasing U_g regardless of U_l, d_p and location of the heater before reaching a plateau at relatively high U_g. For a given U_g, the heat transfer coefficient increased with the addition of solids and decreased with increasing particle diameter (this dependence all but disappears $d_p > 3$ mm and U_g is relatively high). For increasing U_l, the heat transfer coefficient was found to exhibit a maximum value for which the porosity of bed at the maximum h value decreased when d_p was increased. The effect of particles on the heat transfer was attributed to erosion of the thermal boundary layer due to particle motion, which would increase with increasing U_l (i.e. particle motion would be restricted at low U_l due to the lower level of turbulence and at high U_l due to the decrease in ε_s). The enhancement obtained from introducing gas into the column is greatest when the bed is not yet completely fluidized. Baker et al. (1978) represented their data with the with Equations (32) and (33) for gas-liquid and gas-liquid-solid systems, respectively:

$$h = 1592U_l^{0.026}U_g^{0.170} \tag{32}$$

$$h = 1977U_l^{0.070}U_g^{0.059}d_p^{0.106} \tag{33}$$

where U_l and U_g are in mm/s, d_p is in mm, and h is W/m^2.K. The correlation from correlation from Baker et al. (1978) is only good for its conditions (i.e. air-water-glass beads and high U_l) and does not take into account liquid or solid properties (Saberian-Broudjenni et al., 1985).

2.2.3 Kurpiers, Steiff, and Weinspach

Kurpiers, Steiff, and Weinspach investigated heat transfer for stirred and unstirred bubble columns equipped with either sintered plate gas distributors (Steiff and Weinspach, 1978) or spargers (Kurpiers et al., 1985a; 1985b). Column diameters studied ranged from 0.19 to 1.5 m with height to diameter ratios of 1, 2, or 3. Steiff and Weinspach (1978) studied gas-liquid systems consisting of air and water, silicone oil, or baysilone oil. Later studies involved multiphase systems using various combinations of air, water, ethylene glycol, diethylene glycol, glycerol, and glass beads (d_p = 10 to 1800 μm) (Kurpiers et al., 1985a; 1985b). The heat transfer coefficient was measured at the jacketed wall or an internal surface (coiled tube in the former case and a vertical tube in the latter studies). At relatively low U_g, an increase in the stirring speed was found to increase the heat transfer; while at high stirring speeds U_g had no effect: the heat transfer was greatest for the internal coil than from the wall jacket. Furthermore, an increase in the liquid viscosity was found to decrease the heat transfer and this was attributed to a thicker laminar sub-layer at the heat transfer surface. The following equation was proposed for the heat exchange coefficient from the helical coil to an aerated liquid medium (Steiff and Weinspach, 1978):

$$\frac{h}{\rho_l C_{pl} U_g} = 0.137\left[\left\{\left(\frac{\rho_l U_g D_i}{\mu_l}\right)\left(\frac{U_g^2}{gD_i}\right)\left(\frac{\mu_l C_{pl}}{k_l}\right)^2\right\}^{1/3}\right]^{-\left(0.73+1.64\times10^{-5}\,\mathrm{Re}_n\right)} \left(\mathrm{Re}_n+1.0\right)^{0.047}\left(\frac{\mu_w}{\mu_l}\right)^{-0.42} \quad (34)$$

where $\mathrm{Re}_n = \left(\rho_l n D_i^2/\mu_l\right)$ is the liquid Reynolds number based on the stirring speed and D_i is the impeller diameter. A similar equation was proposed for the case of the vertical tube heat exchanger (Kurpiers et al., 1985b), which could be adapted for application to bubble columns by assuming that there is no agitator (i.e. $\mathrm{Re}_n = 0$) as given below:

$$St = 0.1\left[\left(\frac{\rho_l U_g D_c}{\mu_l}\right)\left(\frac{U_g^2}{gD_c}\right)\left(\frac{\mu_l C_{pl}}{k_l}\right)^{2.4}\right]^{-0.25}\left(\frac{\mu_l}{\mu_w}\right)^{0.23} \quad (35)$$

Results from the above authors also indicated the need to take into account the direction of the heat transfer (i.e. cooling or heating) especially in the case of organic liquids. In the case of cooling, the heat transfer coefficients measured where approximately 50 % lower, which was attributed to the increased thickness

of the boundary layer at the heat transfer surface resulting from an increase in the liquid viscosity.

2.2.4 Deckwer and coworkers

The study of Deckwer et al. (1980) was conducted using 0.04 and 0.10 m i.d. columns with a sintered metal distributor (mean pore diameter 75 μm) at pressures of 400 to 1100 kPa, temperatures of 416 – 543 K, and solid concentration up to 16 wt. %. Figure 6 (a) illustrates the larger 10 cm i.d. column. The gas, liquid, and solid phases were comprised of N_2, molten paraffin, and powdered alumina (d_p < 5 μm). The gas velocity used in this study was very low (up to 0.04 m/s) while the liquid flow rate was zero. Accurate measurements of the fluidized bed height were achieved by lowering a hot wire probe [6 mm long, 20.5 μm diameter; refer to Figure 6 (b)] through the bed, where upon coming into contact with the liquid surface the heat removal (and hence the electric current) increased sharply. The gas holdup was found to decrease with increasing temperature in the smaller column before reaching an asymptotic value at 250°C (however this dependence was not observed in the larger column, possibly due to the higher wall effect exerted in the smaller column). No discernible effect of Θ_s or pressure on ε_g was found. However, the heat transfer coefficient did increase with increasing solids concentration. The authors also report an increase in h with

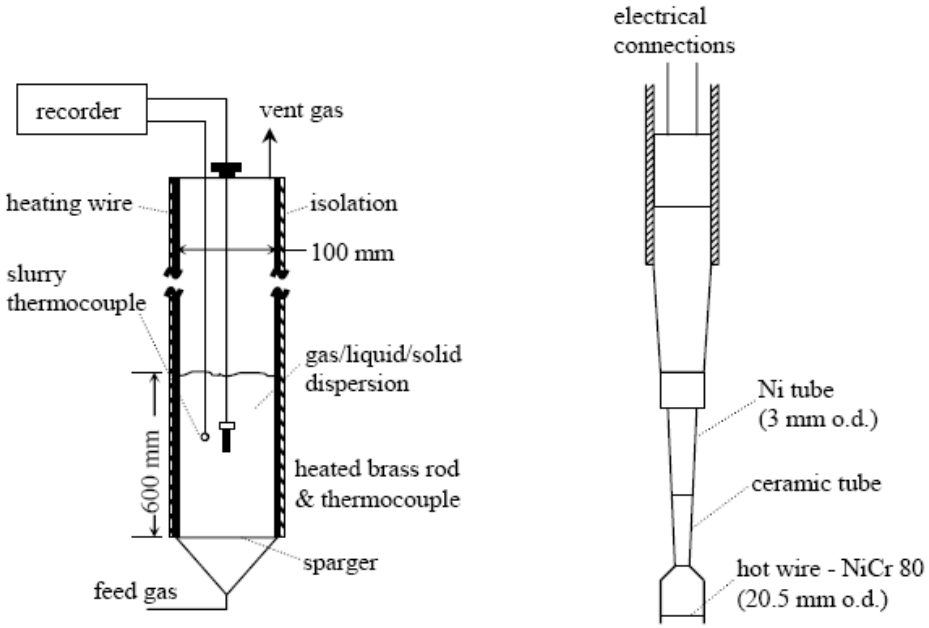

Figure 6. (a) The column and (b) probe utilized by Deckwer and coworkers (after Deckwer et al., 1980).

increasing U_g before levelling off at values above 0.10 m/s. It was demonstrated for such relatively small particles that the suspension could be treated as homogeneous and any changes in the heat transfer could be attributed to changing physiochemical properties.

The correlation proposed by Deckwer et al. (1980) is given below:

$$\frac{h_w}{\rho_{sl} C_{p,sl} U_g} = 0.1 \left[\left(\frac{U_g d_p \rho_{sl}}{\mu_{sl}} \right) \left(\frac{U_g^2}{g d_p} \right) \left(\frac{\mu_{sl} C_{p,sl}}{k_{sl}} \right)^2 \right]^{-0.25} \tag{36}$$

where $C_{p,sl}$, ρ_{sl}, k_{sl} are defined using Equations (11), (10), and (12) and μ_{sl} was determined using Einstein's relation

$$\mu_{sl} = \mu_l \left(1 \quad 4.5\varepsilon_s\right) \tag{37}$$

Zaidi et al. (1990) have studied the effects of highly viscous pseudoplastic solution on hydrodynamics and heat transfer in three-phase fluidized beds using xanthan solutions with air and glass beads (3 and 5 mm) as the gas and solid phases, respectively. The liquid viscosity was varied up to 300 mPa.s while the gas and liquid velocities were varied from 0.01 to 0.14 and 0.013 to 0.09 m/s, respectively. The experiments were conducted in a 0.10 m i.d. Pyrex glass column equipped with a gas sparger and a vertical heater (with a total heat transfer surface area of 64 cm^2) located vertically in the centre of the bed. Their results showed that increasing U_g led to a corresponding increase in ε_g, while the opposite trend occurred for increasing μ_{sl}. It was observed that bed contraction can occur with pseudoplastic solutions. The heat transfer coefficient was found to increase until U_g = 0.06 m/s then levelled off, while it decreased with increasing μ_{sl}. A maximum h values was observed when U_l was increased (the same trend is observed in regards to the bed voidage). The authors explain the appearance of this maximum by relating increased turbulent particle motion to increasing ε, resulting in a corresponding increase in h. However, this effect is "counterbalanced" by the reduced solid concentration at higher bed porosities. The ε corresponding to the maximum h value shifts to higher values with increasing d_p and μ_{sl}. Since most correlations are based on air-water-glass bead systems, and do not explicitly take into account the significant effect of viscosity, Zaidi et al. (1990) proposed the following correlation (standard deviation was 4.5 % for the reported data):

$$h = 1800 U_g^{0.11} \mu_{sl}^{-0.14} U_l^{1.03(0.65-\varepsilon)} d_p^{0.58(\varepsilon-0.68)} \quad (38)$$

where ε is the bed porosity (i.e. $\varepsilon_g + \varepsilon_l$). The equation covers the following range of parameters: $0.01 < U_g < 0.14$ m/s; $0.013 < U_l < 0.09$ m/s; $0.0037 < \mu_{sl} < 0.3$ Pa-s; and $3 < d_p < 5$ mm. Deckwer publish a review of heat transfer in bubble columns in 1984 in German – an English translation is available (Deckwer, 1992).

2.2.5 Kato and coworkers

Heat transfer studies testing horizontal and vertical heat transfer tubes in a vertical cylindrical column were completed by Kato et al. (1985; 1986). Two different columns of 0.12 m i.d. (2.0 m high) and 0.19 m i.d. (2.5 m high) were compared. Air served as the gas phase while water and carboxy-methyl cellulose (CMC) served as the liquid phase. The liquid viscosity was varied from 0.0011 to 0.017 Pa·s. The solid phase consisted of glass beads (d_p = 0.52 to 2.2 mm) or alumina (d_p = 3.2 mm). The column was equipped with a calming section beneath the perforated plate distributor and was operated at ambient pressure and temperature. The heat transfer surface consisted of a copper tube containing a sheathed heating wire (1.6 mm o.d.) surrounded with 5 to 30 μm copper particles and were installed 37 to 57 cm above the distributor. Table 2 summarizes the probe dimensions. Several thermocouples installed to measure heat transfer surface temperature. The temperature difference was maintained at 2 – 3 K. Both studies reported that at low U_l the heat transfer coefficient increased with increasing U_l; and that in the region of stable fluidization h approached an asymptotic value. As well, h increased with U_g and with decreasing μ_l and was found to be independent of D_c. The increase in h with U_g was greater when d_p was relatively small.

Table 2. Probe dimensions used in the studies by Kato et al. (1985; 1986).

Tube orientation	small column		large column	
	d_{tube} (cm)	l_{tube} (cm)	d_{tube} (cm)	l_{tube} (cm)
vertical	2.2	19.6	2.2	19.6
horizontal	1.27	12	1.27 & 3.8	19

In the case of the horizontal tube, the following correlation was proposed (reported accurate to plus or minus 30 %) (Kato et al., 1986):

$$\frac{h d_p \varepsilon_l}{k_l (1-\varepsilon_l)} = 0.12 \left\{ \left(\frac{0.02 + L_c}{L_c} \right)^{0.5} \left(\frac{C_{pl} \rho_l U_l d_p}{k_l (1-\varepsilon_l)} \right)^{0.65+0.12 Fr_h^{0.5}} \right\} + 1.3 \left(\frac{U_g^2}{g d_p} \right)^{0.33} \quad (39)$$

where $Fr_h = \frac{U_g^2}{g d_{tube}}$. In the case of the vertical tube, h appears to be independent of the heater length once it exceeds 6 cm: the correlation for the vertical tube is given by Equation (40) (Kato et al., 1985):

$$\frac{h d_p \varepsilon_l}{k_l (1-\varepsilon_l)} = \left\{ 0.058 \left(\frac{C_{pl} \rho_l U_l d_p}{k_l (1-\varepsilon_l)} \right)^{0.75} + 2.3 \right\} \left(\frac{d_{tube}}{0.022} \right)^{0.5} \tag{40}$$

Although no direct comparison was made by the authors, the heat transfer coefficient appears to be relatively larger for the horizontal tube than for the vertical tube.

2.2.6 Verma

Verma (1989) studied heat transfer in a 0.11 m i.d. by 1.7 m high column equipped with a heat transfer surface that was 0.02 m o.d. by 0.33 m long located 0.57 to 1.18 m above distributor. The heat transfer coefficients were measured at 316 K – at this temperature no foaming was observed and ε_g exhibited a continuous increase with increasing U_g. It was also observed that h increased with increasing U_g and became all but constant above a gas velocity of 0.12 m/s. Furthermore, h was found to be independent of probe location. The authors proposed the following correlation given as Equation (41) based upon the assumption that the heat transfer occurs by conduction to a thin boundary layer of liquid at the heat transfer surface:

$$\frac{h}{\rho_l C_{pl} U_g} = 0.121 \left(1 \quad \varepsilon_g\right) \left(\frac{U_g^3 \rho_l}{\mu_l g} \right)^{-0.25} \left(\frac{C_{pl} \mu_l}{k_l} \right)^{-0.5} \tag{41}$$

where $\varepsilon_g = \frac{1}{2 + \left(0.35 / U_g\right)}$. The correlation showed good agreement with the experimental data.

2.2.7 Chen and coworkers

Neural networks (NN) were utilized in a study by Chen et al. (2003) using an air-water bubble column for modeling heat transfer in terms of bubble and liquid motion. Three different columns were used (D_c = 0.2, 0.4, and 0.8 m i.d. by 3 m

high) equipped with perforated plate distributors. The gas velocities investigated ranged from 0.02 to 0.09 m/s (U_l was nil). The instantaneous local heat transfer coefficient was measured using hot-wire probe with a data acquisition rate of a 1000 Hz. This study concentrated on the time-dependent local hydrodynamics on the assumption that the use of average heat transfer caused the loss of information regarding the effect of instantaneous bubble dynamics on heat transfer. It is for this reason, that the authors surmise that most correlations do not remain valid over a wide range of gas flow rates. The local maximum instantaneous h was associated with the passage of the bubble wake. The data examined using a rescaled range analysis and chaos analysis (including evaluation of the correlation dimension and Hurst exponent), which indicated the behaviour in the bubble column was highly nonlinear and differed with scale. The authors claim that the artificial NN showed good scale-up potential.

2.2.8 Muroyama and coworkers

Muroyama et al. (2001; 2003) have studied heat transfer using air and water/CMC solutions to fluidize glass beads. The glass beads ranged in diameter from 0.1 to 5.2 mm while the solids loading was on the order of 0.01 to 0.1 vol. %. The liquid viscosity was varied from 0.0009 to 0.015 Pa.s by adding CMC concentrations of between 0.7 to 1.7 wt. %. Table 3 summarizes the different column dimensions and fluid velocities. The larger column and the heat transfer probe are illustrated in Figure 7: both columns were equipped with gas spargers and a liquid calming section. The heat transfer probe employed consisted of a brass pipe 25 mm o.d. and 106 mm long placed vertically in the column: placed inside the tube was a 500Z cartridge heater. The authors reported an optimum ΔT of between 3 and 7 K and 4 and 9 K for the water and water/CMC systems, respectively.

In the larger column it was reported that h exhibited a maximum with increasing U_l at relatively low U_g (only slight decrease was observed at relatively high U_l in the smaller column). At relatively high U_g values h varied less with increasing U_l. Generally, ε_g was observed to decrease with increasing Θ_s, which caused d_b (and therefore U_b) to increase due to increase in apparent viscosity (this effect was more pronounced at low U_g). The heat transfer coefficient was

Table 3. Column dimensions and fluid velocities for the studies by Muroyama et al. (2001; 2003).

	(Muroyama et al., 2003)	(Muroyama et al., 2001)
D_c (cm)	8.2	15.0
H_c (cm)	188	203
U_g (cm/s)	0 to 19	0.2 to 15.07
U_l (cm/s)	2.1 to 22	0.89 to 14.88

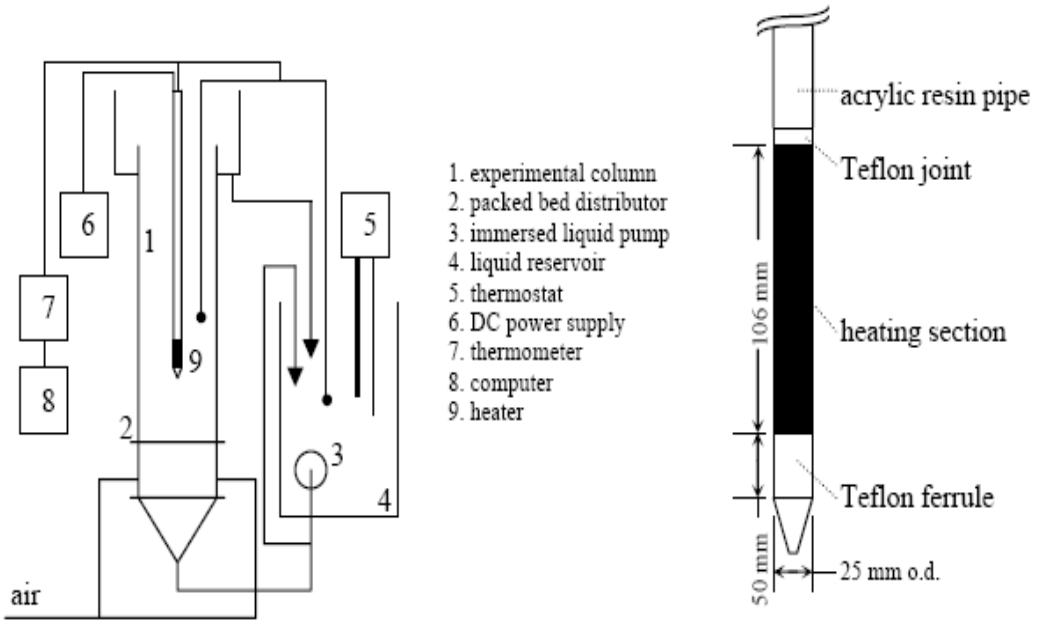

Figure 7. Large column and heat transfer probe used by Muroyama et al. (after Muroyama et al., 2001).

observed to increase slightly with increasing Θ_s. On the other hand, h increased significantly with increasing U_g for water slurry (although the increase was less significant for the 1 wt. % CMC slurry). In general, h was greater in three-phase fluidized bed that in a liquid-solid fluidized bed for an equivalent U_l. Based on their experimental findings, two correlation methods were tested: the modified Chilton- Colburn j_H-factor shown as Equation (42) and the specific power group approach, respectively.

$$j'_H = \frac{h\varepsilon_l \mu_l^{2/3}}{\rho_l k_l^{2/3} C_{pl}^{1/3} U_l} = 0.179 \left(\frac{\rho_l d_p U_l \left(\varepsilon_l + \varepsilon_g \right)}{\mu_l \left(1 - \varepsilon_l - \varepsilon_g \right)} \right)^{-0.273} \tag{42}$$

$$\left(\frac{h d_{tube}}{k_{sl}} \right) \left(\frac{C_{psl} \mu_{sl}}{k_{sl}} \right)^{-1/3} = 0.138 \left(\frac{\rho_{sl} E_{sl}^{1/2} d_{tube}^{4/3}}{\mu_{sl}} \right)^{0.709} \tag{43}$$

where E_{sl} is the energy dissipation rate per unit mass of slurry. Equation (43) was reported to significantly underestimate the heat transfer coefficient for the 1 wt. % CMC slurry data (Muroyama et al., 2003). The authors reportedly found a good analogy between heat and mass transfer.

2.2.9 Kantarci and coworkers

Kantarci et al. (2005b) studied heat transfer in a 0.17 m i.d. by 0.60 m high column equipped with a six-arm gas sparger. The three phases consisted of air, water, and yeast (10 μm) or bacterial cells (0.2 to 0.7 μm) at concentrations of 0.1 and 0.4 dry wt. %. The liquid velocity was zero while the gas velocity was varied from 0.03 to 0.20 m/s. Temperature in the column was varied from 296 to 318 K at ambient pressure. The heat flux probe [the same as described by Li and Prakash (1997)] was mounted flush to 15 mm o.d. brass tube. The dynamic gas disengagement technique was used to distinguish between the small and large bubble hold-up. Results indicated that ε_g increased with increased concentration of cells (cells may disrupt bubble coalescence) and increasing U_g. No significant effect of temperature on ε_g was found. It was suggested by the authors that due to the low concentration of cells that the liquid properties would not be affected. Hence the bubble characteristics were primarily affected by cell adhesion on the bubbles inhibiting bubble coalescence. A significant increase in h when cells added was observed and attributed to enhanced turbulence created by cells. The heat transfer coefficient increased with increasing U_g and decreasing μ_l (i.e. increasing temperature). Larger h values were recorded at the centre and top of the column. Equation (44) presents the correlation derived by Kantarci et al. (2005b) with the coefficients shown air-water-0.4% cell system:

$$\frac{h}{\rho_l C_{pl} U_g} = 0.102 \left(\frac{\rho_g U_g^3}{\mu_l g} \right)^{-0.26} \left(\frac{\mu_l C_{pl}}{k_l} \right)^{-0.54} \left(\frac{z}{H_l} \right)^{-0.07} \left(\frac{r}{R_c} \right)^{-0.013} \tag{44}$$

where z was defined as the axial height below the stationary bed level H_l and r is the radial distance from the column centre. The results were reported accurate to ±15 % for the system studied.

2.2.10 Fan and coworkers

The column used by Kumar et al. (1993a; Kumar and Fan, 1994; 1992; 1993b) was 0.076 m i.d. and 1.5 m high. A small (2.54 x 1.91 x 0.4 cm) heat flux probe was located 52 cm above the distributor (see Figure 8). Each distributor included a calming section filled with 6 mm glass beads. Usually, the gas and liquid phases consisted of air and water (at low pressure) or nitrogen and Paratherm NF (at high pressure or high temperature). The solid phases studied includes polystyrene (PS), polyvinyl acetate (PVA), nylon, calcium alginate, and glass beads. Particle diameters ranged from 0.326 to 3.79 mm (ρ_s = 1040 to 2500 kg/m^3). A mesh screen was placed at the *top* of the column in order to prevent solids from leaving column.

The gas velocities studied by Kumar et al. (1993a) were relatively low (0.85 cm/s or 3.4 cm/s). Three different distributors were evaluated (porous, shell and tube, and secondary nozzle), which are shown in Figure 9. These experiments were performed at ambient temperature and pressure. Tests were conducted by releasing single bubbles using a hemispherical cup (2.5 cm in diameter) inserted through the side wall with air injected via a syringe. Bubble behaviour was then captured using a high-speed camera. Generally, the heat transfer coefficient was observed to increase significantly as the bubble approached the probe with exhibiting a maximum as the bubble wake region with entrained solids passes. This enhancement in h brought about by the bubble wake was reported to be higher for low density particle systems; however, the ε_s values

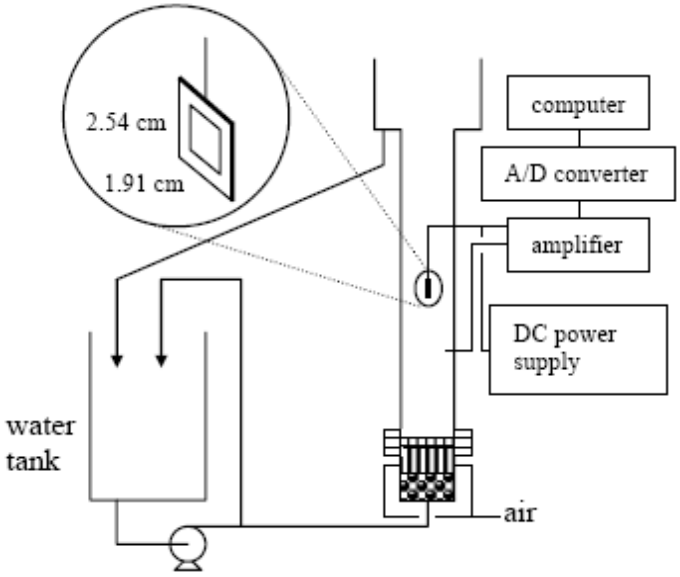

Figure 8. Column and heat transfer probe used by Kumar and coworkers (after Kumar et al., 1993).

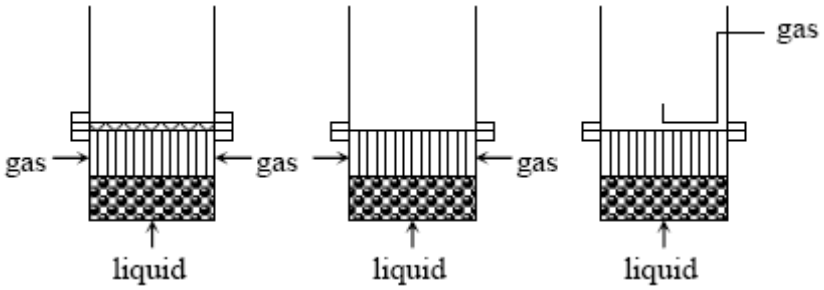

Figure 9. Distributors used by Kumar et al. (after Kumar et al., 1993).

were not the same (the effect on μ_l would have to be considered). When the liquid velocity was varied (from 0.002 to 0.10 m/s) the opposite trend was reported for the average heat transfer coefficient than above. However, ε_s is not stated thereby making any direct comparison difficult. Furthermore, the effect of U_l difficult to ascertain as it is represented on all graphs using a logarithmic scale. The relative increase in h for three-phase systems using low density particles is approaching that of water behaved similarly to two-phase systems (i.e. gas-liquid). The heat transfer was higher in coalesced bubble regime than in dispersed bubble regime (this is affected by grid design). The following correlation for two-phase and three-phase system proposed:

$$\frac{h' d_p \varepsilon_l}{k_l (1-\varepsilon_l)} = 0.0556 \left(\frac{d_p \rho_l C_{pl} U_l}{k_l (1-\varepsilon_l)} \right)^{0.709} \left[\frac{\rho_s - \rho_l}{\rho_l} \right]^{-0.156} \tag{45}$$

where h′ is the heat transfer coefficient from the liquid-solid system (correlation coefficient = 0.99 and standard deviation of 3.3%).

The study by (Kumar and Fan, 1994) studied the effect of viscosity on the bubble behaviour using single bubble injection (as described above) *or* chain bubbling. Liquids utilized included water (μ_l = 0.00086 Pa.s) and aqueous glycerine solutions (μ_l = 0.0385 to 0.0985 Pa.s). Glass beads (d_p = 163 or 760 μm) were used for the solid phase. These tests were conducted at ambient temperature and pressure. Again, as the bubble approached the heat flux probe, the instantaneous h value increased before reaching a maximum as the bubble wake passed. However, the recovery to the value noted prior to the bubble passage is quicker in more viscous systems. Generally, h was observed to increase with increasing bubble diameter and was significantly higher for the chain bubbling system where bubble-bubble interaction would lead to acceleration of any trailing bubble and create higher shear forces. The presence of particles may shorten the critical interaction distance between bubbles by increasing the apparent viscosity and dampening turbulence.

Kumar et al. (1993a) have also studied the effect of high gas hold-up on heat transfer in three-phase systems using surfactants (0.1% t-pentanol aqueous solutions) at ambient temperature and pressure. The solid phase consisted of 2.5 mm nylon beads or 0.76 mm glass beads. The gas velocity was varied from 0.01 to 0.07 m/s, while the liquid velocity was varied from 0.01 to 0.06 m/s (porous distributor) and from 0.007 to 0.016 m/s (perforated distributor). Generally, the heat transfer coefficient exhibited a maximum with U_g for systems that utilized surfactant. It was also observed that the heat transfer coefficient went exhibited a minimum with varying U_l (in the range studied).

Magiliotou et al. (1988) also investigated the effects of relatively high ε_g on the heat transfer in a three-phase system using a vertical heat transfer surface (19 mm in diameter and 66 mm long) located coaxially within columns of 0.076 or 0.15 m i.d (refer to Figure 10). The three-phase consisted of air, water or a 0.5% tert-pentyl alcohol (TPA) aqueous solution, and cylindrical catalyst particles (d_{pe} = 1.09 – 1.57 mm). The presence of the surfactant generally resulted in a higher heat transfer coefficient than that obtained using pure water. Again, h was found to increase with increasing U_g, before reaching an asymptotic value, while exhibiting a maximum value with increasing U_l. The heat transfer coefficient also increased with increasing d_p. The column diameter had no significant effect. Magiliotou et al. (1988) proposed the following relationship for determining the heat transfer coefficient.

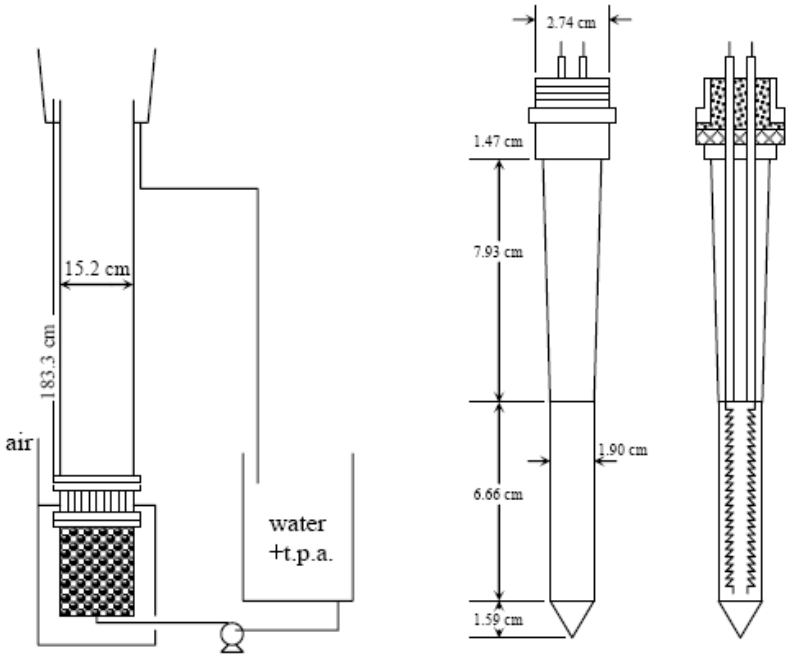

Figure 10. Column and heat transfer probe used by Magiliotou et al. (after Magiliotou et al., 1988).

$$h = c_1\left[k_l\rho_l C_{pl}\left(\rho_l P_v/\mu_l\right)^{1/2}\right]^{1/2} + c_2\left\{k_l\rho_l C_{pl}\left[\varepsilon_s^{1/3}\left(U_l - U_{lmf}\right)/\left(\Phi_s d_{pe}\right)\right]\right\}^{1/2} \qquad (46)$$

where $U_{l,mf}$ is the minimum liquid fluidization velocity and E_{sl} is the energy dissipation rate per unit mass given by Equation (47) and the constants are given in Table 4.

$$E_{sl} = \frac{\left[\left(U_l + U_g\right)\left(\varepsilon_s\rho_s + \varepsilon_l\rho_l + \varepsilon_g\rho_g\right)\right]g}{\varepsilon_s\rho_s + \varepsilon_l\rho_l} \tag{47}$$

Table 4. Coefficients for Equation (46).

	c_1	c_2
Surfactant system	0.071	0.01
Non surfactant system	0.1	0.285

Luo et al. (1997) and Yang et al. (2000) have studied heat transfer at high pressure in 0.051 (0.8 m high) and 0.10 m i.d. columns (1.37 m high), respectively. The latter also studied the effect of high temperature on the heat transfer coefficient. Both columns were equipped with perforated plate distributors and employed the same heat flux probe described above, which is suitable for use at high temperatures and pressures. Typically the ΔT between the heat transfer surface and the bed was maintained at 9 K. Both studies utilized nitrogen as the gas phase and Paratherm NF as the liquid phase. These studies also revealed that the influence of pressure on the hydrodynamics and heat transfer coefficient is significant but differs for systems using relatively small particles (i.e. slurry systems) and those using relatively large particles (i.e. three-phase fluidized beds). Generally, higher pressure leads to smaller bubbles that have a more uniform size distribution that have a lower rise velocity, which in turn increases the gas hold-up. Increasing pressure also increases the transition velocity from dispersed to coalesced bubble flow regime.

The pressure in the study by Luo et al. (1997) was varied between 0.1 and 15.6 MPa while the glass beads were either 2.1 or 3 mm in diameter (ε_s was of the order of 0.49 to 0.55 vol. %). It is important to note that the superficial gas and liquid velocities were relatively small: 0 to 0.09 m/s and 0.004 to 0.026 m/s, respectively. Results indicated that the pressure effects on the hydrodynamics were only significant up to 6 MPa. The heat transfer coefficient was observed to increase with increasing pressure up to about 6 MPa then slowly began to decrease. The authors attributed the increase in h to enhanced erosion of the boundary layer by the motion of the small bubbles. The following correlation was proposed based on their experimental data:

$$h = h'\varepsilon_g^{0.45}\left(\frac{0.396}{U_g^{0.45}} + \frac{0.6768}{U_{t,P0}}\right) \tag{48}$$

where $U_{t,P0}$ is the particle terminal velocity at ambient pressure and h′ is the heat transfer coefficient for the liquid-solid system and is given by Equation (49):

$$\frac{h' d_p}{k_l} = 0.67 \left(\frac{\rho_l d_p U_b}{\mu_l} \right)^{0.62} \left(\frac{C_{pl} \mu_l}{k_l} \right)^{0.33} \left(\frac{\varepsilon_s}{1-\varepsilon_s} \right) \tag{49}$$

The average deviation with experimental values is ± 10 %.

Lin and Fan (1999) have studied heat transfer and bubble characteristics using a single nozzle in a 0.051 m i.d. column (0.8 m high) using nitrogen and Paratherm NF at relatively high pressures (0 to 15.2 MPa). Although not specified, the range of gas velocities through the 1.5 mm i.d. nozzle covered the bubbling and jetting regimes (U_l was nil). The heat flux probe (described above) was submerged directly in the column (i.e. it was the only internal present). The bubble properties were recorded using a high-speed CCD camera (240 frames/s and 1/10000 s shutter speed). The heat transfer coefficient and temperature values were recorded at a rate of 210 Hz. Their results show that pressure has a significant effect on the column hydrodynamics – particularly on the bubble properties. It was determined that d_b decreased with increasing P up to 4 MPa before levelling off (at 15 MPa d_b was reduced by around 15% for all U_g compared to ambient conditions). The effect of P on d_b was greater at relatively larger U_{gn} (gas velocity at the nozzle outlet) since small spherical bubbles appear to be less affected by pressure. As well, the transition velocity from bubbling to jetting behaviour, U_{tran}, decreased with increasing pressure. At a given pressure, h increased linearly with U_{gn} (in bubbling regime) and levelled off (in jetting regime). This behaviour was attributed to their observation that $d_{b,max}$ was reached once the flow regime becomes churn-turbulent.

Yang et al. (2000) employed 53 μm glass beads (ε_s was varied from 0 to 35 vol. %) and varied the pressure and temperature from 0.1 to 4.2 MPa and 35 to 81°C, respectively. The column had an inside diameter of 0.10 m and an overall height of 1.37 m. The liquid velocity was zero while the gas superficial velocity ranged from 0 to 0.20 m/s. The heat transfer coefficient increased with increasing U_g before levelling off when U_g became greater than 0.10 m/s. Contrary to the study by Luo et al. (1997) h was observed to decrease significantly with increasing pressure (on the order of 30%). Generally, h increases with increasing ε_s at relatively low pressures: the effect of ε_s was greatest at ambient pressure but insignificant between 0.20 and 0.35 vol. %. Increasing the temperature cause a significant increase in the heat transfer coefficient (+48%) corresponding to a decrease in μ_l of 78%. The correlation proposed for the results of this study is presented in Equation (50).

$$\frac{h}{\rho_{sl} C_{p,sl} U_g} = 0.037 \left[\left(\frac{U_g d_b \rho_{sl}}{\mu_{sl}} \right) \left(\frac{U_g^2}{g d_b} \right) \left(\frac{C_{pl} \mu_l}{k_l} \right)^{1.87} \left(\frac{\varepsilon_g}{1-\varepsilon_g} \right) \right]^{-0.22} \tag{50}$$

The same research group has studied heat transfer and hydrodynamics using a 2D transparent Plexiglas column (50 cm wide, 1.2 cm deep, and 220 cm high) (Lin and Hung-Tzu, 2003; Lin and Wang, 2001). The gas flow rates were on the order of 0 to 4 cm/s while the liquid velocity was zero. The flow patterns were studied using a high speed camera as well as non-invasive PIV system and less than < 0.1% neutrally buoyant Pliolite particles (200 – 300 μm) as a liquid tracer. The heat flux probe used was the same as that described above. The lowest heat transfer coefficients were measured in the descending region near the sidewalls in the dispersed bubble flow regime (U_g < 1 cm/s) due to the relative absence of bubbles. In the coalesced bubble flow regime the radial heat transfer coefficient was relatively flat in the central region and reached a maximum of 12.5 cm away from the sidewall (1 < U_g < 3 cm/s) before decreasing again at the wall. Finally, for even higher gas flow rates (> 3 cm/s) an increased rate of descent in liquid at the walls resulted in improved transfer.

2.2.11 Field and coworkers

Field and Rahimi (Field and Rahimi, 1988b) and Lewis et al. (1982) studied heat transfer in a gas-liquid bubble column which was 1.5 m high with an inner diameter of 0.29 m. Sailcloth was placed on the perforated plate distributor to increase the pressure drop and ensure a more uniform distribution of gas. The systems studied included air-water, nitrogen-cumene, and nitrogen-glycol. Typical gas velocities varied from 0.01 to 0.18 m/s, bulk bed temperatures from 5 to 82°C, and fluid viscosity from 0.00038 to 0.023 Pa·s. Liquid velocity in all the experiments was zero. The heat transfer probe was inserted vertically or horizontally (see Figure 11) and the dimensions varied (length from 10 – 150 mm and diameter from 20 – 50 mm). Experiments indicated that the radial variation in ε_g was small but increased slightly with vertical distance while the variation in h showed exactly the opposite trend. Equation (51) presents the so-called Cambridge model proposed by Field and Rahimi (1988b). It is an adaptation of the correlation derived by Lewis et al. (1982) although the thermal boundary layer thickness (δ_T) is not taken as laminar sub-layer thickness (δ) and takes into account aspects of the Ruckenstein and Smigelshi model. The model considers heated surface and by unsteady-state diffusion to liquid packets and is only applicable to inviscid systems (i.e. μ_l < 0.004 Pa-s).

$$h = \left[\frac{\delta_T}{k_l} + \left\{ \frac{\pi L_c}{4 k_l \rho_l C_{pl} U_c} \right\}^{1/2} \right]^{-1} \tag{51}$$

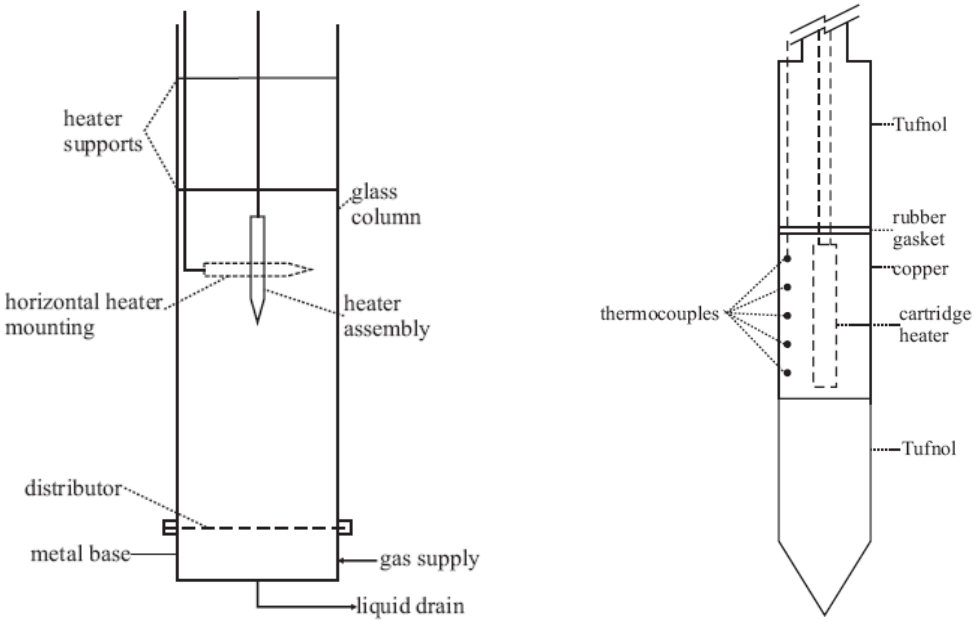

Figure 11. The column and heat transfer probe employed by Lewis et al. (1982).

where $\delta_T = 0.045 + 1.08\mu_l$, L_c is the characteristic vertical dimension, and U_c is the average circulation velocity which is considered a key parameter for both axial dispersion and heat transfer and is given by Equation (52):

$$U_c = 1.36\left[gH_0 \left(U_g - \varepsilon_g U_{slip}\right)\right]^{0.33} \tag{52}$$

where H_0 is the static bed height and U_{slip} is the bubble slip velocity. For high U_g the first term on RHS increases in importance, which forces h to tend to a constant value – something which the correlation of Deckwer (1980) and other similar correlations fail to predict. The correlation fits the presented data to ±20%.

2.2.12 Wild and coworkers

The study of Nore et al. (1992) was conducted in Plexiglas column that was 0.10 m i.d. and 2 m high. The twenty-three pressure taps installed were equipped with capillaries to reduce the manometer level fluctuations. The liquid used consisted of 4 wt. % NaCl entered the column via a 25 cm high calming section filled with 0.01 m Raschig rings before passing through a perforated plate distributor. Polypropylene particles were embedded with mica particles to create particles with densities ranging from 1130 to 1700 kg/m^3. The fluidization gas was either air or nitrogen. The heat transfer was measured using a self-heating thermistor

probe (2.7 mm o.d.) protected by an epoxy shell. The typical temperature difference (ΔT) was between the probe and the bed was 1 – 3 K: it required approximately 2 s to reach steady state. The probe surface temperature was obtained by measuring the electrical resistance. In all cases, increasing the superficial gas velocity (U_g) increased h especially at relatively low U_g and small particle diameters. The authors correlated their data using Equation (53) and reported an accuracy of ±25%.

$$h = 32300\left(\frac{U_l}{\varepsilon_l}\right)^{0.15} U_g^{0.21} d_p^{-1.5} \tag{53}$$

Del Pozo et al. (1994) and Briens et al. (1993) studied heat transfer in 0.08 m i.d. column using the same heat transfer thermistor probe as that used by Nore et al. (1992). Five different liquids were tested (pure deionized water, 0.5 wt. % NaCl solution, 5 wt. % NaCl solution, 5 wt. % NaCl and 100 wppm benzoic acid, and 5 wt. % NaCl and 25 wppm tert-amyl-alcohol). In every experiment 2.44 kg of 3 mm glass beads was added to the column. The gas enters the column via a four-arm sparger at 0.06 to 0.09 m/s while the liquid entered the column via perforated plate at 0 to 0.085 m/s. A 0.08 m high calming section of 0.019 m ceramic saddles was included just below the distributor plate. The experiments revealed that the effect of salt and surfactants in the three-phase systems were different from that observed using two-phase systems. Contrary to many other studies, the present study observed a decrease in ε_g with increasing salt concentration. The gas hold-up increased with addition of tert-amyl-alcohol but decreased with addition of benzoic acid. The results were interpreted as indicating that salt and surfactants may affect small (U_{slip} < 0.4 m/s) and large bubbles (U_{slip} > 0.5 m/s) differently. The largest heat transfer coefficient was obtained for the 0.5 wt. % NaCl solution and smallest for the pure water system. Not only was no correlation found between mass and heat transfer but salt tracer studies indicated negligible liquid back-mixing as well.

Dhaouadi et al. (2006) performed their heat transfer study using a circulating fluidized bed with a 0.10 m i.d. riser that was 3 m high and equipped with a gas sparger. The three phase system consisted of air (U_g < 0.10 m/s), water, and glass beads (d_p = 90 μm and Θ_s = 3 – 7 vol. %) system. Bubble rise velocity and frequency was measured using an ultrasound probe. The heat transfer probes had an outside diameter of 15 mm o.d. and was installed horizontally (Figure 12 shows the relative locations of the probes while Figure 13 shows the probe in greater detail). The probe consists of a central brass core (5 mm o.d.) wrapped with a 1 m of heating resistance (1 mm o.d.) that consumed 12 – 500 W at 12 – 80 V. Surrounding the core is an interstitial mix of 50 μm copper

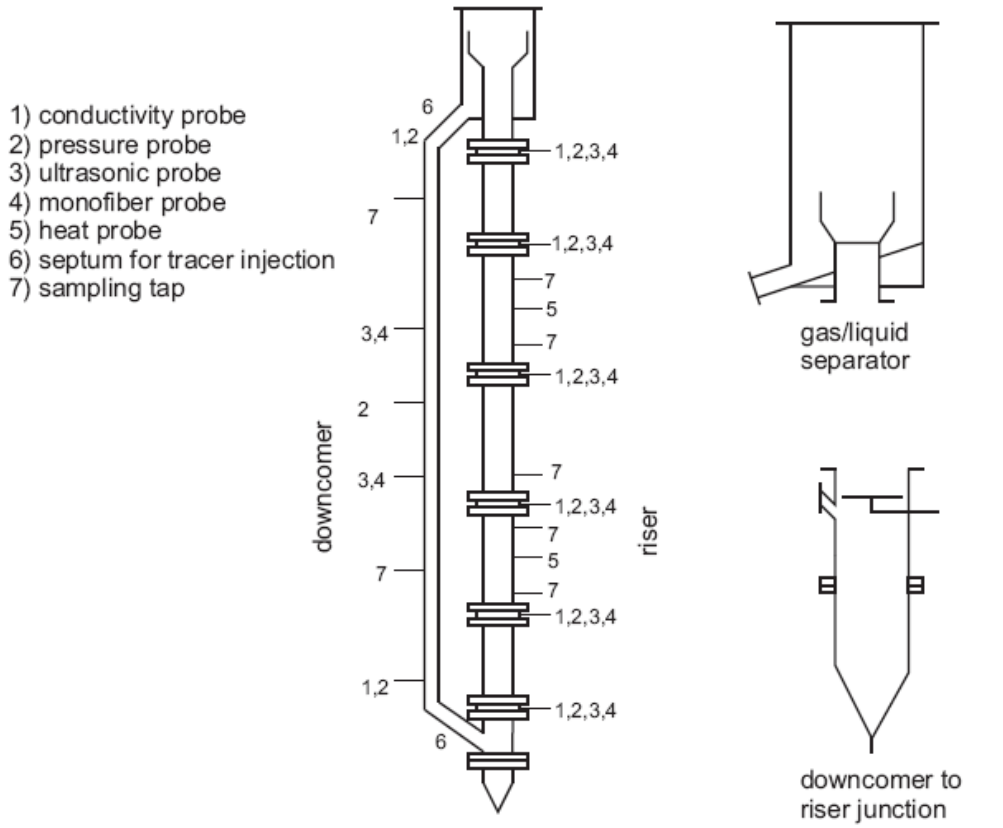

Figure 12. Circulating fluidized bed apparatus of Dhaouadi and coworkers (after Dhaouadi et al., 2006).

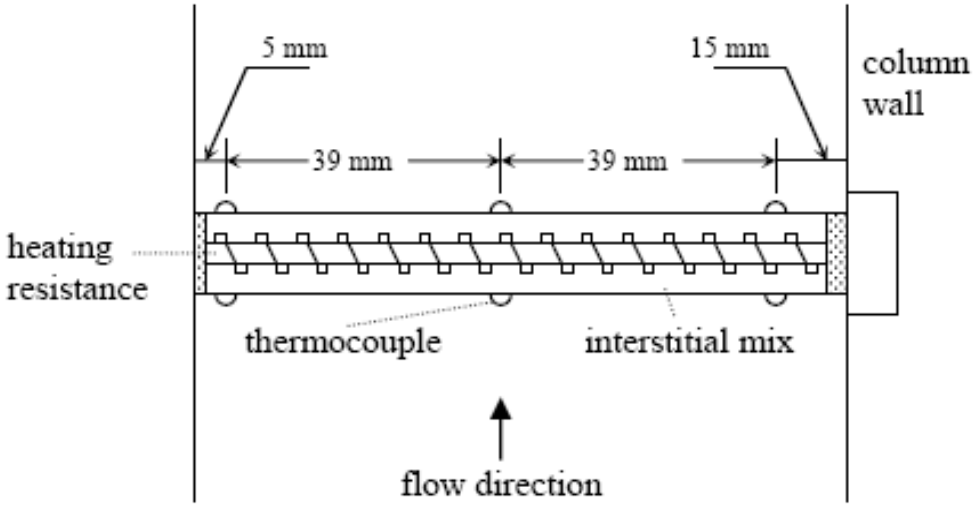

Figure 13. Horizontal heat transfer probe used by Dhaoudi and coworkers (after Dhaouadi et al., 2006).

particles, water, and a wetting agent. The solids hold-up was determined using the so-called Wenge method: the feed gas supply is shut off and the resulting pressure drop profile with respect to time recorded (refer to Figure 14).

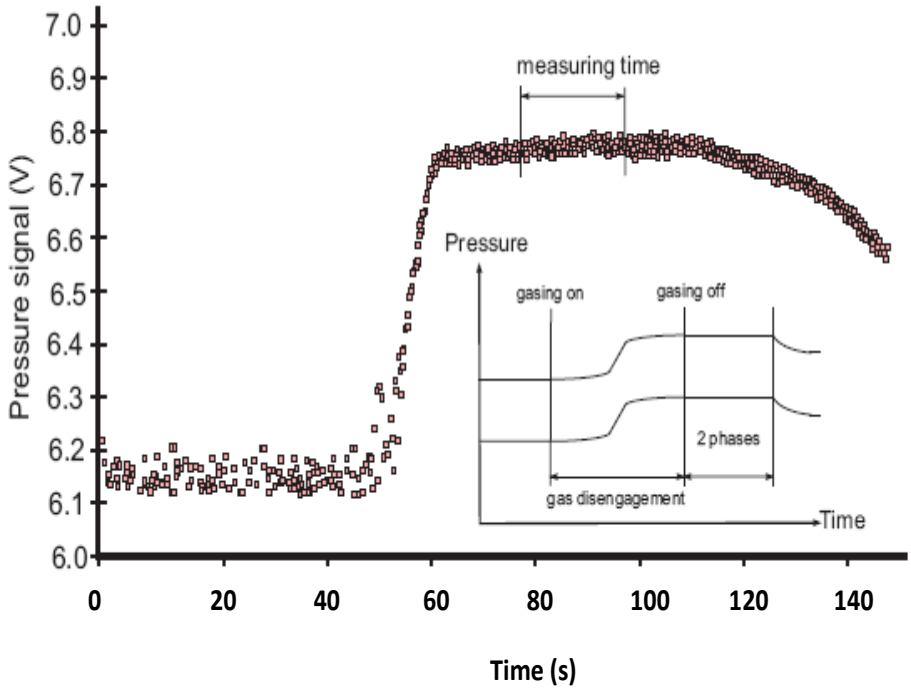

Figure 14. Illustration of the Wenge method for determining ε_s (after Dhaouadi et al., 2006).

The recorded pressure drop will initially increase before stabilizing for a period of 10 to 20 s during which time the solids hold-up may be calculated according to Equation (54):

$$\varepsilon_s = \frac{\rho_l}{\rho_l - \rho_g}\left(1 - \frac{\Delta P}{\Delta P_0}\right) \tag{54}$$

the gas phase hold-up is then given by Equation (55):

$$\varepsilon_g = 1 - \frac{\Delta P}{\Delta P_0} + \varepsilon_s\left(\frac{\rho_s - \rho_l}{\rho_l}\right) \tag{55}$$

where ΔP_0 is the baseline pressure prior to the interruption of the gas supply. The authors report that h was found to decrease with increasing solids concentration and increase with increasing gas velocity. Their correlations (only validated for

their system) for the homogeneous and heterogeneous regimes are presented as Equations (56) and (57), respectively:

$$h = 26090 U_{gr}^{0.48} \tag{56}$$

$$h = 15950 U_{gr}^{0.33} \tag{57}$$

where U_{gr} is the superficial gas velocity in the riser expressed in m/s.

2.2.13 Prakash and coworkers

Numerous studies have been conducted by Prakash and coworkers using a column 0.28 m i.d. and 2.4 m high under ambient conditions in semi-batch mode (i.e. U_l = 0): Figure 15 shows a the typical experimental setup used. The parameters studied in regards to their effects on heat transfer and hydrodynamics include high solids concentration (Li and Prakash, 1997), micron sized particles (Li et al., 2003), particle type (i.e. yeast cells) (Prakash et al., 2001), and flow patterns (Li and Prakash, 1999; 2002; 2001). Another study at high pressures was conducted in a 0.16 m i.d. and 2.5 m high column (Wu et al., 2007). The majority of these studies employed air, water, and 35 μm glass. The column was equipped with a six-arm gas sparger, an electric heater which maintained the bed temperature at approximately 296 K, and several pressure taps with purge meters. Several copper-constantan thermocouples sheathed in stainless steel were employed to measure the bulk fluid temperature. The typical data acquisition rate was on the order of 50 Hz.

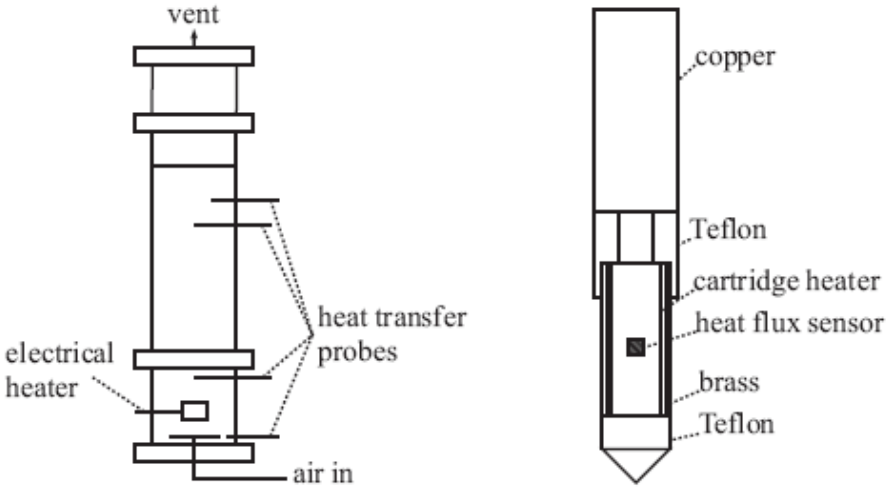

Figure 15. Column and heat transfer probe used by Prakash et al. (after Prakash et al., 2001).

The local instantaneous heat transfer measurements were carried out using a specially designed microfoil heat flow sensor measuring 2.54 x 1.91 x 0.4 cm. The sensor consists of 2 foil-type thermocouples bounded to both sides of a known thermal barrier and measures the heat flux and surface temperatures with a fast response time (0.02 s). The local heat flux is proportional to the difference in temperature across the thermal barrier and is obtained directly from the output voltage of the sensor. Figure 15 shows the heat flux sensor mounted flush on the surface of a brass cylinder (11 mm o.d. by 150 mm long) inside of which is located the cartridge heater. The position of heat transfer probe was adjustable in the radial direction and could be used to study bubble passage in the column.

Quantitative analysis of the instantaneous h versus time graphs was accomplished by deriving a peak fitting method which gives the average peak area and peak height distribution (Li and Prakash, 1999). Generally, peak height and area are increasing functions of U_g and are indicative of the level of turbulence and the intensity of the heat transfer. The three-phase system showed a reduction in "peak intensity" (but an increase in the baseline value) compared to an air-water system indicating that the solid particles decreased the turbulence intensity of the bubble wakes. In terms of solids concentration, both the peak height and area decrease when solids were initially added (ε_s = 5 vol. %), increased with increasing ε_s (5 to 20 vol. %). When ε_s > 20 vol. % the peak height increased only slightly while the peak area decreased.

Further study of the heat transfer coefficients indicated the existence of four main "mixing" regions consisting of (from bottom to top): a distributor region, a developing region, a bulk region, and a disengagement region. Plots of the instantaneous heat transfer coefficient versus time revealed that the h baseline value and variance were 30 – 80% (Li and Prakash, 2001) higher in the central bulk region of the column, while less variance was observed at the wall and in the developing and disengagement regions (Li and Prakash, 1997; 2002). These differences were attributed to the mixing behaviour in these regions (e.g. due to the presence of larger and faster bubbles in the central bulk region and primarily jets in distributor region, hence the bubble wakes are not yet fully formed) with the difference increasing with increasing U_g (Li and Prakash, 2002). The radial h profiles were similar in the distributor, developing, and disengagement regions indicating similar mixing behaviour. Radial profiles of the heat transfer coefficient in the bulk region were similar for U_g > 0.1 m/s and when ε_s = 20 vol. % the radial profiles were similar at all values of U_g, thereby indicating that the onset of heterogeneous flow regime begins at lower U_g in the presence of solids (Li and Prakash, 2002). Furthermore, the radial h profiles agree with observed liquid velocity profiles (highest in the middle and decreasing towards the walls; however, U_l is lowest at $r/R_c \approx 0.7$ but h is lowest right at wall). The heat transfer probe was also used to determine liquid flow direction and estimate U_l and

indicated that at high U_g most of column was occupied by large-scale liquid circulation cell (liquid rising in the middle and descending at the wall). Li and Prakash (2002) proposed a phenomenological mixing model summarized as follows:

- the distributor region is well-mixed (especially at high U_g) and dominated by jets and bubble formation; h is low indicating relatively poor mixing and exchange rates,
- the developing region has a better mixing rate (indicated by higher h) dominated by bubble wake formation; downward flowing liquid entrained into upward flowing region (reducing exchange below at the distributor)
- bulk region characterized by large radial variation but small axial variation in h consisting of up-flowing central core and downward flowing annular region,
- as U_g increases the bulk region extends lower,
- the core and annulus may be modeled using plug flow with axial dispersion term,
- exit region assumed to be well mixed.

Li and Prakash (1997) investigated the effects of high solids concentrations (up to 40 vol. %) on the gas hold-up and heat transfer coefficient. The gas superficial velocity was varied between 0.05 and 0.35 m/s. The gas hold-up was reported to increase with increasing U_g for all solids concentrations studied. For a given U_g, ε_g initially was observed to decrease relatively quickly with increasing ε_s. The rate of decrease slowed as ε_s reached approximately 20 vol. % indicating the presence of a fairly stable bubble size (a slight increase was noted at ε_s > 30 vol. %). The effect of ε_s on ε_g was associated with an increase in d_b due to an increase in the apparent slurry viscosity in the presence of fine solids. This would cause the gas hold-up to decrease as a result of the increased bubble rise velocity. Fine particles may also hinder bubble break-up by dampening the turbulence intensity (Li and Prakash, 1997). The instantaneous h peak values were higher for 20 vol. % slurry than for a 5 vol. % slurry while the baseline value decreased with increasing ε_s in both bulk and distributor regions (the rate of decreases levels of above 20 vol. %). The average heat transfer coefficient increased with increasing U_g (before levelling off at U_g = 0.20 m/s). Based on these observations, the authors recommend that no internal heat transfer surfaces be placed in the wall region (r/R_c = 1 to 0.75) and that the column operate in the heterogeneous flow regime to achieve higher heat transfer rates (Li and Prakash, 2002; 2001).

The substitution of yeast cells in place of the solid particles drastically altered the slurry bubble column behaviour – mostly attributed to changes in the bubble characteristics (Prakash et al., 2001). The three-phase system had a high

foaming tendency (foam formation increases ε_g due to an accumulation of small bubbles). The foam layer was reduced at higher U_g. The measured h values were higher in the bulk region than in foam region. It was also observed that the ε_g estimated from ΔH_{bed} method were generally higher than the values estimated using ΔP method. Furthermore, the large bubble rise velocities were higher here than for air-water-glass bead system at similar ε_s. It was proposed that the contribution to ε_g of ε_s due to large bubbles decreases while the contribution from small bubbles increases. Addition of yeast cells increased h in the centre, decreased it at the wall in bulk and developing regions.

Prakash et al. (Li and Prakash, 2001; 2001) based on their work, developed the following model for determining the heat transfer coefficient based on the film and surface renewal model:

$$h = \frac{2k_{sl}}{\sqrt{\pi\alpha\theta_c}} + \frac{k_{sl}\delta}{\alpha\theta_c}\left\{\left[1 - erf\left(\frac{\sqrt{\alpha\theta_c}}{\delta}\right)\right]\exp\left(\frac{\alpha\theta_c}{\delta^2}\right) - 1\right\} \tag{58}$$

where h is in kW/m^2K, $\alpha = k_{sl}/\rho_{sl}C_{p,sl}$, δ is the film thickness, and θ_c is the contact time of the fluid element. The latter two parameters are given by Equations (59) and (60), respectively:

$$\delta = \frac{1.25 d_{tube}}{\left(\frac{\rho_{sl} U_b d_{probe}}{\mu_{sl}}\right)^{0.5}\left(\frac{C_{p,sl}\mu_{sl}}{k_{sl}}\right)^{0.33}} \tag{59}$$

$$\theta_c = \left\{\frac{\mu_{sl}}{U_g \rho_{sl} g}\right\} \tag{60}$$

Prakash and coworkers (Li et al., 2003) reported h increased with decreasing particle size (d_b increases for decreasing d_p). The effect is most significant in the bulk region than at the wall (region dominated by back flow circulation created by radial gradient in ε and not by bubble wake). The heat transfer coefficient decreased with increasing ε_s (the effect decreases at $\varepsilon_s > 10$ vol. % or with slurries of relatively fine particles). Again, h increased with increasing U_g in both centre and wall region for all d_p. It was determined that h values were lower in slurries of fine glass particles than for g-l systems and this was attributed to turbulence intensity reduction due to apparent increase in viscosity even though d_b increases with increasing μ_l. The radial profile, correlated by Prakash et al. as Equation (61) (Li and Prakash, 2001), widens when

d_p decreases and at relatively high U_g and ε_s the radial profile is flat up to half the column diameter (the effect of d_p is smaller at low U_g):

$$\frac{h(r)-h_w}{h_w} = 0.217\left[1 \quad \left(\frac{r}{R_c}\right)^{0.2}\right] \tag{61}$$

where h(r) is the heat transfer coefficient at the radial position r and h_w is the heat transfer coefficient at the wall. It should be noted that the above equation is applicable for $\varepsilon_s < 10$ vol. % and that the coefficient is dependent on d_p.

In the most recent study from Prakash and coworkers they studied the effect of high pressure on heat transfer coefficients in a gas-liquid bubble column using air and water (Wu et al., 2007). For this study a perforated plate distributor was used and the column was constructed of stainless steel. Before each experiment the static liquid height was varied in order to maintain a constant dynamic bed height. It was reported that pressure has significant effect on column hydrodynamics. As the pressure increases, ρ_g increases which caused the initial bubble size (d_{b0}) to decrease and increases the rate of bubble break-up which decreases the overall bubble size and bubble size distribution. Increasing the pressure (0.1 – 1 MPa) resulted in a decrease in the measured heat transfer coefficient at both the wall and in the centre of the column. From this it would appear that bubble size is a dominant factor in determining the heat transfer rate and that the positive effect due to increasing bubble number is not as strong as the negative effect of decreasing bubble diameter (Wu et al., 2007). The decrease in h due to the increase in pressure was more pronounced at low U_g. Finally, the radial profile of h was observed to flatten as P increased.

2.2.14 S.D. Kim and coworkers

A number of studies on heat transfer involving gas-liquid, liquid-solid, and gas-liquid-solid have been conducted by S.D. Kim and coworkers. Most of these studies were conducted in a 3 m high and 0.152 m i.d. column. The cone shaped heater used in all studies was 0.03 m o.d. and 0.356 m long and coaxially located with the tip touching the distributor (see Figure 16). Four iron-constantan thermocouples encased in stainless steel sheaths were located at different radial locations 0.20 m above the distributor to measure the bed temperature while four thermocouples were flush mounted to the heat transfer surface. The typical temperature difference between the probe surface and the bed was 2.75 to 3.89 K (Kang et al., 1991). Air, entering the column via a sparger, was used in all studies as the gas phase while glass beads (d_p = 1.7 to 8 mm) were used for the solid

phase. Typically, the gas and liquid velocities varied from 0 – 0.14 m/s and 0.02 to 0.09 m/s, respectively.

Kang et al. (1991) employed water as the liquid phase in their study. Measurements indicating a steep radial temperature profile at the heater surface were interpreted as two resistances in series (i.e. heater boundary layer and the bed proper). It was later determined that the bed resistance accounts for less than 10% of overall resistance. As U_l was varied, h adjacent to the heater exhibited a maximum and the boundary layer thickness exhibited a minimum. This corresponded with a maximum axial particle dispersion coefficient (i.e. enhanced particle motion led to erosion of the thermal boundary layer). The boundary layer was found to be thinner for relatively larger particles. The data was correlated using two approaches based on the modified and standard Colburn-Chilton j-factors (Equations (62) and (63), respectively). The correlation coefficients (r^2) were 0.988 and 0.954, respectively.

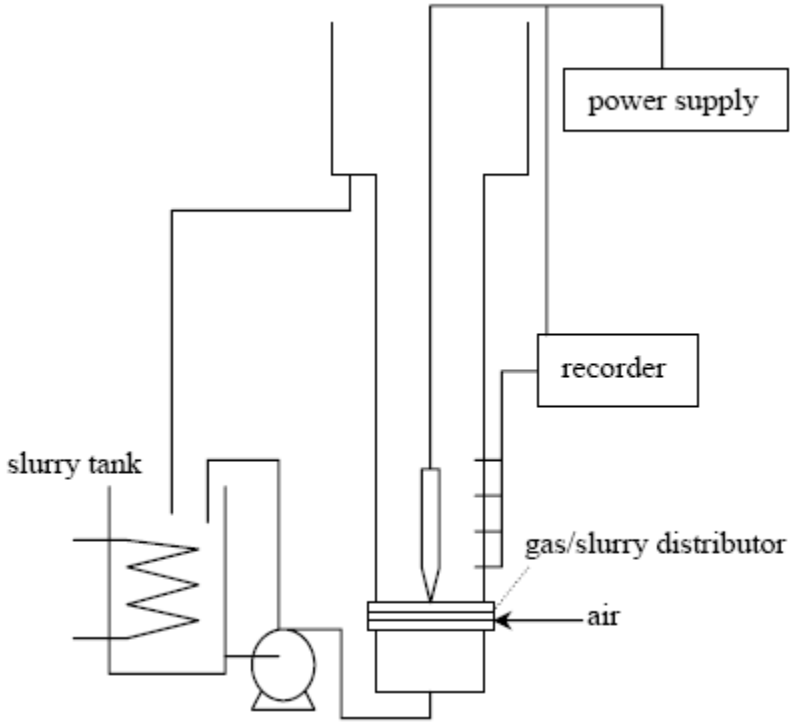

Figure 16. Column and heat transfer probe used by Kim et al. (after Kim et al., 1987).

$$j'_H = \left(\frac{h\varepsilon_l}{\rho_l C_{pl} U_l}\right)\left(\frac{C_{pl}\mu_l}{k_l}\right)^{2/3} = 0.191\left(\frac{d_p U_l \rho_l}{\mu_l (1-\varepsilon_l)}\right)^{-0.310} \quad (62)$$

$$j_H = \left(\frac{h\varepsilon_l}{\rho_l C_{pl} U_l}\right)\left(\frac{C_{pl}\mu_l}{k_l}\right)^{2/3} = 0.021\left(\frac{d_p U_l \varepsilon_l}{D_p\left(1-\varepsilon_l\right)}\right)^{-0.453} \tag{63}$$

In two studies by Kim et al. (1987; 1986) a slurry consisting of pulverized bituminous coal (< 150 μm) in mineral oil (at 1, 6, or 10 wt. %) or in kerosene (at 17.5 wt. %) was employed as the "liquid" phase. The slurry viscosity ranged from 0.001 to 0.028 Pa·s and the slurry viscosity was varied between 0.03 and 0.12 m/s. The heat transfer coefficient generally increased with increasing U_g and d_p but decreased with increasing μ_l and goes through a maximum with increasing U_{sl} (at relatively high U_{sl}, the increase in h with increasing U_g is negligible). It was observed that the bed porosity corresponding to the maximum h decreased with increasing d_p but increased with increasing μ_l. The data was correlated using Equation (64) ($r^2 = 0.95$):

$$h = 0.072\left(k_{sl}\rho_{sl}C_{pl}\right)^{0.5}\left\{\frac{\left[\left(U_{sl}+U_g\right)\left(\varepsilon_s\rho_s+\varepsilon_{sl}\rho_{sl}+\varepsilon_g\rho_g\right)-U_{sl}\rho_{sl}\right]g}{\varepsilon_{sl}\mu_{sl}}\right\}^{0.25} \tag{64}$$

Suh et al. (1985) also derived an equation similar to Equation (64) with a leading coefficient of 0.065.

Different shapes (cubic, cylindrical, or hexagonal) and sizes of floating bubble breakers were investigated by Kim et al. (1990) using a 0.142 m i.d. by 2 m high column. The bubble breakers were made of acrylic resin and were with varying amounts of lead and paraffin (for densities ranging from 1500 to 1800 kg/m^3): the volume ratio of bubble breaker to particle (V_f/V_s) ranged from 1 to 0.25. Similar to the other studies, h increased with U_g and was greatest for hexagonal shaped bubble breakers (the maximum h being 30% higher than in the corresponding system without breakers). The optimum V_f/V_s ratio was found to be 0.15. The heat transfer increased with increasing contact angle, increasing breaker density, and projected area of the bubble breaker. Kim et al. (1990) proposed Equation (65) to correlate their data ($r^2 = 0.92$):

$$h = 0.0685\left(k_l\rho_l C_{pl}\right)^{0.5}\left\{\frac{\left[\left(U_l+U_g\right)\left[\left(1-x\right)\varepsilon_s\rho_s+\varepsilon_l\rho_l+\varepsilon_g\rho_g\right]-U_l\rho_l\right]g}{\varepsilon_l\mu_l}\right\}^{0.25} \tag{65}$$

where $x = \dfrac{V_f/V_s}{1+V_f/V_s}$.

Equations (66), (67), and (68) (with correlation coefficients of 0.92, 0.96, and 0.94, respectively) were derived from a study using CMC solutions to study the effect of viscosity (0.001 to 0.039 Pa·s) on the heat transfer coefficient (Kang et al., 1985).

$$h = 2290 U_g^{0.10} U_l^{0.05} \mu_l^{-0.18} d_p^{0.04} \tag{66}$$

$$\frac{h d_p \left(1-\varepsilon_s\right)}{k_l \varepsilon_s} = 0.036 \left(\frac{C_{pl}\mu_l}{k_l}\right)^{0.65} \left(\frac{d_p \rho_l \left(U_g + U_l\right)}{\mu_l \varepsilon_s}\right)^{0.81} \tag{67}$$

$$\left(\frac{h}{\rho_l C_{pl} \sqrt{U_l U_g}}\right) \left(\frac{d_p \rho_l \left(U_l + U_g\right)}{\mu_l \varepsilon_s}\right)^{0.11} \left(\frac{C_{pl}\mu_l}{k_l}\right)^{0.33} \log\left(7.58\right) = 0.72 \left(\varepsilon_l \quad \varepsilon_g\right) \tag{68}$$

Cho et al. (2001) have studied heat transfer from the wall to an air-water-glass bead (d_p = 2.1 mm) system using a circulating fluidized bed (CFB) operating at ambient temperature and pressure. The riser diameter was 0.102 m and was 3.5 m high. The heater probe was 0.03 m o.d. and equipped with 5 thermocouples with the cone-shaped lower end placed directly on the gas-liquid distributor (see Figure 17). The gas and liquid velocities were varied between 0.01 to 0.07 m/s and 0.25 to 0.33 m/s, respectively, while the solids mass flux was varied between 2 and 8 kg/m^{2}s. The heat transfer measurements and temperature fluctuations were analyzed using the mutual information function, phase space portraits, and Shannon entropy. The heat transfer coefficient increased with increasing U_g and M_s, but did not change significantly with U_l. The h values measured in the CFB were found to be slightly greater than those of a conventional three-phase fluidized bed. Their data was correlated as given by Equation (69):

$$h = 2776 U_g^{0.0799} U_l^{0.0317} M_s^{0.0654} \tag{69}$$

where M_s is the mass flux of solids in kg/m^2.s.

A similar study to that described above was performed by Cho et al. (2002) in a gas-liquid bubble column (0.152 m i.d. by 2.5 m high) while varying the gas velocity (0 to 0.12 m/s), pressure (0.1 to 0.6 MPa), and liquid viscosity (1 to 38 mPa·s). The authors reported that h increased with increasing pressure (which caused d_b to decreases thereby increasing ε_g which increases turbulence which increases h) and U_g. However, it was observed that the fluctuations in the measured h and ΔT values decreased with increasing pressure. The correlation dimension increased with increasing U_g (i.e. indicating increased level of chaos

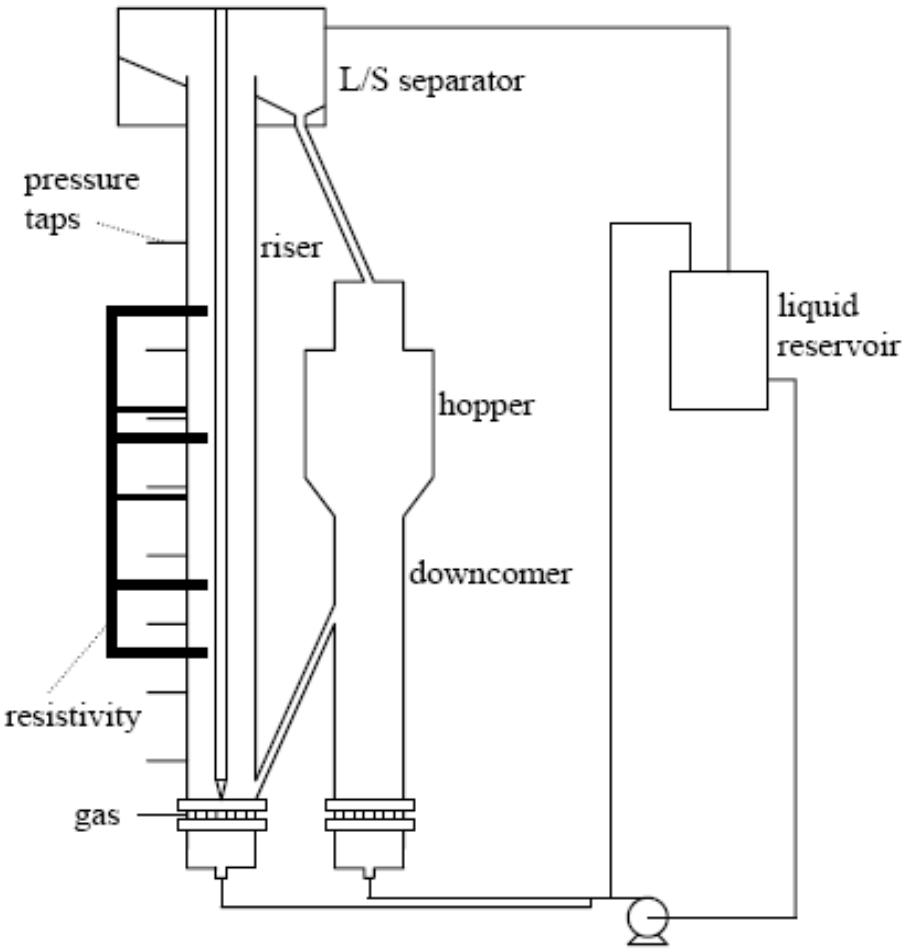

Figure 17. Circulating fluidized bed utilized by Cho and coworkers (after Cho et al., 2001).

and non-homogeneity) and decreased with increasing P (i.e. indicating decreased level of chaos and non-homogeneity). The heat transfer coefficient decreased gradually with increasing μ_l. This was associated with a decrease in the fluctuations of the measured h values. The following correlation ($r^2 = 0.974$) was proposed based on acquired data:

$$h = 11710 U_g^{0.445} \mu_l^{-0.060} P^{0.176} \tag{70}$$

where the liquid viscosity μ_l is in mPa.s and the pressure P in MPa. It was determined that the predictability of h improved with increasing P or decreasing μ_l.

2.2.15 Nishikawa and coworkers

Both cooling coils (1 cm o.d. by 31 cm high helical shape) and wall jacket heat exchanger (15 cm high) were studied by Nishikawa et al. (1977) using 5.1 and 15 cm i.d. columns. The liquids studied include water, millet jelly solutions, and glycerine solutions. The superficial gas velocity was varied between 0.0056 and 0.56 m/s while the liquid velocity was nil. Both columns were 180 cm high and were equipped with 8 and 10 thermocouples, respectively. Air and liquid entered via a common single nozzle (3 cm i.d.) located flush at the bottom of the column. The heat transfer coefficient was obtained by quantifying the amount of steam condensed or by measuring the inlet and outlet temperatures of the bed and coils. The correlation derived is reported to be suitable for either wall or internal heat transfer (Nishikawa et al., 1977):

$$\left(\frac{h}{\rho_l C_{pl}}\right)\left[\frac{\rho_l^2}{\mu_l g\left(\rho_l-\rho_g\right)}\right]^{1/3}\left(\frac{C_{pl}\mu_l}{k_l}\right)^{2/3}\left(\frac{\mu_w}{\mu_l}\right)^{-0.05}=a \qquad (71)$$

where a is determined according to Table 5:

Table 5. RHS components of Equation (71) (from Nishikawa et al., 1977).

A	U_l (m/h)	U_g (m/h)
$0.054U_g^{1/4}$	< 54	< 1000
0.3	< 54	> 1000
$0.054U_g^{1/4}\left(U_l/54\right)^{1/4}$	> 54	

The units reported are as follows: h (kcal/m^2·h·°C); μ_l and μ_w (kg/m·h); g (m/h^2); C_{pl} (kcal/kg·°C); k_l (kcal/m·h·°C); U_g (m/h).

2.2.16 Michael and Reichert

The study by Michael and Reichert (1981) utilized an 65 mm long electrically heated 19 mm o.d. copper tube located in a 10 cm i.d. (150 cm high) column. Liquids studied included n-heptane, cyclohexane, toluene and Excol D80. The gas phase used was ethylene gas while polyethylene (0 to 34 wt. % in Exsol D80) served as the solid phase in certain studies. Gas velocities ranged from 0.9 to 12 cm/s. Results indicated that the type of distributor (porous plate or sparger) had no effect on the heat transfer coefficient. However, h was observed to increase with increasing U_g (approaching an asymptotic value at high velocities). The heat transfer coefficient decreased with increasing solids concentration and d_p when Θ_s

> 16 wt. %. It was reported that increasing Θ_s increased the apparent liquid viscosity and that this effect decreased as the particle size increased. Equation (72) gives the correlation derived by Michael and Reichert (1981):

$$\frac{h}{\rho_{sl}C_{p,sl}U_g} = 0.12\left[\left(\frac{\rho_{sl}U_g d_b}{\mu_{sl}}\right)\left(\frac{U_g^2}{gd_b}\right)\left(\frac{\mu_{sl}C_{p,sl}}{k_{sl}}\right)^2\right]^{-0.25} \tag{72}$$

where ρ_{sl}, $C_{p,sl}$, and k_{sl} where calculated using Equations (10), (11), and (12), respectively. For liquid hydrocarbon systems (i.e. without solids) the leading coefficient becomes 0.11.

2.2.17 Kubie

Kubie (1975) conducted studies in a small column (dimensions not reported) to investigate the heat transfer mechanism two-phase gas-liquid bubbling flow. This was simulated using single gas nozzle (0.8, 1.6, 2.8 mm i.d.) to generate continuous stream of discrete bubbles into a stationary liquid. The heat transfer probe consisted of an electrically heated thin platinum wire (4.45 mm long stretched between 2 copper plates), which could reportedly detect the difference between conductive and convective heat transfer (see Figure 18). The probe designed also allowed the measurement of the bubble passage frequency. The gas phase consisted of air, while water, n-heptane, or 50 wt. % aqueous glycerol served as the liquid phase. It was reported that the choice of liquid had little effect on the measured heat transfer; however, the wire diameter had a significant effect with the thinnest wire having greatest sensitivity. To analyze the results Kubie (1975) employed the surface renewal and penetration theory. It was determined that the bubble wakes were primarily responsible for the surface renewal and that transient conduction was responsible for 75% of total heat transfer. Furthermore, in order to maximize heat transfer the bubble frequency should be maximized: to achieve this bubble size should be minimized. It appears that the relatively small increase in h due to larger wakes generated by faster rising relatively larger bubbles was outweighed by the negative effects of increased bubble residence time and decreased frequency.

2.2.18 Khoze and coworkers

Khoze and coworkers have utilized a 120 mm square column equipped with a single horizontal electrically heated copper tube of varying diameter (8, 13, 18 mm o.d.) to measure heat transfer in a two-phase bubble column (Khoze, 1971;Khoze and Scharov, 1977; Tarat et al., 1970). The liquids studied by Tarat et al. (1970) included water, aqueous ethanol (0 – 85 wt. %) or aqueous glycerol

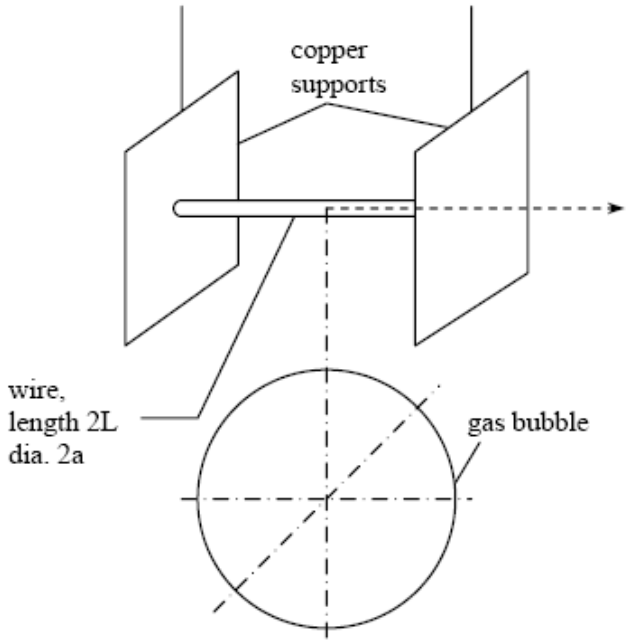

Figure 18. Heat transfer probe used by Kubie (1975).

(0 –60 wt. %) solutions. Air was used for the gas phase. The superficial gas velocity ranged from 0.1 to 2.0 m/s. Six thermocouples measured the bed temperature while 9 were placed flush to the heat transfer surface. The heat transfer coefficient was found to be independent of the tube diameter, while it decreased with μ_l, k_l, and σ_l. The effect of increasing temperature was reported to be insignificant. The data was correlated as Equation (73):

$$\frac{h}{\rho_l C_{pl} U_g} = 0.108\left[\left(\frac{\rho_l U_g^3}{g\mu_l}\right)\right]^{-0.26}\left(\frac{\mu_l C_{pl}}{k_l}\right)^{-0.52} \tag{73}$$

Khoze and Scharov (Khoze, 1971; Khoze and Scharov, 1977) used air and water mixed with either glycerine, sodium oleate, or ethanol. The superficial gas velocity was varied from varied from 0.4 to 4.5 m/s while the temperature of the generated foam ranged from 20 to 50°C. The heat transfer coefficient increased with increasing U_g up to about 3.2 m/s then began to decrease. While h was reported to decrease with increasing υ_l (kinematic viscosity = 0.8 – 4.5 m^2/s) and ethanol concentration (0-93%) it increased moderately with increasing σ_l (30-73 N/m). Khoze and Scharov (Khoze, 1971; Khoze and Scharov, 1977) correlated their data using Equation (74):

$$\frac{h}{U_g C_{pl} \rho_l} = 0.108 \left(\frac{\rho_l U_g d_{tube}}{\mu_l} \right)^{-0.28} \left(\frac{U_g^2}{g d_{tube}} \right)^{-0.26} \left(\frac{\mu_l C_{pl}}{k_l} \right)^{-0.52} \quad (74)$$

2.3 Experimental Investigations in Columns with Multiple Internals

2.3.1 Fair and coworkers

Fair et al. (1962) measured the heat transfer coefficient from the wall in a 0.457 m and a 1.07 m diameter bubble columns to an air-water system at 300 K for liquid velocities of 0.0038 to 0.0050 m/s and gas velocities of 0 to 0.09 m/s. Both columns are illustrated in Figure 19. Heat transfer was determined using the conventional method of recording the electrical energy consumed by the heater. Twenty perforated plates with holes of varying diameter and open area were installed at 0.14 m intervals throughout the smaller column. A reciprocating motion of 1050 cycles per minute was reported to increase the h_w coefficient by 10 – 15% in comparison to the stationary set of baffles. In the larger column, 42 vertical tubes, 0.038 m o.d. by 2.77 m high, were installed – one tube serving as the heater. Bubble flow was observed to be essentially vertical, but liquid temperature measurements indicated a significant degree of liquid back-mixing. Neither the column diameter nor the type of heat transfer surface appears to have significantly influenced the heat transfer. Furthermore, it was determined that the baffles increased the gas holdup by up to 50% (with moving baffles increasing it a further 25 – 30%). In general, mechanical agitation does not significantly increase h in sparged vessels – the bubble action is sufficient to agitate the liquid film at the heat transfer surface (Fair et al., 1962). Based on their results, Fair et al. (1962) proposed the following relationship for determining the heat transfer coefficient.

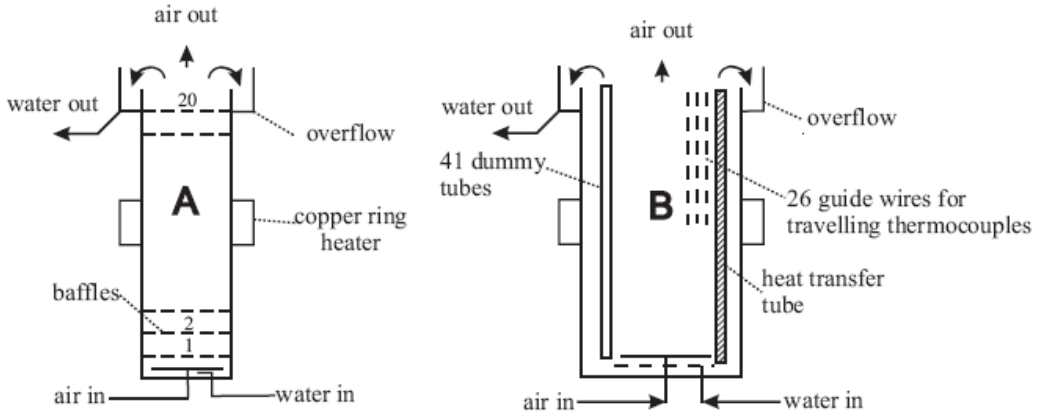

Figure 19. Large and small columns used by Fair and coworkers (after Fair et al., 1962).

$$h_w = 1200 U_g^{0.22} \quad (75)$$

(Note: the units for h_w and U_g are B.t.u/hr.ft^2.°F and ft/s, respectively).

2.3.2 Korte

Korte (1987) performed heat transfer studies testing horizontal and vertical heat transfer tubes in a vertical gas-liquid cylindrical column at ambient pressure and temperatures ranging from 20 or 60 °C. Three different columns of 0.12 m i.d. (4.5 m high), 0.196 m i.d. (6.8 m high) and 0.45 m i.d (6.2 m high) were compared. Air served as the gas phase while pure water, saline water (10% NaCl), glycerine-water (52 wt. % glycerine) or 1,2-propylene-glycol served as the liquid phase. The liquid viscosity and gas velocity was varied from 0.001 to 0.055 Pa·s and up to 1 m/s, respectively. The number of column internals was varied between 1 heat transfer tube and up to 18 "dummy" tubes installed vertically above the perforated plate distributor. Another configuration studied consisted of a horizontal tube bundle, comprising 3 to 5 rows of up to 13 tubes, installed midpoint of the column. Figure 20 illustrates the location of the tubes and the different configurations studied. The heat transfer was measured with an electrical heater acting as a heat flux probe (25 mm in diameter, 150 mm long). Four iron-constantan thermocouples were installed to measure the heat transfer surface temperature. A 15 mm microturbine velocimeter was used to determine fluid velocity profiles through the column.

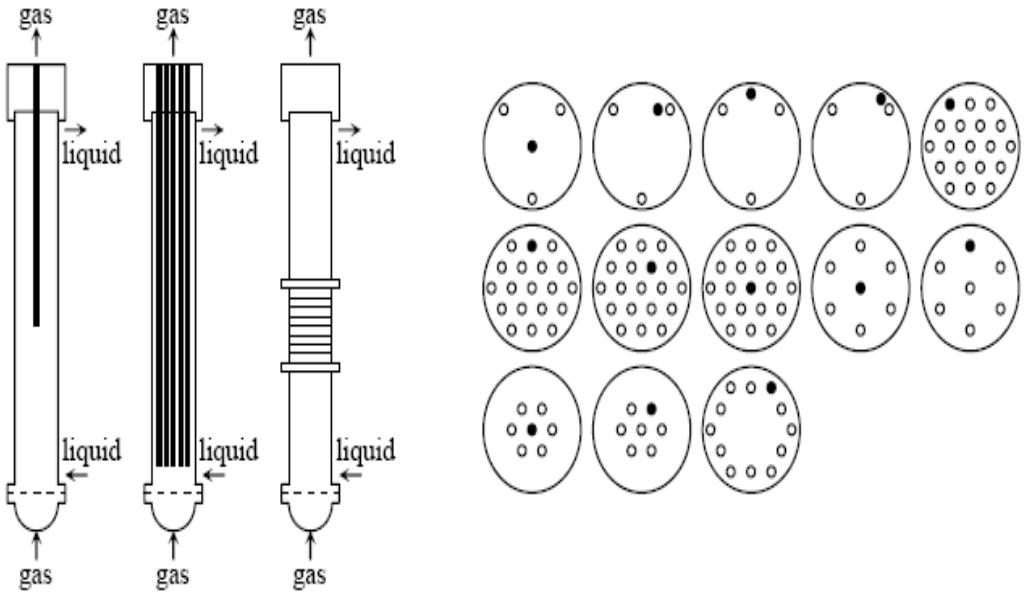

Figure 20. Tube configuration for the studies by Korte (1987).

The thesis presents several correlations including one for calculating the radial profile for the case of a single vertical tube [see Equation (76)] and heat transfer correlations for all configurations studied.

$$V_{lr} = U_l + 0.68 \exp\left[\left(\left|0.76 - \left(r/R_c\right)^{1.69}\right|\right)^{1.54}\right] U_g^{0.39} D_c^{(0.40-0.24r/R_c)} \tag{76}$$

Generally, the effect of U_g on the heat transfer coefficient is significant for $U_g < 0.20$ m/s: the heat transfer coefficient increased with increasing U_g , then approaches an asymptotic value in the stable fluidization region. Furthermore, h increased with decreasing μ_l and was found to be independent of D_c. It was determined that the heat transfer coefficient of the horizontal tube bundle was two times that of the vertical tube bundle. Equations (77) through (80) show the heat transfer coefficient correlation for the horizontal tube bundle. It is expressed as the sum of the single liquid single phase heat transfer coefficient (Nu_{1Ph}) obtained experimentally (or derived from available correlations) and a two phase heat transfer coefficient (N_{2Ph}). The latter is derived from the single tube experiment multiplied by a correction factor (C) that takes into account the liquid physical properties, velocity, and tube configuration (i.e. number of rows, rod diameter and pitch).

$$Nu = Nu_{1Ph} \quad CNu_{2Ph} \tag{77}$$

$$Nu_{1Ph} = \frac{h_{1Ph}\left(\pi/2\right) d_{tube}}{k_l} \tag{78}$$

$$Nu_{2Ph} = \frac{h_{2Ph}\left(\pi/2\right) d_{tube}}{k_l} \tag{79}$$

$$C = 10.2\,\mathrm{Re}_l^{-0.29}\,\mathrm{Pr}_l^{-0.35}\,N_R^{-0.30}\left(\frac{t_{tube}}{d_{tube}}\right)^{0.54} \tag{80}$$

where N_R is the number of tube rows t_{tube} is the tube pitch (m), and Re_l and Pr_l are the liquid Reynolds and Prandtl numbers given by Equation (81) and (82), respectively.

$$\mathrm{Re}_l = \frac{\rho_l U_l d_{tube}}{\mu_l} \tag{81}$$

$$\mathrm{Pr}_l = \frac{\mu_l C_{pl}}{k_l} \tag{82}$$

Finally, Equation (83) and Equation (84) show the correlations for the single and multiple vertical tube configurations, respectively:

$$\mathrm{St} = 0.163\left(\mathrm{Re}_g\, Fr_g\, \mathrm{Pr}_l^{2.2}\right)^{-1/3}\left(\frac{\mu_l}{\mu_w}\right)^{0.30} \tag{83}$$

$$St = 0.139\left[\left(\mathrm{Re}_g\, Fr_g\, \mathrm{Pr}_l^{2.26}\right)^{-1/3}\right]^{0.84} A_f^{-0.20}\left(\frac{t_{tube}}{d_{tube}}\right)^{0.14}\left(\frac{\mu_l}{\mu_w}\right)^{0.30} \tag{84}$$

where A_f is the free cross-sectional area of the column (i.e. the area not occupied by the tubes) and the Stanton number, gas Reynolds number, and gas Froude number are given below:

$$\mathrm{St} = \frac{h}{\rho_l C_{pl} U_g}$$

$$\mathrm{Re}_g = \frac{\rho_l D_c U_g}{\mu_l} \text{ and } \mathrm{Fr_g} = \frac{U_g^2}{gD_c}$$

2.3.3 Saxena and coworkers

Figure 21 and Figure 22 illustrate the two basic experimental setups employed by Saxena et al. for studying heat transfer in two-phase and three-phase systems. All studies make use of one of two different columns. The smaller column was built using Plexiglas with an internal diameter of 0.108 cm, and an overall height of 2.25 m comprising a calming section (0.15 m), a test section (1.7 m), and a gas disengagement section (0.4 m). The calming section consisted of 5 symmetrical bubble cap distributors. Typically a perforated plate type distributor was installed in all cases, with the exception of Saxena et al. (1990l) who utilized a porous distributor. Ten pressure taps were installed at 0.152 m intervals above the distributor, while 5 thermocouples recorded the bulk bed temperature. The pressure taps were equipped with purgemeters and bottle traps in order to prevent liquid form entering the pressure lines. The arrangement of the larger column (0.305 m i.d. and 3.30 m high) was similar, while it was fabricated using Pyrex glass and had 4 pressure ports and 4 thermocouple ports installed 0.04, 0.52, 1.61, and 2.19 m above the grid. The air circuit consisted of a compressor, refrigeration

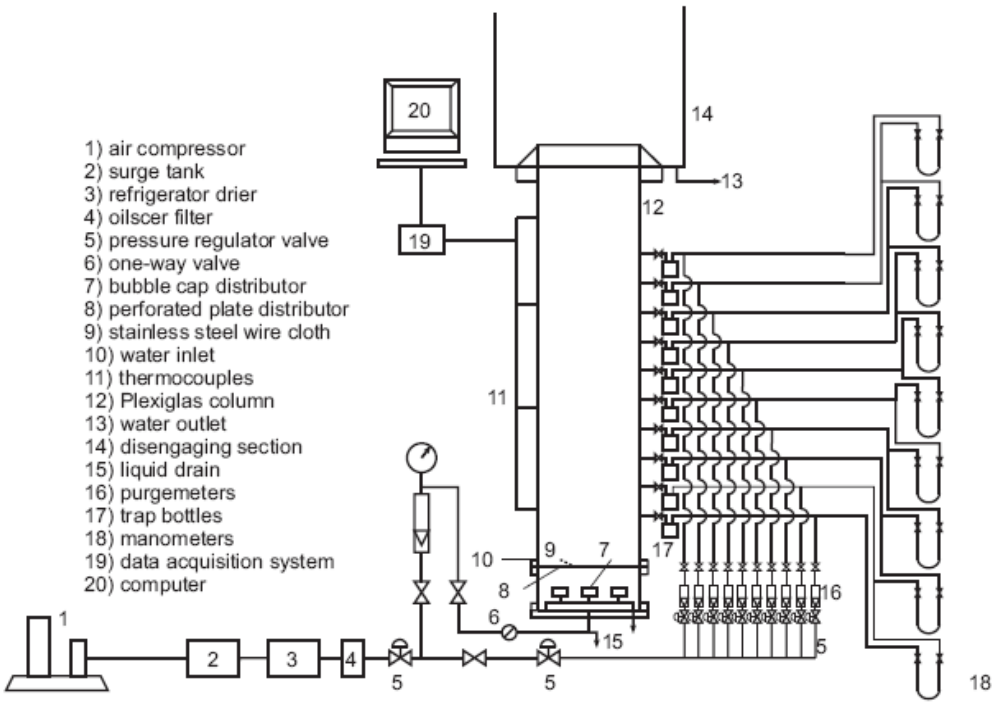

Figure 21. Equipment setup for the small column used by Saxena et al. (after Saxena and Vadivel, 1988).

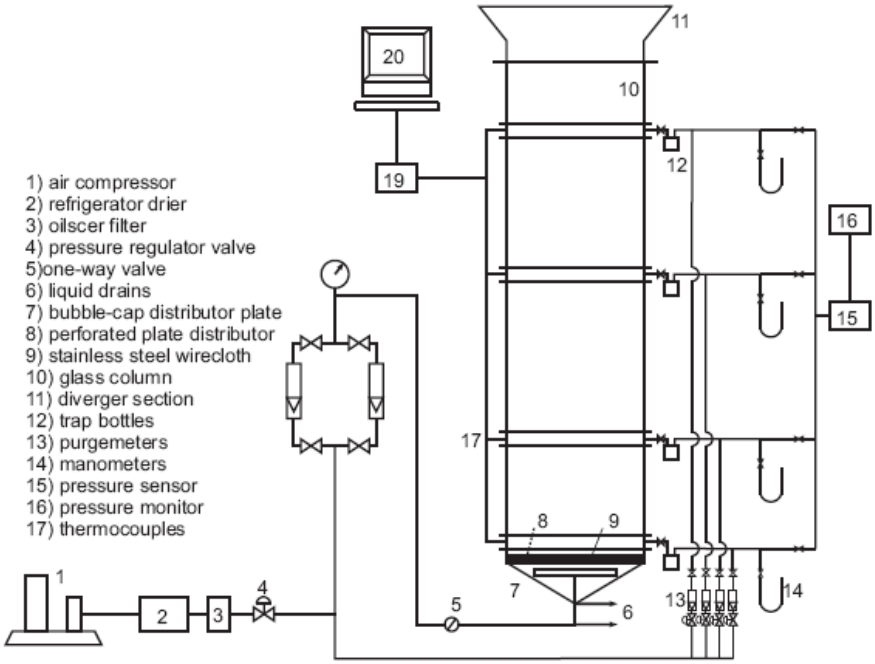

Figure 22. Equipment setup for the large column used by Saxena et al. (after Saxena et al., 1989b).

dryer, and three filters (cyclone type oil filter, oilscer cartridge filter, and an activated charcoal filter) (Saxena and Rao, 1991). The primary components of the liquid/slurry circulation loop were a stirred tank, variable speed pump, and a Venturi meter.

All columns were equipped with internals consisting of tubes with built-in heaters. The tubes themselves may be divided into three main components interspersed by two Delrin connectors. Installed at the bottom was a tapered Teflon cone used to promote smooth liquid flow around the probe. The middle component (340 mm in length) was built from brass and held the Calrod heater (305 mm in length) (1991). The brass section surface temperature was measured using 5-10 copper-constantan thermocouples copper cemented into milled grooves equally spaced both radially and axially. The top section was constructed of either Plexiglas or stainless steel. The length of the bottom and top components were varied in order to be able to study the effect of heater location, but the overall tube length was approximately equal to the column height. The tube outer diameter was typically 19 mm although some selected studies tested 31.8 and 50.8 o.d. tubes as well (Saxena and Rao, 1991; Saxena et al., 1991b; 1991c). A specially designed telescoping three-armed clamp held the internals in place and minimized movement caused by the gas, liquid, and solids circulation. The radial temperature profile was measured using a specially designed probe containing several thermocouples extending to various locations throughout the stainless steel or Acrylic resin tube. Figure 23 shows the basic design of the heat transfer probes and radial temperature probe. Studies conducted in the 0.108 m i.d column had 1, 5, or 7 tubes while there was 1, 5, 7, or 37 tubes placed in the 0.305 m i.d. column. For single tube studies, the heat transfer tube was axially aligned at the centre of the column. For the five and seven tube configurations in the smaller column additional “dummy” tubes were inserted around the central tube in a 36.5 mm square and triangular pitch arrangement, respectively (refer to Figure 24). The five, seven, and thirty-seven tube configurations in the larger column were arranged as shown in Figure 25. The 37 tube configuration in the larger column was also arranged using a 36.5 mm equilateral triangular pitch but contained four heat transfer probes located in four separate tubes with each test section located at a different height (refer to Figure 26 for side view and top view). Table 6 summarizes the tube diameters, number of tubes, and percent of the column cross sectional area occupied by the tubes (Saxena and Chen, 1994).

All studies conducted by Saxena et al. were conducted at ambient pressure and virtually all in semi-batch mode (i.e. $U_l = 0$) (Saxena and Chen, 1994). The major parameters studied included the bed temperature, the particle diameter, solids concentration, gas velocity, and the number and configuration of the internals.

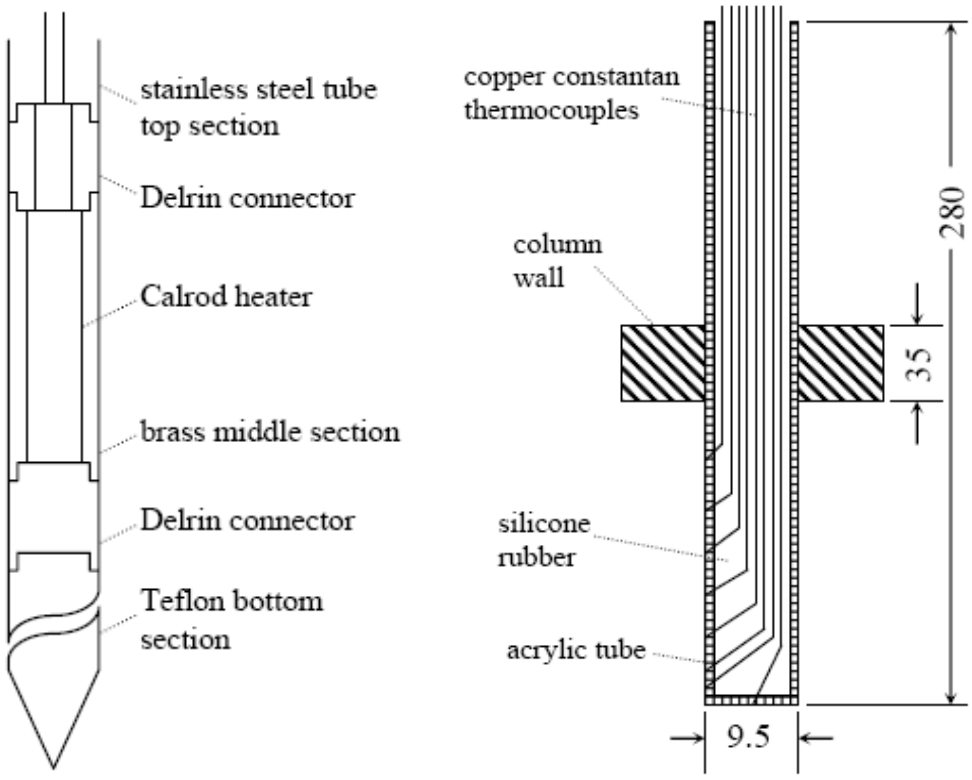

(a) **(b)**

Figure 23. Design and dimensions of (a) the 19 mm o.d. heat transfer probe and (b) radial thermocouple probe used by Saxena and coworkers (after Saxena and Chen, 1994).

Table 6. Column diameter, number of tubes, and percent occupied area of the column for the selected studies from Saxena and coworkers.

D_c (m)	No. of Tubes	d_{tube} (mm)	% area occupied
0.108	1	19	3.1
0.108	1	31.8	8.7
0.108	1	50.8	22.1
0.108	5	19	15.5
0.108	7	19	21.7
0.305	1	19	0.4
0.305	5	19	1.9
0.305	7	19	2.7
0.305	37	19	14.4

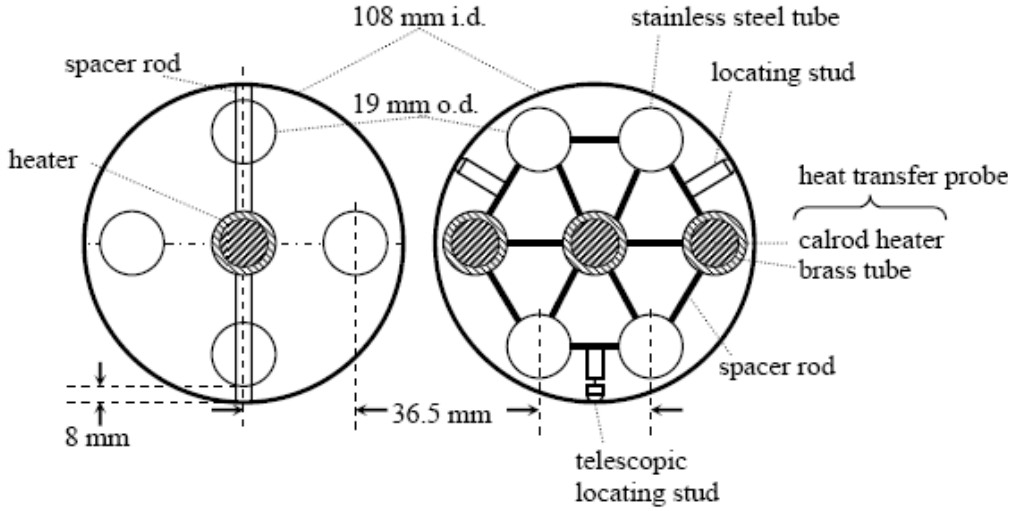

Figure 24. Five and seven tube arrangments in the 10.8 cm i.d. column (after Saxena and Chen, 1994).

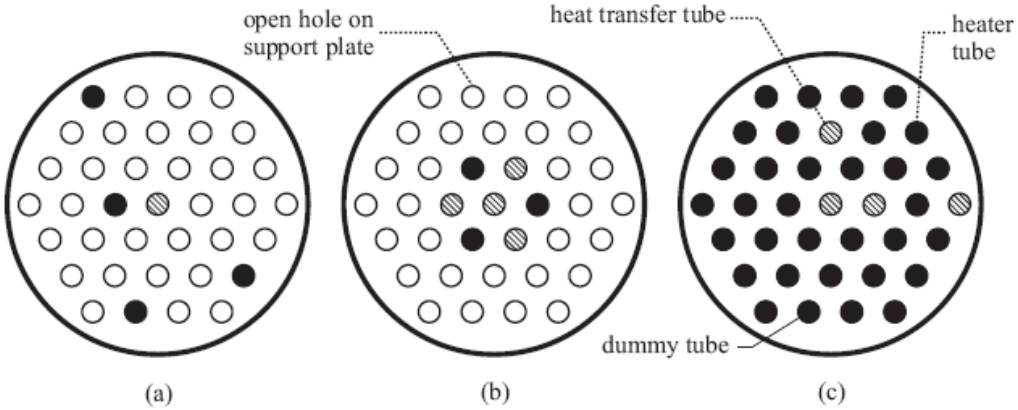

Figure 25. Five, seven, and thirty-seven tube bundle configurations in the 30.5 cm i.d. column (Saxena and Rao, 1993).

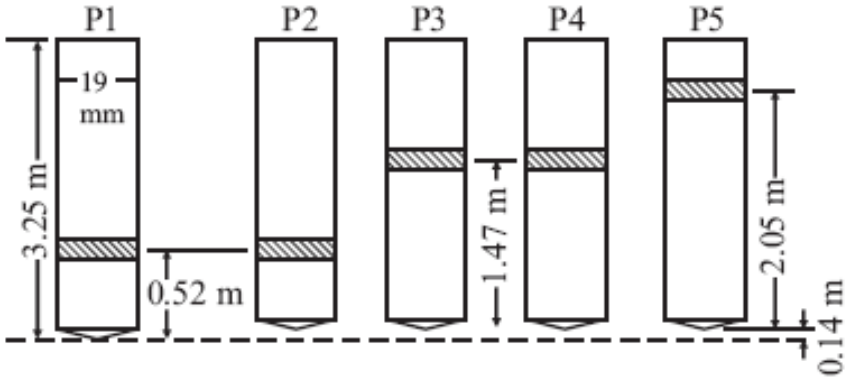

Figure 26. Side view of the heat transfer tubes showing the relative location of the heat transfer surfaces (after Saxena et al., 1992b).

2.3.3.1 ***Single Tube Studies: Glass Bead Systems***

In the small column Saxena and Patel (1991) studied the gas hold-up and heat transfer using the three different heat transfer probe diameters mentioned above. Three different sizes of glass beads (50, 119, 143 μm) were used at concentrations of 0 and 10 wt. %, while the gas and liquid phases consisted of air and water. The gas hold-up and heat transfer coefficient were both reported to be independent of the particle diameter and solids concentration. The gas hold-up was also reported to be independent of the tube probe diameter; however, the heat transfer coefficient decreased with increasing d_{tube} (due to the poorer mixing resulting from the decrease in the spacing between the tube and outer wall). The difference between the heat transfer coefficients for the 10 mm o.d. tube and the 51 mm o.d. tube was approximately 50%. The following correlation incorporates the hydraulic diameter of the column:

$$h = 1483 U_g^{0.21} \left(\frac{D_c - D_{probe}}{D_c} \right) \tag{85}$$

A wider range of solid concentration (10 to 30 wt. %) values was tested in the study by Saxena et al. (1989i) again using the small column and a single 19 mm tube and using the same sizes of glass beads. This study reported a slight negative influence of d_p on ε_g for relatively small particles at low concentrations in the foaming region of the column. However, at higher superficial gas velocities the gas hold-up decreased as the particle agitation suppressed the foaming. The heat transfer coefficient was observed to initially increase rapidly with increasing U_g and then reach an asymptotic value and was systematically greater in the three-phase system than for two-phase system (air-water). This difference was found to increase with increasing Θ_s. Again, d_p was found to have a negligible effect on h; however, it was observed to increase slightly with increasing Θ_s.

Saxena et al. (1989c) compared the heat transfer and gas hold-up in the small and large column for both two- and three-phase systems (air-water and air-water-glass beads, respectively). It was observed that ε_g was consistently higher when the initial static bed height was set at 0.95 m compared to when it was set at 1.40 m. The hydrodynamics of the two columns was reported as being similar except when foaming was significant: with less foaming observed in the larger column. Furthermore, the foaming increased with distance above the distributor plate leading in turn to higher gas hold-up. Measurements also indicated that ε_g increased monotonically with increasing U_g and decreased in the presence of the solid particles – in agreement with studies on glass beads (Saxena et al., 1989j)

Table 7. Experimental summary table of select articles from Saxena and coworkers.

	Gas	Liquid	Solid	Column						
Source	**Type**	**Ug (m/s)**	**Type**	**Type1**	**dp (μm)**	**Θ_s wt. %**	**Dc (cm)**	**Hc (cm)**	**T (°C)**	**Internals (No. of tubes)**
(Saxena and Rao, 1991)	air	0.02-0.33	water	-	-	-	10.8	2.25	27-71	1
(Saxena et al., 1989a)	air	0.02-0.38	water	glass beads	143.3	10	10.8/30.5	2.25/3.3	25	1
(Saxena and Patel, 1991)	air	0.02-0.36	water	glass beads	50-143	0-10	10.8	2.25	36	1
(Saxena et al., 1989k)	air	0.10-0.35	water	glass beads	50-143	10-30	10.8	2.25	40-49	1
(Saxena et al., 1990o)	air	0.02-0.33	water	Fe3O4	36-138	0-30	10.8	2.25	35	1
(Saxena et al., 1989g)	air	0.11-0.36	water	Fe3O4 Fe2O3	44 1.0-2.4	0-404 kg/m3	10.8	2.25	22-51	1
(Saxena et al., 1991m)	N2	0.01-0.24	Therminol66	Fe2O3	1.7	0-50	10.8	2.25	28-45	1
(Saxena et al., 1991g)	N2	0.03-0.20	Therminol66	Fe3O4	23-46	0-50	10.8	2.25	29-45	1
(Saxena and Vadivel, 1988)	air	0.04-0.42	water	-	-	-	10.8	2.25	~46	5
(Saxena and Patel, 1990c)	air	0.03-0.37	water	glass beads	50-143	0-30	10.8	2.25	36	1,7
(Saxena et al., 1990f)	air	0.02-0.28	water	glass beads	50-143	0-20	10.8/30.5	2.25/3.3	24-70	7
(Thimmapuram et al., 1993a)	air	0.02-0.30	water	glass beads	125-212	0-30	30.5	3.3	25-82	1,5,7,37
(Saxena and Patel, 1990g)	air	0.02-0.38	water	Fe2O3	1.0-2.4	0-20	10.8	2.25	36	7
(Saxena et al., 1990b)	air	0.02-0.43	water	Fe3O4	31-138	10-30	10.8	2.25	24-36	7
(Saxena et al., 1991a)	air	0.02-0.28	water	Fe3O4	50-90	0-10	30.5	3.3	24-80	7
(Saxena and Rao, 1992)	N2	0.02-0.11	Therminol66	Fe3O4	36	0-40	30.5	3.3	23-250	37
(Saxena et al., 1992b)	air	0.02-0.26	water	sand	65	5-10	30.5	3.3	24-70	1,5,7

and red iron oxide powders (Saxena et al., 1989h). The heat transfer coefficients for the three-phase system were reported as being consistently higher than the two-phase system. In all cases, the heat transfer coefficient was greater in the large column (attributed to better mixing).

2.3.3.2 ***Single Tube Studies: Iron Particle Systems***

Several studies performed by Saxena and coworkers used iron particles for the solid phase (magnetite or red iron oxide) and water or Therminol-66 as the liquid phase. The major difference between the two types of particles was their size: the red iron oxide particles were typically no larger than 2.38 μm while the smallest magnetite particles ranged from 22 to 137 μm on average. Tests using Therminol-66 were conducted in order to evaluate the effect of increased liquid viscosity on the systems under consideration. The next four studies described below were all conducted using the small diameter column. In general, the gas hold-up was found to be consistently higher for the two-phase systems (air-water) than for the three-phase systems while the opposite was observed in terms of the heat transfer coefficient (Saxena et al., 1990k). The heat transfer coefficient was highest for the magnetite particle systems.

Using air, water, and magnetite particles ranging in size from 35.7 to 137.5 μm at up to 30 wt. % Saxena et al. (1990j) observed that the gas hold-up was dependent on particle size and concentration. For particles smaller than 100 μm, solids concentration had a negligible effect on ε_g. When $d_p > 100$ μm ε_g initially increased with increasing Θ_s before levelling off at relatively high solid concentrations. The gas hold-up decreased with increasing d_p particularly in the bubbling regime. For engineering applications, Saxena et al. (1990i) recommend Equations (86) and (87) for determining the lower and upper bounds of the gas hold-up, respectively:

$$\varepsilon_g = \left\{ 2.25 \quad \left(\frac{33.9}{U_g} \right) \left(\frac{\rho_{sl}\sigma_l}{72} \right)^{0.31} \mu_{sl}^{0.016} \right\}^{-1} \tag{86}$$

$$\varepsilon_g = 0.009 \quad 296 U_g^{0.43} \rho_l^{-0.98} \sigma_l^{-0.16} \rho_g^{0.19} \tag{87}$$

where μ_{sl} is determined using Equation (9) [from Smith et al. (1984) and Reilly et al. (1986) as cited in (Saxena et al., 1990n)]. The heat transfer coefficient exhibited a similar dependence on the solids concentration and particle size as the gas hold-up values as summarized in Table 8 (these effects were more pronounced at higher U_g). A slight negative dependence of h with increasing particle size was observed.

Table 8. Effect of d_p and Θ_s on the heat transfer coefficient from the study of Saxena et al. (1990e).

d_p (μm)	Θ_s (wt. %)	Effect on h
< 100	< 10	small
> 100	10 to 20	increases
	20 to 30	negligibly increases

For both magnetite and red iron oxide particle systems the h value increased with increasing superficial gas velocity before reaching an asymptotic value. However, the red iron oxide system only showed a relatively weak dependence on d_p and decreased in value when the solid concentration was increased (Saxena et al., 1989d). It was noted in this study that any foaming occurred most often at relatively low U_g and disappeared when the red iron oxide particles were added (Saxena et al., 1989e).

Saxena et al. (1991f; 1991l) also studied red iron oxide (1.7 μm) and magnetite (23 – 46 μm) particles using N_2 and Therminol-66 at weight concentrations of up to 50%. Single probes, of three different diameters as described above, were also compared. There was no foaming or hysteresis observed with the use of Therminal-66 as the liquid phase: gas hold-up increased with increasing U_g over the entire range of velocities studied. In general, there were no cellular liquid circulation patterns observed and bubbles always flowed upwards through the column. Variation of the gas hold-up with Θ_s and d_p was within experimental error, especially when the gap was either large or small, and most likely could be "neglected in most design studies" (Saxena et al., 1991k). The gas hold-up was consistently smaller when the smallest probe was installed: there was a negligible difference between the results for the two larger probes. Generally, the heat transfer coefficient increased with increasing Θ_s and U_g while it decreased with increasing tube diameter (1991e; Saxena et al., 1991j). The effect of d_p was reported to be relatively small (Saxena et al., 1991d).

Two similar equations were derived from the studies of Saxena et al. (1991i) and Saxena et al. (1991c). The major difference between the two is the inclusion of the effect of the tube size included in the latter. These equations are shown below as Equation (88) and Equation (89), respectively.

$$h = 1024\left(\frac{\mu_l}{\mu_{sl}}\right)^{-0.34} U_g^{0.316} \tag{88}$$

$$h = 1050\left(\frac{\mu_l}{\mu_{sl}}\right)^{-0.6} U_g^{0.27}\left(\frac{D_c - D_{tube}}{D_c}\right)^{0.65} \tag{89}$$

where μ_{sl} was determined using Equation (29).

2.3.3.3 ***Multiple Tube Studies: Air-Water Systems***

Air-water systems were also studied using the small column equipped with 5 tubes by Saxena and Vadivel (1988). It was observed that ε_g and h increased with increasing U_g up to about 0.15 m/s and 0.26 m/s, respectively, before reaching asymptotic values. The gas hold-up values were determined to be significantly higher with the tube bundle in place and this was attributed to the limitation in bubble size. It was also observed that foaming was distributed evenly throughout the column and that ε_g was dependent on the initial static bed height: increasing H_0 leads to increased bubble coalescence which decreases ε_g. No comparison between the heat transfer with and without the tubes was reported.

2.3.3.4 ***Multiple Tube Studies: Glass Bead Systems***

Multiple tube arrangements (1 and 7 tubes) were studied using glass bead particles by Saxena et al. (Saxena et al., 1990e; Saxena and Patel, 1990b). Several general conclusions were made in both studies in terms of gas hold-up and the heat transfer coefficient. Both were found to be consistently higher for 7 tube configuration. The overall gas hold-up was lower for the three-phase systems than for the air-water system and showed no dependence on d_p. For solid concentrations of less than 10 wt. % no effect on ε_g was observed: when Θ_s increased further ε_g decreased. In general, the heat transfer coefficient increases with the addition of solids for both the single and 7 tube configurations. The effect of Θ_s on h was found to be negligibly small for 7 tube arrangement. Particle diameter had only a small negative effect on h as d_p increased from 50 to 90 μm; at 143 μm this effect disappeared. The following two correlations were proposed by Saxena et al (1990g):

$$h = 8273 U_g^{0.194} \tag{90}$$

$$h = 8108 \quad 1058 \ln\left(U_g\right) \tag{91}$$

Thimmapuram et al. (1993b) also studied a glass bead system in the large column using a wider range of temperatures (25 to 80°C) and tube configurations (1, 5, 7, or 37 tubes – refer to Figure 25). The glass beads ranged in size from 125 to 212 μm and the concentration was varied up to 30 wt. %. Again, h was found to vary weakly with particle size or concentration only for relatively small particles and at ambient temperature; h increased with d_p up to Θ_s = 15 wt. %. However, it varied significantly with U_g and temperature. It was reported that the

average bubble size increased with increasing temperature (this combined with the decreased liquid viscosity would likely increase the turbulence generated by the bubble wake). It was reported that h increased with increasing axial distance from the distributor, while it exhibited a maximum with increasing radial distance from the centre of the column. The heat transfer coefficient was also sensitive to the number of tubes and configuration. At lower temperatures (and higher μ_l) if the bubble size (d_b) was less than the tube pitch then h was independent of the tube configuration. However, if the bubble size and pitch are similar then h will be dependent on the bubble hydrodynamics and liquid mixing. The authors report that h generally tended to be lowest for the 37 tube bundle configuration. However, this is most likely related to the relative positioning of the tubes. In the 37 tube configuration the bubbles would be more evenly distributed whereas in the other configurations the bubble coalescence would tend to concentrate larger bubbles in the centre of the column – where the only heat transfer tube was located.

2.3.3.5 ***Multiple Tube Studies: Iron Particle Systems***

The heat transfer coefficient for a 7 tube bundle in the small column using magnetite or red iron oxide was also reported to be larger than for the single tube configuration when air and water were used for the gas and liquid phases, respectively. The magnetite particles where 31 μm to 138 μm in diameter and were tested at concentration 10 and 30 wt. % (Saxena et al., 1990d). The red iron oxide particles were considerably smaller (1.02 and 2.38 μm) but were employed at similar concentrations of 0 to 20 wt. % (Saxena and Patel, 1990f). The gas hold-up measured was higher in the two-phase system than in the three-phase system: ε_g was also greater for the 7 tube bundle than for the single tube. The authors expressed their concern at the lack of applicability of existing correlations for evaluating the gas hold-up for their so-called "baffled" systems. Saxena et al. (1990a) reported that ε_g decreased with increasing d_p and, for a given particle size, decreased with increasing Θ_s. Furthermore, particle size appeared to be more significant for dilute slurries. The dependence of h on d_p was characterized as "small" for particles of magnetite and negligible for red iron oxide. However, h was reported to decrease with increasing particle concentration for the former while decreasing for the latter. Mixing was reported to be poorer in the lower 1/3 of the column, which translated to lower h values, otherwise it was independent of the location of the heat transfer probe. It was observed that the heat transfer coefficient was consistently larger in the three-phase systems than in the two-phase systems (i.e. gas-liquid) but increased with increasing U_g in both. The authors caution against extrapolating these results to systems at higher values of Θ_s or d_p (Saxena and Patel, 1990e).

The tests conducted by Saxena et al. (1991a) were conducted in the larger column and over a wider range of temperatures (24 to 80°C) than in the study by (Saxena et al., 1990c). However, the particles and concentrations used were smaller (50 to 90 μm and 10 wt. %, respectively). The gas hold-up was observed to increase monotonically with increasing U_g but decreased with increasing temperature. Furthermore, the bubbles appeared to be larger and flatter as T increased. The presence of solids did not appreciably influence ε_g and measured values were similar in both the small and large columns for the 7 tube configurations. This is significant as it may indicate that when baffles create similar hydrodynamics that the column diameter does not affect ε_g. The heat transfer coefficient increased significantly with increasing temperature and exhibited the same increasing tendency with U_g tending towards an asymptotic value. The effects of particle concentration and size were rated as negligible. Even though it was reported that many current correlations failed to predict the effect of temperature on h, even for air-water systems, the heat transfer coefficients were correlated using a relatively simple correlation shown in Equation (92):

$$h = aU_g^b \tag{92}$$

While b was set to a value of 0.16 for all conditions it was determined that a was dependent on temperature.

Saxena and Rao (1992) also tested 36 μm magnetite particles at to 40 wt. % in the large column using the 37 tube bundle configuration. Again, h was found to increase with increasing U_g before reaching an asymptotic value (for U_g > 0.05 m/s). The heat transfer was also observed to increase with increasing temperature and solid concentration. Equation (93) shows the correlation proposed for their results with an average absolute deviation of 11.4%:

$$\frac{h}{\rho_{sl}C_{p,sl}U_g} = 0.179\left[\left(\frac{d_bU_g\rho_{sl}}{\mu_{sl}}\right)\left(\frac{U_g^2}{gd_b}\right)\left(\frac{C_{p,sl}\mu_{sl}}{k_{sl}}\right)^{2.54}\right]^{-0.25} \tag{93}$$

2.3.3.6 ***Multiple Tube Studies: Sand System***

Saxena et al. (1992c) studied an air-water-sand system using the large column equipped with 1, 5, or 7 tubes. The sand particles were 65 μm in diameter and the concentrations used were 5 and 10 wt. %. The gas hold-up was reported to decrease as the temperature was increased from 24 to 70°C while the heat transfer coefficient increased monotonically. Temperature appeared to be the most sensitive parameter in this study – even more than the superficial gas velocity

(Saxena et al., 1992e). Overall, ε_g was lower in the columns with 5 or 7 tubes than in the case of a single tube. The gas hold-up was reported to be slightly sensitive to Θ_s in the discrete bubbling regime (decreasing slightly with increasing Θ_s) with the effect becoming negligible at higher U_g. The solids concentration only appeared to have a nominal effect on h in the discrete bubbling regime with increasing slightly with increasing Θ_s. Based on their results Saxena et al. proposed the following correlation:

$$h = 0.0035\left(k_{sl}\rho_{sl}C_{p,sl}\right)^{0.5}\left(\frac{\rho_{sl}g}{\mu_{sl}}\right)^{0.47}U_g^{0.25} \tag{94}$$

with average absolute deviation of 13%.

2.3.4 Westermeyer

The work by Westermeyer Benz (1992) may be seen as an extension of the thesis by Korte (1987) but with the addition of a solid phase. Different columns of 0.12 m i.d. (3.62 m high), 0.19 m i.d. (4.75 m high) 0.20 m i.d (6.05 m high), 0.29 m i.d. (4.27 m high) and 0.45 m i.d (6.68 m high) were compared. Air served as the gas phase while pure water, saline water (10% NaCl), ethylene-glycol or 1,2-propylene-glycol served as the liquid phase. The liquid viscosity was varied from 0.001 to 0.055 Pa·s. The solid phase consisted of glass beads, plastic, or corundum powder; with Sauter mean diameters ranging from 60-440 μm. The column internals consisted of 1 heat transfer tube (150 to 280 mm long) and anywhere from 4 to 36 "dummy" tubes installed vertically above the perforated plate distributor (see Figure 27). The column was operated at ambient pressure while the temperature was varied from 20 to 60 °C. Three different tube diameters (15, 25, 63 mm) and tube pitch were studied (40 to 159 mm). A conductivity probe was installed midway up the 0.19 m i.d. column to measure the radial solid phase hold-up.

Westermeyer (1992) concluded that the effect of the superficial gas velocity on the heat transfer coefficient was pronounced when U_g < 20 cm/s: h increased with increasing U_g, then in the region of stable fluidization h approached an asymptotic value. Furthermore, h increased with decreasing μ_l and was determined to be independent of D_c. The experimental results were summarized by Equation (95).

$$St = 0.115\left[\left(\mathrm{Re}_g\, Fr_g\, \mathrm{Pr}^2\right)^{1/3}\right]^{-1}\left[\mathrm{Re}_g^{1/36}\, Fr_g We_g^{5/48}\right]A_f^{-1/6} \tag{95}$$

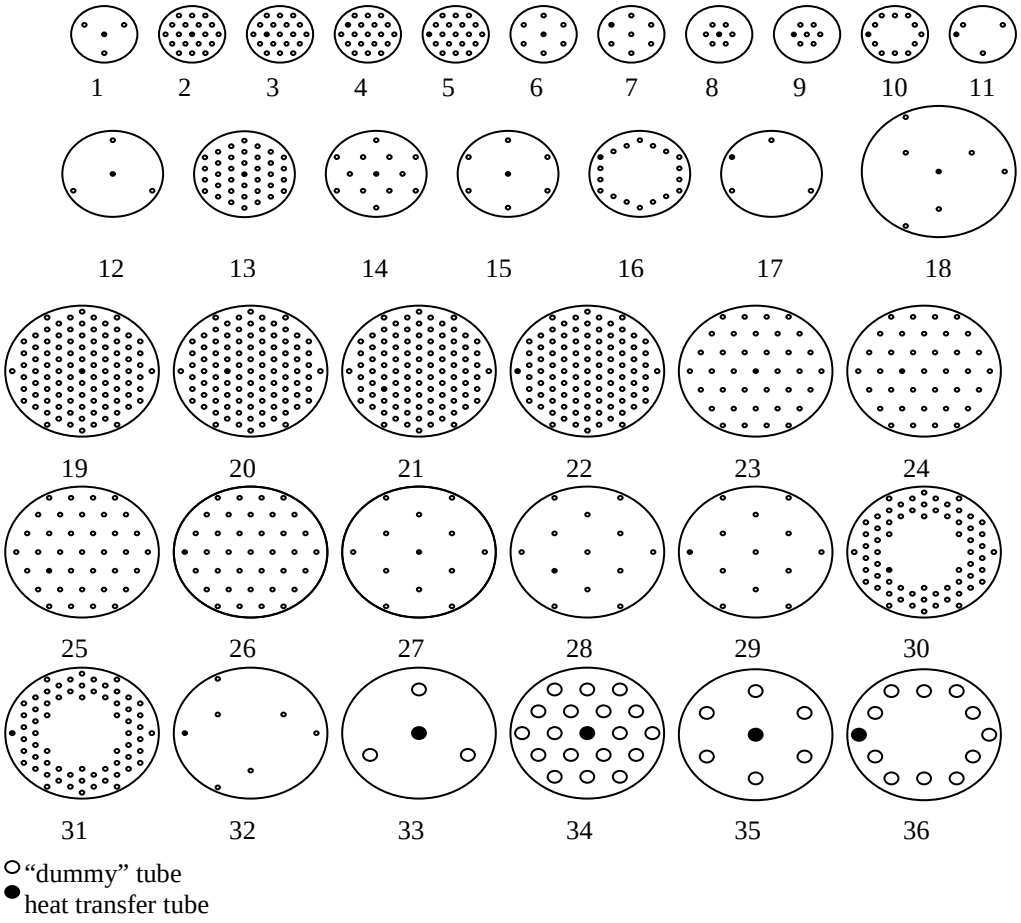

Figure 27. Tube arrangements studied by Westermeyer (after Westermeyer, 1992).

where A_f is the free cross-sectional area of the column (i.e. the area not occupied by the tubes) and the dimensionless groups are defined below:

$$St = \frac{h}{C_{pl}\rho_l U_g}; \quad \mathrm{Re}_g = \frac{\rho_l U_g D_c}{\mu_l}; \quad Fr_g = \frac{U_g^2}{gD_c}; \quad \mathrm{Pr} = \frac{\mu_l C_{pl}}{k_l}; \text{ and } \quad We_g = \frac{\rho_l D_c U_g^2}{\varphi}$$

2.4 Summary of Experimental Studies and Additional Heat Transfer Correlations

Table 9 presents some additional correlations found in the literature. The first 4 correlations correspond to correlations obtained on a theoretical only basis as indicated in the last column. The remaining correlations are from select

references originally written in German – in these cases the last column contains notes with details on the experimental system where provided.

Table 10 and Table 12 summarize the experimental studies for columns without and with internals, which were described in Section 2.1 through 2.3.

3 Specific Effects of Process Parameters on Heat Transfer

The purpose of this section is to summarize the key effects of each variable in regards to the heat transfer in two- and three-phase bubble columns.

3.1 Superficial Gas Velocity (U_g)

The introduction of the gas into the column enhances the turbulence in the medium, which enhances the heat transfer (Kantarci et al., 2005a). The effect of the superficial gas velocity on the heat transfer coefficient has been widely investigated and the general consensus is that h increases with U_g up to a given velocity and thereafter attains an asymptotic value (Kantarci et al., 2005a; Saxena and Chen, 1994). It is important to note that the majority of correlations do not predict this effect. This effect is more pronounced at relatively low U_g and appears to be independent of the solid and liquid phase properties or column diameter (Kantarci et al., 2005a). The dependence of h on U_g has been reported with a power between 0.059 to 0.34 (Kim and Laurent, 1991). The exponent selected is dependent in part on how the contact time of the fluid element at the heat transfer surface is defined (Lewis et al., 1982).

The initial increase in U_g results in a larger bubble diameter (Kim and Laurent, 1991). However, as U_g continues to increase the flow becomes churn-turbulent and the rate of bubble coalescence and break-up reaches an equilibrium (Li and Prakash, 1997): further increases in U_g do not significantly contribute to the gas hold-up or h (Kim and Laurent, 1991; Li and Prakash, 1997). It has been reported that the increase in h with increasing U_g decreases by an order of magnitude with increasing d_p and μ_l (Kim and Laurent, 1991). Heat transfer tends to be poorest in the homogeneous flow regime and best in the churn-turbulent regime (Lin and Hung-Tzu, 2003).

3.2 Superficial Liquid Velocity (U_l)

Generally, the heat transfer coefficient increases with U_l, reaches a maximum, then decreases (Kim and Laurent, 1991). It has been reported to be insignificant at relatively low values by Saxena and coworkers (Saxena and Chen, 1994) and

Table 9. Additional heat transfer coefficient correlations.

Reference	Correlation	Note(s) / Comment(s)
(Konsetov, 1966)	$\frac{h_w D_c}{k_l} = 0.25\varepsilon_g^{1/3}\left(\frac{g\rho_l^2 D_c^3}{\mu_l^2}\right)^{1/3}\left(\frac{\mu_l C_{pl}}{k_l}\right)^{1/3}\left(\frac{\mu_l}{\mu_w}\right)^{0.14}$ (96)	1) Theoretical treatment only
	$\frac{h d_{tube}}{k_l} = 0.18\varepsilon_g^{1/3}\left(\frac{g\rho_l^2 d_{tube}^3}{\mu_l^2}\right)^{1/3}\left(\frac{D_c}{d_{tube}}\right)^{1/3}\left(\frac{\mu_l C_{pl}}{k_l}\right)^{1/3}\left(\frac{\mu_l}{\mu_w}\right)^{0.14}$ (97)	
(Suh and Deckwer, 1989)	$h = 0.1\left[k_l\rho_l C_{pl}\left(\frac{P_v}{\eta_{sl}\mu_l}\right)^{1/2}\right]^{1/2}$ (98) where $P_v = \frac{\left[\left(U_l+U_g\right)\left(\varepsilon_s\rho_s+\varepsilon_l\rho_l+\varepsilon_g\rho_g\right)-U_l\rho_l\right]g}{\varepsilon_l}$; $\eta_{sl} = \frac{2.5\beta}{1-39\beta/64}$; and $\beta = \frac{\varepsilon_s}{1-\varepsilon_g}$	1) For both wall and internal heat transfer 2) r^2 = 0.98 and maximum deviation of ±15% 3) Theoretical treatment only
(Kawase and Moo-Young, 1987)	$\frac{hD_c}{k_l} = 0.134\left(\frac{\mu_l C_{pl}}{k_l}\right)^{1/3}\left(\frac{U_g^2}{gD_c}\right)^{-1/4}\left(\frac{\rho_l D_c U_g}{K}\right)^{3/4}$ (99)	1) For Newtonian fluids 2) K = power-law consistency index ($Pa{\cdot}s^n$) 3) Theoretical treatment only
(Joshi et al., 1980)	$\frac{h_w D_c}{k_l} = 0.48\left[\frac{\rho_l D_c^{1.33} g^{0.33}\left(U_g-\varepsilon_g V_{b\infty}\right)^{0.33}}{\mu_l}\right]^{0.66}\left(\frac{C_{pl}\mu_l}{k_l}\right)^{0.33}\left(\frac{\mu_l}{\mu_w}\right)^{0.14}$ (100)	3) Theoretical treatment only
(Kast, 1962; Kast, 1963)	$\frac{h_w}{\rho_l C_{pl} U_g} = 0.1\left[\left(\frac{\rho_l D_c U_g}{\mu_g}\right)\left(\frac{U_g^2}{gD_c}\right)\left(\frac{\mu_l C_{pl}}{k_l}\right)^2\right]^{-0.22}$ (101)	1) D_c = 0.29 m i.d.; H_c = 4 m 2) Air/water/isopropanol (45 wt. %) 3) U_g = 0.0025 to 0.06 m/s

Table 9. (cont.) Additional heat transfer correlations.

Reference	Correlation	Note(s) / Comment(s)
(Burkel, 1972)	$\frac{h}{\rho_l C_{pl} U_g} = 0.11\left[\left(\frac{\rho_l U_g D_c}{\mu_l}\right)\left(\frac{U_g^2}{g D_c}\right)\left(\frac{\mu_l C_{pl}}{k_l}\right)^{2.48}\right]^{-0.22}$ (102)	1) Immersed coil in air-water system 2) D_c = 0.19 m 3) U_g < 0.5 m/s – h constant for U_g > 0.1 m/s 4) Correlation cited from (Schluter et al., 1995)
(Bieszk, 1986; Bieszk and Hammer, 1988)	$\frac{h}{\rho_l C_{pl} U_g} = 0.15\left[\left(\frac{\rho_l U_l d_b}{\mu_l}\right)\left(\frac{U_g^2}{g d_b}\right)\right]^{-0.25}\left(\frac{\mu_l C_{pl}}{k_l}\right)^{-0.69}$ (103)	1) D_c = 15 cm i.d.; H_c = 1.85 m 2) Single heat probe 3) U_g = 2 to 10 cm/s 4) Solids: 0.46 mm glass beads (Θ_s = 5 wt. %) 5) Water and glycerine solutions: μ_l = 0.89 to 9.35 MPa.s; ρ_l = 998 to 1155
(Pauli, 1988)	$\frac{h}{U_g \rho_l C_{pl}} = 0.097\left[\left(\left(\frac{\rho_l U_g d_{tube}}{\mu_l}\right)\left(\frac{U_g^2}{g D_c}\right)\left(\frac{\mu_l C_{pl}}{k_l}\right)^2\right)^{1/3}\right]^{-0.78}$ (104)	1. industrial chlorine liquefaction plant 2. gas and liquid phase: chlorine 3. tube bank: 100 mm o.d. 2 m high
(Mersmann, 1976; Mersmann, 1977)	$h = 0.107 k_l \sqrt[8]{\frac{g}{\nu_l a_l}}\left(\frac{\nu_l}{a_l}\right)^{0.226}$ (105) $h = 0.12\left(\frac{g^2}{\nu_l}\right)^{1/6}\left(\frac{\rho_l - \rho_g}{\rho_l}\right)^{1/3}\left(k_l \rho_l C_{pl}\right)^{1/2}$ (106)	1. Equation (105) for 0.03 < Pr < 100 2. Equation (106) for 1 < Pr < 100 3. D_c = 200 mm, H_0 = 900 mm 4. Probe: 39.5 mm o.d.; 111.4 mm long 5. liquid-liquid column: toluene in water, or water in tetrachlorethylene 6. dispersed phase velocity = 0.002 to 0.15 m/s 7. 6.9 < d_b < 15.1
(Zaidi et al., 1987)	$\frac{h}{\rho_l C_{pl} U_g} = 0.076\left(\frac{\mu_l C_{pl}}{k_l}\right)^{-0.49}\left[\left(\frac{U_g D_c \rho_l}{\mu_l}\right)\left(\frac{U_g^2}{g D_c}\right)^2\right]^{-0.29}$ (107)	1. D_c = 0.10 m and H_c = 1.6 m 2. U_g = 0.01 to 0.10 m/s 3. biomass reactor 4. air/Xanthan solutions of varying concentrations and flow indices between 0.18 and 0.70 5. inserted heating elements (64 cm^2 total surface area) 6. cross-flow

Table 9. (cont.) Additional heat transfer correlations.

Reference	Correlation	Note(s) / Comment(s)
(Napp and Hammer, 1983)	$\frac{h}{\rho_l C_{pl} U_g} = 0.25\left(\mathrm{Re}\, Fr\right)^{-0.26} \mathrm{Pr}^{-0.78}$ (108)	1. D_c = 15 cm; H_c = 125 cm 2. U_g = 0.005 to 0.11 m/s; U_l = 0 to 0.01 3. water/PE-glycol/KCl/benzoic acid 4. glass beads: 0.095, 0.145, 0.275. 0.460 mm 5. μ_l = 0.92 to 20 mPa.s 6. no general correlation for taking into account solid suspension effect
(Zehner, 1982; Zehner, 1986a; Zehner, 1986b)	$h_w = 0.18\left(1 \quad \varepsilon_g\right)\sqrt[3]{k_l^2 \rho_l C_{pl}\left(\frac{\rho_l U_f^2}{l_b \mu_l}\right)}$ where $l_b = d_b \sqrt[3]{\frac{\pi}{6\varepsilon_g}}$ and $U_f = \sqrt[3]{\frac{\left(\rho_l - \rho_g\right) g D_c U_g}{2.5\rho_l}}$ (109)	1. D_c = 0.139 m and H_c = 0.298 m 2. l_b is mean distance between bubbles and U_f is the eddy velocity 3. liquid circulation model based on transversely layered cylindrical eddies 4. compared to data obtained using sucrose, ethanol, spindle oil, water, glycerine, and glycol solutions 5. liquid velocity was measured using a fan-wheel anemometer
(Fazeli et al., 2008)	$h = 2.03 + 0.0276\Theta_s + 0.155H_p + 5.26R_p + 2.91U_g + 0.0027\Theta_s H_p - 0.158\Theta_s R_p + 0.140\Theta_s U_g - 7.20H_p R_p + 3.38H_p U_g - 21.5R_p U_g + 0.0287\Theta_s H_p R_p - 0.0576\Theta_s H_p U_g + 24.2H_p R_p U_g$	1. See Table 11 for experimental details.

Table 10. Experimental summary table of heat transfer studies conducted in columns without internals.

Source	Gas		Liquid		Solid			Column		
	Type	U_g (m/s)	Type	U_l (m/s)	Type[1]	d_p (mm)	Θ_s wt. %	D_c (cm)	H_c (cm)	T (°C)
(Hikita et al., 1981)	air	0.053-0.34	water/sucrose water/alcohol	-	-	-	-	10/19	162/240	22-45
(Kato et al., 1981; 1982)	air	0.03-0.15	water/CMC	0.003-0.15	glass beads porous alumina	0.42-2.2 3.3		5.2/12	150	
(Chiu and Ziegler, 1983; 1985)	air	0-0.14	water	0.063-0.15	glass beads γ-Al	0.05-3 3.5-5.3		5.1	152	
(Hatate et al., 1987)	air	0.15-9	water	0.08-1.6	glass beads	0.029-0.096	0.2-54	1.5/2.7	400	
(Kim and Lee, 2001)	-	-	water	0.3-1.7	glass beads	1.5-3	0.5-1.5	1.4	140	
(Holcombe et al., 1983)	N_2	0-0.60	water	0-0.02	-	-	-	7.8	180	23-42
(Shaykhutdinov et al., 1971)	air	0.002-1.0	water/5 or 50 wt% glycerin	0.004-0.016	-	-	-	4.8	40	
(Zehner, 1986a; Zehner, 1986b)		0.05-0.20			-	-	-	14/30	2.5	

Table 11. Experimental summary table of heat transfer studies conducted in columns with internals.

Source	Gas		Liquid		Solid			Column				
	Type	U_g (m/s)	Type	U_l (m/s)	Type	d_p (mm)	Θ_s wt. %	D_c (cm)	H_c (cm)	T (°C)	Internals (mm o.d.)	
(Kölbel et al., 1958b)	air	0-0.35	water/sugar		-	-	-	9.2/29	200		1 tube	30
(Fair et al., 1962)	air	0-0.09	Water	0.0038-0.0050	-	-	-	45.7	305		20 plates	
				0.0007-0.0009				107			42 tubes	38.1
(Baker et al., 1978)	air	0-0.24	Water	0.006-0.13	glass beads	0.5-5		24	275		1 tube	64
(Steiff and Weinspach, 1978)	air	< 0.15	water or oil	< 0.04	-	-	-	19/45/70	1,2,3[1]	40	coils	
(Deckwer et al., 1980)	N_2	< 0.04	paraffin	-	Al_2O_3	0.005	0-16	10	> 100	143-270	1 tube	21
(Kato et al., 1985)	air	0.02-0.16	water/CMC	0.005-0.08	glass beads Al_2O_3	0.52-2.2 3.2		12/19	200/250		1 tube	22
(Kato et al., 1986)											1 tube	13/38
(Magiliotou et al., 1988)	air	0-0.06	water/TPA	0.01-0.06		1.09-1.57		7.6-15	183		1 tube	19
(Verma, 1989)	air	0.033-0.35	Water		-	-	-	10.8	170	43	1 tube	19
(Zaidi et al., 1990)	air	0.01-0.14	xanthan	0.013-0.09	glass beads	3-5	0.4-5.5 kg/m^3	10	160		cone	
(Lin and Fan, 1999)	N_2	bubbling/ jetting	Paratherm NF	-	-	-	-	5.1	80	27	flux probe	25x19 x4
(Lin and Hung-Tzu, 2003; Lin and Wang, 2001)	air	0-0.04	NaI	-	glass beads	0.586	0-22 vol. %	50 x 1.2	220		flux probe	25x19 x4
(Chen et al., 2003)	air	0.02-0.09	Water	-	-	-	-	20/40/80	300		hot wire probe	
(Muroyama et al., 2001; 2003)	air	0-0.19	water/CMC	0.009-0.15	glass beads	0.25-5.2	1-10 vol. %	8.2/15	188/203		1 tube	25
(Kantarci et al., 2005b)	air	0.03-0.20	Water	-	yeast	0.0002-0.01	0.1-0.4	17	60	23-45	1 tube	15
(Field and Rahimi, 1988a; Lewis et al., 1982)	air/N_2	0-0.18	water/cumene/ glycol	-	-	-	-	29.2	150	5-82	1 probe	20-50
(Nore et al., 1992)	air/N_2	0-0.08	4 wt % NaCl	0.0098-0.041	PP	2.1-3.1	2.2-3.3 kg	10	200	25	1 probe	2.7
(Del Pozo et al., 1994)	air	0.06-0.09	water/NaCl/ alcohol/acid	0-0.085	glass beads	3	2.44 kg	8			1 probe	2.7

Table 11. (cont.) Experimental summary table of heat transfer studies conducted in columns with internals.

Source	Gas		Liquid		Solid			Column				
	Type	U_g (m/s)	Type	U_l (m/s)	Type	d_p (mm)	Θ_s wt. %	D_c (cm)	H_c (cm)	T (°C)	Internals (mm o.d.)	
(Dhaouadi et al., 2006)	air	0-0.10	Water	-	glass beads	0.09	3-7 vol. %	10	300		1 probe	15
(Li and Prakash, 1997; 1999; 2002; 2001)	air	0.05-0.30	Water	-	glass beads	0.035	0-40 vol. %	28	240		1 probe	11.4
(Li et al., 2003)	air	0.05-0.30	Water	-	glass beads	0.011-0.093	0-40 vol. %	28	240		1 probe	11.4
(Prakash et al., 2001)	air	0.05-0.30	Water	-	yeast	0.008	0.1-0.4	28	240		1 probe	11.4
(Wu et al., 2007)	air	0.03-0.30	Water	-	-	-	-	16	250		1 probe	11.4
(Cho et al., 2001)	air	0.01-0.07	Water	0.28-0.33	glass beads	2.1	2-8 kg/m^2s	10.2	350		1 tube	30
(Kim et al., 1987; Kim et al., 1986)	air	0-0.14	mineral oil/ kerosene	0.03-0.12	glass beads/ coal	1.7-8	8-62 vol. %	15.2	300		1 tube	30
(Kim et al., 1990)	air	0.02-0.14	water/CMC	0.02-0.09	glass beads	1-1.7		14.2	200		1 tube	30
(Kang et al., 1991)	-	-	water	0.04-0.12	glass beads	1.7-4		15.2	300		1 tube	30
(Cho et al., 2002; Kang et al., 1985)	air	0-0.12	water/CMC	0-0.16	glass beads	1.7-8		15.2	300		1 tube	30
(Luo et al., 1997; Yang et al., 2000)	N_2	0-0.20	Paratherm NF	-	glass beads	2.1-3	0-35 vol. %	10	137	34-81	flux probe	25x19x4
(Kumar and Fan, 1994; Kumar et al., 1992)	air	single bubble	water/glycerin	-	glass beads	0.16-0.76		7.62	150		flux probe	25x19x4
(Kumar et al., 1993ba)	air	single bubble	water	-	PS/PVA/nylon/ Ca alginate	0.33-3.79		7.62	150		flux probe	25x19x4
(Kumar et al., 1993ab)	air	0.01 to 0.07	t-pentanol	0.007-0.06	glass beads/ nylon	0.76/2.5		7.62	150		flux probe	25x19x4
(Korte, 1987)	air	0-1.0	water/glycerine/ salt water/ 1,2-$C_3H_8O_2$	0.01-0.038	-	-	-	12/20/45	450/ 680/ 620	20-60	1-49 tubes	25
(Westermeyer, 1992)	air	0.01-0.60	water/$C_2H_6O_2$ salt water/ 1,2- $C_3H_8O_2$	0.0-0.04	plastic/glass/ corundum	0.06-0.44	0-28 vol. %	12-45	362-668	20-60	1-36 tubes	15/25/63
(Hart, 1976)	air	0.0003-0.020	water/glycol	negligible	-	-	-	9.91	107	71-84	1 tube	6.4
(Nishikawa et al., 1977)	air	0.0056-0.56	water/ millet jelly/CMC	0-0.14	-	-	-	5.1/15	180	25-45	1 coil	10

Table 11. (cont.) Experimental summary table of heat transfer studies conducted in columns with internals.

Source	Gas		Liquid		Solid			Column				
	Type	U_g (m/s)	Type	U_l (m/s)	Type	d_p (mm)	Θ_s wt. %	D_c (cm)	H_c (cm)	T (°C)	Internals (mm o.d.)	
(Kubie, 1975)	air	bubble chain (up to 40 bubbles/s)	water/n-heptane/ 50% glycerol	0	-	-	-	14		25	1 wire	0.041 to 0.31
(Michael and Reichert, 1981)	C_2H_4	0.009-0.118	various liquid hydrocarbons	-	PE	0.047-0.241	0-34	10	150	50-70	1 probe	19
(Tarat et al., 1970)	air	0.1-2.0	water/C_2H_5OH /glycerol	-	-	-	-	12x12		23-50	1 tubes	8,13,18
(Khoze, 1971; Khoze and Scharov, 1977)	air	0.5-3.5	water/$C_{18}H_{33}NaO_2$/ $C_3H_8O_3$/C_2H_6O	-	-	-	-	12x12		15-90	1 tube	4,8,13,18
(Fazeli et al., 2008)	air	0.026 – 0.23	paraffin	0	SiO_2	0.050	10,20,30	30	300	-	1 tube	19

[1]Three different column height to diameter ratios were studied.
[2]Three different "hydraulic" diameters (i.e. $D_c - d_{tube}$) were used: 0.024, 0.030, and 0.036 m.

Hikita et al. (1981) for U_l < 0.012; however Saxena and Chen cite work by Holcombe et al. (1983) and Knickle et al. (1983) which reported that h increased in the range 0 to 0.02 m/s. The liquid flow rate corresponding to the maximum h value increase as the particle size and density increase and decreases with increasing liquid viscosity (Kim and Laurent, 1991).

Increasing liquid velocity will initially increase the liquid phase turbulence and particle motion. However, further increases in U_l leads to a significant decrease in the solid phase hold-up. The reported exponent for power-law relationship between h and U_l ranges from 0.03 to 0.07 (Kim and Laurent, 1991).

3.3 Gas and Liquid Properties

The heat transfer coefficient has been observed to increase with increasing liquid heat capacity and thermal conductivity (Lin and Fan, 1999; Wu et al., 2007). Surfactants have been added to the column in some studies in order to mimic the effect of higher pressure. Magiliotou et al. (1988) and Kumar et al. (1993a) have both reported studies where the presence of surfactants increased the heat transfer coefficient. However, the presence of surfactants may also increase foaming (Kantarci et al., 2005b). Surfactants decrease the small bubble rise velocity (especially at relatively low U_g) but increase the large bubble velocity (Prakash et al., 2001). Generally, the bed hydrodynamics and heat transfer are not affected by the gas properties (Lewis et al., 1982; Saberian-Broudjenni et al., 1985).

3.4 Viscosity(μ_l)

Liquid viscosity has a significant effect on heat transfer through its impact on the system hydrodynamics (i.e. bubble properties and mixing) (Lin and Fan, 1999). The general consensus is that h decreases with increasing μ_l regardless of the particle diameter. This is attributed to reduced turbulence due to increased frictional losses (even though bubble coalescence increases) and decreased solids mobility (Kantarci et al., 2005a; Quiroz et al., 2003; Saxena and Chen, 1994). The laminar sub-layer thickness will increase as the apparent viscosity increases, which will further reduce heat transfer (Saxena and Chen, 1994). The effect of viscosity is highest in small diameter columns (high wall area to volume ratio) (Field and Rahimi, 1988b). Care should be taken in applying correlations derived for a wide range of μ_l as these generally do not account for the corresponding changes in hydrodynamics (Lewis et al., 1982). Finally, Saxena et al. (1991o) stress the importance of quantifying the apparent slurry viscosity for varying solids concentrations and particle diameters simultaneously.

3.5 Liquid Surface Tension (σ_l)

There are few reported studies on the effect of liquid surface tension. Kölbel et al. (1958b) reported that h increased with decreasing surface tension at relatively low values of U_g and that this effect decreased at higher superficial gas velocities. Surface tension affects foam formation, which increases the gas hold-up but decreases the heat transfer coefficient. Increased foaming will also increase the liquid viscosity, which hinders bubble motion, thereby further decreasing h (Saxena and Chen, 1994).

3.6 Particle Diameter (d_p)

The effect of solid loading and particle diameter on the heat transfer in bubble columns is complex (Kantarci et al., 2005a). Kim and Laurent (1991) have reported that h was observed to increase with increasing particle diameter at relatively low superficial gas velocity (< 0.05 m/s). Quiroz et al. (2003) cite a study from Kölbel et al. (1960) who also determined that h increased with increasing particle diameter. Relatively smaller particles may enhance bubble coalescence creating larger and more stable bubbles (Kim and Laurent, 1991; Li et al., 2003). Generally smaller particles (< 100 μm) minimize the intraparticle resistance and enhance the mass transfer rate, but particles that are too small may lead to problems with separation (Li and Prakash, 2001).

On the other hand, relatively large particles (mm size) do not have a significant effect on the heat transfer coefficient in low viscosity solutions such as water (Kim and Laurent, 1991). However, a local maximum was observed for relatively viscous CMC solutions (μ_l = 0.039 Pa.s) (Kang et al., 1985). Initially, relatively smaller particles would enhance the turbulence and may act to disrupt the thermal boundary at the heat transfer surface. However, relatively larger particles increase the energy dissipation of the liquid and may also contribute to bubble break-up. Saxena and coworkers report that particle size had a negligible effect on the heat transfer, especially in a well-baffled system (Saxena et al., 1991p). Turbulence dissipation in sparger region would be expected to increase with increasing d_p (Li et al., 2003). It has been noted that the use of mono-dispersed spherical glass particles may not be suitable for low U_l studies as the formation of stable flow patterns formed were observed (Saberian-Broudjenni et al., 1985).

3.7 Solid Loading (Θ_s)

The effect of solid concentration appears to be dependent in part on the particle size, particle density, and liquid properties (i.e. viscosity). Kölbel et al. (1960)

found that h increased with Θ_s using 120 μm sand particles up to 50 wt. % (Quiroz et al., 2003; as cited in Saxena and Chen, 1994) as did Deckwer et al. (1980) using 5 μm alumina particles at up to 16 wt. %. Similar tendencies were observed by Saxena and coworkers using air-water-red iron oxide (d_p = 1.02 and 2.38 μm; ρ_s = 5100 kg/m^3; Θ_s up to 40 wt. %) (Saxena et al., 1989f); magnetite (d_p = 28 to 143 μm; Θ_s up to 50 wt. %); and air-water-glass beads (d_p = 50 to 143 μm; Θ_s up to 30 wt. %) (Saxena and Chen, 1994).

The initial increase has been attributed to the increasing contact frequency between the particles and heat transfer surface acting to disrupt the film boundary layer and cause enhanced renewal (Lin and Hung-Tzu, 2003). An increase in the apparent slurry viscosity may also lead to increased bubble coalescence causing U_b to increase, which would increase the system turbulence (Kantarci et al., 2005a). The interaction between the fluid and solid particles may also enhance the turbulence (Dhaouadi et al., 2006; Ozbelge, 2001). However, as Θ_s continues to increase it will eventually begin to dampen heat transfer as the pseudo slurry viscosity increases (Li and Prakash, 1997; Ozbelge, 2001). High solids loading may also lead to problems of poor mixing and low heat and mass transfer rates (Li and Prakash, 2001). However, Saxena et al. (1992a) did not observe a significant effect of solid loading for 65 μm sand particles at up to 10 wt. %. They also observed that h decreased for a N_2-Therminol-red iron oxide system (d_p = 1.7 μm) (Saxena et al., 1991q). Li and Prakash (1997) also reported a decrease in h with increasing Θ_s attributed to an increase in the apparent slurry viscosity with increase in Θ_s, which in turn decreased the system turbulence.

Saxena and Chen (1994) attribute these discrepancies to the particle diameter and apparent slurry viscosity. They conjecture that h increases with increasing Θ_s for relatively large particles regardless of the liquid properties. However, h will decrease with increasing Θ_s in relatively low viscosity solutions and increase in relatively high viscosity systems. Saxena and Chen (1994) urge further research in terms of the effect of particle size and concentration.

3.8 Bubble Properties

Larger bubbles tend to congregate in the centre of the column (Kantarci et al., 2005a). This creates more turbulence and higher shear rates there than at the wall since bubble rise velocity increases with increasing d_b (Li and Prakash, 1997). The bubble diameter tends to increase with increasing U_g, which in turn leads to a decrease in ε_g. The heat transfer coefficient has been observed to increase with increasing bubble size due to the enlarged wake region (Kumar and Fan, 1994; e.g. Kumar et al., 1992; Li and Prakash, 2001). The bubble-wake effect is enhanced by the so-called “chain bubbling” effect described by Kumar and Fan

(1994): trailing bubbles tend to be accelerated by the wake-effect of the leading bubble thereby increasing the rate of surface renewal. However, smaller bubbles were observed to create better mixing than larger coalesced bubbles (Saxena and Patel, 1990a). Larger bubbles on the other hand, were reported to rise more slowly in confined annular spaces, which led to decreases in the heat transfer coefficient (Saxena et al., 1991b).

The terminal bubble rise velocity was found to increase with increasing Θ_s up to 30 vol. % but decreased for a slurry concentration of 40 vol. % (Li et al., 2003). The rate of increase was higher for relatively smaller particles. The bubble terminal rise velocity is a good indication of the bubble size distribution and higher $U_{b\infty}$ indicates the presence of larger bubbles. The bubble rise velocity is also a function of the bubble size, liquid and gas properties, column diameter, and pressure (Lin and Fan, 1999).

3.9 Column and Probe Characteristics

The heat transfer coefficient was reported to be independent of the column diameter in the majority of studies that investigated more than one column diameter: e.g. Deckwer et al. (1980), Korte (1987), Fair et al. (1962). The value of D_c at which this occurs may vary from 0.05 m to 0.19 m depending on the system under study (Kim and Laurent, 1991; Saxena and Chen, 1994). Saxena and Chen (1994) stress the importance of the presence of a suitably designed gas distributor in order to ensure an initially uniform distribution of bubbles. The gas hold-up is not dependent on D_c (or column height) if the column diameter is larger than 0.10 m (Kantarci et al., 2005b; Saxena and Chen, 1994). However, there is no information on heat transfer in columns greater than 0.5 m in diameter. It has been observed that as the column diameter increase there is a significant increase in the axial liquid circulation velocity while the radial liquid circulation velocity decreases (Forret et al., 2006) and in one study Saxena et al (1990h) reported an increase in the heat transfer rate with increasing D_c (10.8 and 30.5 cm i.d. columns). Wu et al. (2007) reported that the column diameter should be greater than 0.15 m in order to avoid wall effects.

The column height will affect the bubble characteristics and column hydrodynamics by affecting the bubble coalescence. The column should be high enough that the rate of bubble coalescence and break-up has reached equilibrium and the bubble size has stabilized. Generally, industrial scale columns are designed with a height to diameter ratio greater than 5 (Kantarci et al., 2005b).

The location of the heat transfer probe will affect the values of h obtained. Differences may be attributed to liquid circulation and flow patterns and bubble distribution. Bubbles generally tend to be smaller in the distributor region (which extends upwards 3 to 4 column diameters), while h is generally higher in the

upper portion of the reactor due to the presence of larger bubbles with a higher U_b and more turbulent wakes (Kantarci et al., 2005a). Generally, higher heat transfer coefficients are reported at the column centre than those near the wall since larger bubbles tend to concentrate in the centre of the column (Li and Prakash, 1997). According to Li and Prakash (2002) the distributor design will effect the size of the distributor region to a large extent, but developing region relatively less. In general though, the heat transfer coefficient has been found to be relatively independent of the sparger design in a well aerated column (i.e. at relatively high U_g) (Saxena and Chen, 1994). The probe diameter may negatively affect the heat transfer coefficient by altering the hydrodynamics and bubble characteristics. This effect is pronounced when the gap between adjacent tubes, or the outer column wall, is small (Saxena and Patel, 1991).

The presence of internals drastically altered the hydrodynamics and heat transfer of the columns studied by Saxena and coworkers (Saxena and Chen, 1994; e.g. Saxena and Vadivel, 1988). The heat transfer coefficient was observed to be significantly higher for a 10.8 cm i.d. column studied by Saxena and Rao (1991) than for a single tube configuration. This was attributed in large part to bubble coalescence inhibition. Saxena and Chen (1994) reported better liquid mixing and circulation as a result of the larger number of smaller bubbles since their movement was not hindered by the heat transfer tubes. However, there is currently no correlation that explains the dependence of the heat transfer coefficient on tube bundle configuration and pitch (Saxena and Chen, 1994). Liquid phase back mixing was reported to decrease when multiple tubes were present (Saxena and Patel, 1990d). Saxena and Chen (1994) also discuss the concept of "similarly baffled" columns whereby control of the bubble size and distribution may be achieved in order to achieve similar hydrodynamics between small and larger columns. Internal heat transfer surfaces such as those described herein are generally preferred to external wall heat exchangers. However, Saxena and Chen emphasize the importance the heat transfer surface is well secured because any vibration induced in the test surface will enhance the heat transfer rates making comparison between columns more difficult (Saxena and Chen, 1994).

3.10 Temperature (T)

Increasing temperature causes the liquid/slurry viscosity to decrease. The liquid/slurry heat capacity (C_{pl} or $C_{p,sl}$) and thermal conductivity (k_l, k_{sl}) also increase with increasing T although the effect of these variables is less pronounced than effect of the change in viscosity (Saxena and Chen, 1994).

In terms of measuring temperature, studies revealed by Saxena and Vadivel (1988) indicated that the bulk fluid temperature was reliably obtained

when the probe was located anywhere from 15 to 25 mm away from the heat transfer surface. For their studies, the difference between the heat transfer surface and the bulk fluid was typically between 3.4 and 13.2 K (Saxena et al., 1991r).

3.11 Pressure (P)

Pressure can have a significant effect on the system hydrodynamics and bubble characteristics. However, there are only a limited number of studies that have been conducted using bubble columns at high pressure and the effects of pressure on heat transfer are still inconclusive (Cho et al., 2002; Wu et al., 2007). Furthermore, the effect of pressure on bubbles in the distributor region is poorly understood even though the hydrodynamics and heat transfer in this region are important to overall performance (Lin and Fan, 1999). Increasing pressure generally causes the bubble size and rise velocity to decrease and the bubble number density to increase (Lin and Fan, 1999). This is largely attributed to the corresponding increase in gas density with increasing pressure, which causes bubble to detach sooner from the gas distributor (Lin and Fan, 1999). Pressure may cause the liquid viscosity to increase and surface tension to decrease, but does not significantly effect the liquid density, heat capacity or thermal conductivity (Lin and Fan, 1999; Wu et al., 2007). The effect of pressure on the heat transfer coefficient appears to be dependent on particle size as well. Yang et al. (2000) reported a negative influence of P on h while others have found h to increase with increasing pressure, reach a stable value at moderate pressures, before decreasing at relatively high pressures (Cho et al., 2002; Lin and Fan, 1999; Luo et al., 1997). This would seem to indicate that, while smaller bubbles and increased liquid viscosity would generally tend to decrease h, that the increased bubble frequency may become the more dominant factor in enhancing the heat transfer under certain conditions (Lin and Fan, 1999).

Table 12 presents a summary of the general consensus as to the effect of key process parameters on the heat transfer coefficient. Where the consensus is not clear, the varying conclusions are presented along with a reference to the relevant sources.

4 Conclusions and Recommendations

In the above review, a relatively large number of experimental investigations into heat transfer in two- and three-phase bubble columns with and without internals have been reviewed. In this section, significant general conclusions which are relevant in the design, scale-up, and operation of slurry bubble columns for Fischer-Tropsch synthesis are reported. To close, recommendations are made to

Table 12. Summary table of the relative effects of increasing the selected process variables on h.

Independent Variable	Relative Magnitude of Independent Variable		Comments
	low	high	
U_g	↗	→	Initial increase is rapid; approaches asymptotic value
U_l	↗	↘	Local maximum
μ_l	↘		
σ_l	↘	→	Initially decreases; approaches asymptotic value
d_b	↗		"unbaffled" column (i.e. single tube)
	↘		"baffled" column
d_p	↗		e.g. Quiroz et al. (2003)
	←→		e.g. Saxena and Chen (1994)
	↗	↘	e.g. Kang et al. (1985)
Θ_s	↗		large d_p all liquids; small d_p in viscous liquids
	↘		small particles in relatively low viscosity liquids
	←→		e.g. Saxena et al. (1992d)
d_{tube}	↘		
N_{tube}	↗	↘	
D_c	↗	↗	No studies for $D_c > 0.45$ m
H_c			
T	↗	→	
P	↘		for relatively small particles (d_p = 53 μm)
	↗→↘		relatively large d_p (d_p = 2.1 to 3 mm) or g-l only

guide future study in terms of reactor configuration and key measurements required for scale-up to commercial scale.

The results reported here from the majority of studies cannot be directly extrapolated to relatively large scale systems without a great deal of uncertainty. All bubble columns studied were relatively small – with no heat transfer data reported for columns near or greater than 0.45 m in diameter. In the studies involving solid particles, most utilized particles that were relatively large (a few hundred microns or more). Heat transfer measurements reported indicate differences in the behaviour of systems employing relatively small particles compared to those using relatively large particles. Furthermore, a clear majority of studies were conducted at ambient temperature and pressure. However, pressure and temperature are two variables that have a significant effect on heat transfer – impacting bubble size and slurry viscosity, respectively. Another concern is the relatively low superficial gas velocities employed in most studies, which may not properly mimic hydrodynamic and heat transfer phenomena relevant to industrial operating conditions. Finally, in terms of the heat transfer probes, it should be emphasized that most columns were only equipped with a single tube, and in some cases only a small heat flux probe. In both cases, only

the local heat transfer would be measured and would not properly take into account the effect of multiple heat transfer tubes commonly found in highly exothermic gas-liquid-solid applications. Even those studies reported that included multiple internal heat transfer tubes only measured localized heat transfer at a single point within the column since only a few tubes were equipped with heaters (that did not run the entire tube length) and heat flux probes while the remaining probes were "dummy" tubes (i.e. not active). Furthermore, no studies utilizing multiple internal heat transfer tubes employed active heat transfer tubes (with the exception of the study of Kolbel and Ralek (1980), which did not provide any information in terms of heat transfer).

Similar concerns that prevent generalization of the experimental results to larger scale columns apply to the corresponding heat transfer correlations. Reviewing the correlations reveals great deal of diversity between correlations and the lack of any standardized approach in their derivation. As well, there is no consensus on the best method of determining the key parameters of such correlations (e.g. the characteristic length and residence time). Virtually every correlation is dependent upon the equipment and/or properties of the gas, liquid, solid components studied – resulting in very limited applicability to other systems or for scale-up. Virtually no study takes into account the effect of multiple internals (especially 1-D models like the axial dispersion model) and most are not directly coupled with the system hydrodynamics. Furthermore, most correlations reported only concern steady-state operation and would therefore be unsuitable for start-up, shut-down, and other transient situations.

From the literature reviewed the parameters having the most pronounced impact on heat transfer in slurry bubble columns and three-phase fluidized beds are the superficial gas velocity and liquid properties (e.g. viscosity). Given the impact of the pressure and temperature on the bubble characteristics and liquid viscosity it is important that these variables are included in any further study and if possible testing conducted under actual FT conditions.

It is recommended that future experimental work be conducted in bubble columns at large diameter in order to better understand the effect of column diameter on liquid circulation patterns. A large diameter column would also permit experimentation using multiple internal heat transfer tube configurations. The presence of multiple column internals was observed to have a significant effect on the column hydrodynamics in liquid circulation and bubble size. Consistent data sets will only be generated if comparable mixing patterns of the two phases exist in different experimental arrangements and provided the heat transfer surface is adequately designed (Saxena and Rao, 1991). Although Saxena and coworkers have reported numerous studies involving such internals (see for example Saxena and Chen, 1994) this parameter was not investigated. Although some authors reported that the heat transfer coefficient became

independent of the column diameter this is mostly likely attributable to the relatively small column diameters studied. However, as reported in Section 3.9, Forret et al. (2006) report that the liquid axial velocity is a significant function of column diameter but the impact on the heat transfer remains unknown. The gas distributor type showed no obvious effects on the heat transfer as long as it was properly designed and the gas is well distributed. To this end, Saxena (1995) strongly recommends the inclusion of a calming section prior to the distributor to promote more even distribution of the gas and liquid entering the column.

Systematic studies of the relative effects of particle diameter, concentration and the impact of these parameters on the apparent liquid viscosity and heat transfer are missing from the literature. Furthermore, no detailed investigation describing the effects of particle density, particle size distribution, or shape have been located in the literature despite the impact such parameters may have on the fluidization behaviour. It will also be important in future studies to comprehensively characterize the bubble properties (i.e. bubble diameter, rise velocities, holdup, and bubble size distribution) especially in the presence of multiple internals to facilitate scale-up. Finally, proper characterization of the liquid behaviour is important as well and the liquid velocity distribution profiles and mixing behaviour should be studied in addition to measurements of temperature profiles throughout the column. The critical aspect of these studies will be to identify appropriate measurement techniques suitable for large scale equipment operating at high temperatures and pressure, and eventually in the presence of solids. Simultaneous study under identical conditions using a relatively smaller column would allow for comparison and identification of any parameters that are scale independent.

5 Nomenclature

A_c column cross-sectional area (m^2)
Ar Archimedes number
C_{pg}^* enthalpy increase of air saturated with water per unit increase of temperature ($J/K \cdot kg_{dry\ air}$)
C_{pl} liquid phase specific heat ($J/kg \cdot K$)
C_{ps} solid phase specific heat ($J/kg \cdot K$)
d_b bubble diameter (m)
d_o gas inlet orifice diameter (m)
d_p particle diameter (mm)
d_{pe} equivalent particle diameter (mm)
d_{tube} outer diameter of heat transfer tube/probe (m)
D_c column diameter (m)

D_i impeller diameter (m)
D_p particle dispersion coefficient (m^2/s)
E_{zl} liquid axial dispersion coefficient (m^2/s)
E_{zs} solid axial dispersion coefficient (m^2/s)
Fr Froude number
Fr_g gas Froude number
g gravitational acceleration (m/s^2)
h heat transfer coefficient from an internal surface to the surrounding medium (W/m^2K)
h_w wall heat transfer coefficient (W/m^2K)
H_0 slumped or static bed height (m)
H_c column height (m)
H_e expanded or fluidized bed height (m)
Hp height of probe measured from grid surface (m)
j_H Colburn-Chilton j-factor
j'_H modified Colburn-Chilton j-factor
k_{ez} axial effective thermal conductivity ($W/m{\cdot}K$)
k_l liquid phase thermal conductivity ($W/m{\cdot}K$)
k_s solid phase thermal conductivity ($W/m{\cdot}K$)
k_{sl} apparent slurry phase thermal conductivity ($W/m{\cdot}K$)
l_{tube} length of the heat transfer tube (m)
L_c characteristic vertical dimension of heater (m)
L_p cylindrical particle length (m)
M_g gas phase mass flow rate (kg/m^2s)
M_l liquid phase mass flow rate (kg/m^2s)
m_s mass of solids in the column (kg)
M_s solid phase mass flow rate (kg/m^2s)
n impeller stirring speed
N_{tube} number of tubes
P system pressure (Pa)
ΔP pressure drop (Pa)
Pr Prandtl number
Q_g volumetric gas flow rate (m^3/s)
r radial coordinate (m)
R radial distance from column centre (m)
R_c column radius (m)
Re Reynolds number
Re_n impeller Reynolds number
S_p particle specific area $S_p = 6/d_p$ (spherical) and $S_p = 2\left(2L_p \quad d_p\right)\big/ d_p L_p$ (cylindrical)
St Stokes number
T system temperature (K)

T_b medium bulk temperature (K)
T_w wall temperature (K)
ΔT temperature difference between the heat transfer surface and the surrounding medium (K)
U_b single bubble rise velocity (m/s)
U_g gas superficial velocity (m/s)
U_{gr} gas superficial riser velocity (m/s)
U_{gn} gas velocity exiting nozzle (m/s)
U_l liquid superficial velocity (m/s)
U_{sl} slurry superficial velocity (m/s)
U_{slip} bubble slip velocity (m/s)
U_t particle terminal velocity (m/s)
U_{tran} transitions velocity from bubbling to jetting regime (Lin and Fan, 1999) (m/s)
V_f total volume of floating bubble breakers in column (m^3)
V_s total volume of solids in column (m^3)
Δz axial distance separating two pressure taps (m)
z axial coordinate (i.e. distance above distributor) (m)

Greek Letters

α thermal diffusivity (m^2/s)
δ thermal boundary layer thickness (m)
ε bed porosity (i.e. $\varepsilon = \varepsilon_l + \varepsilon_g$)
ε_g gas phase hold-up
ε_l liquid phase hold-up (ε_{l2} = liquid phase hold-up for liquid-solid system)
ε_s solid phase hold-up
θ_c contact time at heat transfer surface (s)
Θ_s solids concentration (i.e. mass of solids divided by mass of slurry) (wt. %)
μ_b liquid or slurry viscosity at average bulk temperature (Pa·s)
μ_g gas viscosity (Pa.s)
μ_l liquid viscosity (Pa·s)
μ_{sl} apparent slurry viscosity (Pa.s)
μ_w liquid viscosity at the given wall temperature (Pa·s)
ρ_g gas phase density (kg/m^3)
ρ_l liquid phase density (kg/m^3)
ρ_s apparent particle density (kg/m^3)
ρ_{sl} apparent slurry density (kg/m^3)
σ_l surface tension (dynes/cm or mM/m)

6 References

Baker, C.G.J., Armstrong, E.R., and Bergougnou, M.A. "Heat transfer in three-phase fluidized beds." Powder Technology 21 (1978): 195 - 204.

Bieszk, H. "Zum wärmeübergang von einer festen wand an ein disperses zweiphasensystem. (Heat transfer from solid wall to the two phase dispersions.)." Chemische Technik (Leipzig) 38.12 (1986): 518 - 521.

Bieszk, H., and Hammer, H. "Zum einfluß suspendierter feststoffe auf den wärmeübergang von einer festen wand an die disperse phase in blasensäulen." Chemie Ingenieur Technik 60.5 (1988): 403 - 404.

Briens, C.L., Del Pozo, M., Chiu, K., and Wild, G. "Modeling of particle-liquid heat and mass transfer in multiphase systems with the film-penetration model." Chemical Engineering Science 48.5 (1993): 973 - 979.

Burkel, W. "Der wärmeübergang an heiz- und kühlflächen in begasten flüssigkeiten. (Heat transfer at heating and cooling surfaces in gassed liquids.)." Chemie Ingenieur Technik 44.5 (1972): 265 - 268.

Chen, W., Hasegawa, T., Tsutsumi, A., Otawara, K., and Shigaki, Y. "Generalized dynamic modeling of local heat transfer in bubble columns." Chemical Engineering Journal 96 (2003): 37 - 44.

Chiu, T.M., and Ziegler, E.N. "Heat transfer in three-phase fluidized beds." AIChE Journal 29.4 (1983): 677 - 685.

Chiu, T.M., and Ziegler, E.N. "Liquid holdup and heat transfer coefficient in liquid-solid and three-phase fluidized beds." AIChE Journal 31.9 (1985): 1504 - 1509.

Cho, Y.J., Kim, S.J., Nam, S.H., and Kim, S.D. "Heat transfer and bubble properties in three-phase circulating fluidized beds." Chemical Engineering Science 56 (2001): 6107 - 6115.

Cho, Y.J., Woo, K.J., Kang, Y., and Kim, S.D. "Dynamic characteristics of heat transfer coefficient in pressurized bubble columns with viscous liquid medium." Chemical Engineering and Processing 41 (2002): 699 - 706.

Deckwer, W.D., Louisi, Y., and Ralek, M. "Hydrodynamic properties of the Fischer-Tropsch slurry process." Industrial & Engineering Chemistry Process Design and Development 19 (1980): 699 - 708.

Deckwer, W.D. Bubble Column Reactors. New York: Wiley (1992).

Del Pozo, M., Briens, C.L., and Wild, G. "Effect of liquid coalescing properties on mass transfer, heat transfer and hydrodynamics in a three-phase fluidized bed." Chemical Engineering Journal and Biochemical Engineering Journal 55.1-2 (1994): 1 - 14.

Dhaouadi, H., Poncin, S., Hornut, J.M., and Wild, G. "Solid effects on hydrodynamics and heat transfer in an external loop airlift reactor." Chemical Engineering Science 61 (2006): 1300 - 1311.

Dhotre, M.T., and Joshi, J.B. "Two-dimensional CFD model for the prediction of flow pattern, pressure drop and heat transfer coefficient in bubble column reactors." Chemical Engineering Science 82.A6 (2004): 689 - 707.

Dhotre, M.T., Vitankar, V.S., and Joshi, J.B. "CFD simulation of steady state heat transfer in bubble columns." Chemical Engineering Journal 108 (2005): 117 - 125.

Dudukovic, M.P., Larachi, F., and Mills, P.L. "Multiphase catalytic reactors: a perspective on current knowledge and future trends." Catalysis Reviews 44.1 (2002): 123 - 246.

Fair, J.R., Lambright, A.J., and Andersen, J.W. "Heat transfer and gas holdup in a sparged contactor." Industrial & Engineering Chemistry Process Design and Development 1.1 (1962): 33 - 36.

Fazeli, A., Fatemi, S., Ganji, E., and Khakdaman, H.R. “A statistical approach of heat transfer coefficient analysis in the slurry bubble column.” Chemical Engineering Research and Design 86 (2008): 508 – 516.

Field, R.W. and Rahimi, R. "Hold-up heat transfer in bubble columns." Fluid Mixing III, Sep 8-10 1987, Bradford, Engl: Publ by European Federation of Chemical Engineering, Amarousion-Pefki, Greece, 1988. 257-270.

Forret, A., Schweitzer, J.M., Gauthier, T., Krishna, R., and Schweich, D. "Scale up of slurry bubble reactors." Oil & Gas Science and Technology 61 (2006): 443 - 458.

Hart, W.F. "Heat transfer in bubble-agitated systems. A general correlation." Industrial & Engineering Chemistry, Process Design and Development 15.1 (1976): 109 - 114.

Hatate, Y., Tajiri, S., Fujita, T., Fukumoto, T., Ikari, A., and Hano, T. "Heat transfer coefficient in three-phase vertical upflows of gas-liquid-fine solid particles system." Journal of Chemical Engineering of Japan 20.6 (1987): 568 - 574.

Hikita, H., Asai, S., Kikukawa, H., Zaike, T., and Ohue, M. "Heat transfer coefficient in bubble columns." Industrial & Engineering Chemistry, Process Design and Development 20.3 (1981): 540 - 545.

Holcombe, N.T., Smith, D.N., Knickle, H.N., and O'Dowd, W. "Thermal dispersion and heat transfer in nonisothermal bubble columns." Chemical Engineering Communications 21.1-3 (1983): 135 - 150.

Joshi, J.B., Sharma, M.M., Shah, Y.T., Singh, C.P.P., Ally, M., and Klinzing, G.E. "Heat transfer in multiphase contactors." Chemical Engineering Communications 6.4-5 (1980): 257 - 271.

Joshi, J.B. "Computational flow modelling and design of bubble column reactors." Chemical Engineering Science 56 (2001): 5893 - 5933.

Kang, Y., Fan, L.T., and Kim, S.D. "Immersed heater-to-bed heat transfer in liquid-solid fluidized beds." AIChE Journal 37.7 (1991): 1101 - 1106.

Kang, Y., Suh, I.S., and Kim, S.D. "Heat transfer characteristics of three phase fluidized beds." Chemical Engineering Communications 34 (1985): 1 - 13.

Kantarci, N., Borak, F., and Ulgen, K.O. "Bubble column reactors." Process Biochemistry 40 (2005a): 2263 - 2283.

Kantarci, N., Ulgen, K.O., and Borak, F. "A study on hydrodynamics and heat transfer in a bubble column with yeast and bacterial cell suspensions." The Canadian Journal of Chemical Engineering 83.August (2005b): 764 - 773.

Kast, W. "Analyse des wärmeübergangs in blasensäulen." International Journal of Heat and Mass Transfer 5 (1962): 329 - 336.

Kast, W. "Investigations into heat transfer in bubble columns. Untersuchungen zum Waermeuebergang in Blasensaeulen." Chemie Ingenieur Technik 35.11 (1963): 785 - 788.

Kato, Y., Uchida, K., Kago, T., and Morooka, S. "Liquid holdup and heat transfer coefficient between bed and wall in liquid-solid ang gas-liquid-solid fluidized beds." Powder Technology 28.2 (1981): 173 - 179.

Kato, Y., Kago, T., Uchida, K., and Morooka, S. "Wall-bed heat transfer characteristics of three-phase packed and fluidized bed." Heat Transfer - Japanese Research 9.3 (1982): 32 - 40.

Kato, Y., Koyama, M., Kago, T., and Morooka, S. "Heat transfer coefficient between bed and inserted horizontal tube in a three-phase fluidized bed." Heat Transfer - Japanese Research 15.1 (1986): 1 - 14.

Kato, Y., Taura, Y., Kago, T., and Morooka, S. "Heat transfer coefficient between an inserted vertical tube and a three-phase fluidized bed." Heat Transfer - Japanese Research 14.3 (1985): 21 - 31.

Kawase, Y., and Moo-Young, M. "Heat transfer in bubble column reactors with Newtonian and non-Newtonian fluids." Chemical Engineering Research & Design 65 (1987): 121 - 126.

Khoze, A. "Heat transfer in a dynamic two-phase bed at reduced pressures." Journal of Applied Mechanics and Technical Physics 12.5 (1971): 782 - 785.

Khoze, A., and Scharov, J. "Wärmeübergang an Schaumshichtböden." Luft- und Kältetechnik 5 (1977): 248 - 251.

Kim, J.O., Park, D.H., and Kim, S.D. "Heat transfer and wake characteristics in three-phase fluidized beds with floating bubble breakers." Chemical Engineering Processing 28 (1990): 113 - 119.

Kim, N.-H., and Lee, Y.-P. "Hydrodynamic and heat transfer characteristics of glass bead-water flow in a vertical tube." Desalination 133 (2001): 233 - 243.

Kim, S.D., Kang, Y., and Kwon, H.K. "Heat transfer in gas-solid-coal slurry fluidized beds." Particulate and Multiphase Processes.Volume 1: General Particulate Phenomena, Miami Beach, 1987. Eds. T. Ariman and T.N. Veziro. Washington: Hemisphere Publishing Corporation, 1987. 645-658.

Kim, S.D., and Laurent, A. "The state of knowledge on heat transfer in three phase fluidized beds." International Chemical Engineering 31.2 (1991): 284 - 302.

Kim, S.D., Kang, Y., and Kwon, H.K. "Heat transfer characteristics in two- and three-phase slurry-fluidized beds." AIChE Journal 32.8 (1986): 1397 - 1400.

Kim, S.D., and Kang, Y. "Heat and mass transfer in three-phase fluidized bed reactors - an overview." Chemical Engineering Science 52.21-22 (1997): 3639 - 3660.

Knickle, H.N., O'Dowd, W., Holcombe, N.T., Smith, D.N. "Backmixing and heat transfer coefficients in bubble columns using aqueous glycerol solutions." AIChE Symposium Series, 79.225 (1983): 352 - 359.

Kölbel, H., Borchers, E., and Martins, J. "Wärmeübergang in blasensäulen. III. Messungen an gasdurchströmten suspensionen." Chemie Ingenieur Technik 32.2 (1960): 84 - 88.

Kölbel, H., Borchers, E., and Müller, K. "Wärmeübergang in blasensäulen. II. Messungen an viscosen suspension." Chemie Ingenieur Technik 30.11 (1958a): 729 - 734.

Kölbel, H., and Langemann, H. "Warmeubergang in blasensaulen." Erdoel Zeitschrift 80.10 (1964): 405 - 415.

Kölbel, H., and Ralek, M. "The Fischer-Tropsch synthesis in the liquid phase." Catalysis Reviews 21.2 (1980): 225 - 274.

Kölbel, H., Siemes, W., Maas, R., and Müller, K. "Heat transfer in bubble columns." Chemie Ingenieur Technik 20.6 (1958b): 400 - 404.

Konsetov, V.V. "Heat transfer during bubbling of gas through liquid." International Journal of Heat and Mass Transfer 9 (1966): 1103 - 1108.

Korte, H.J. "Wärmeübergang in blasensäulen mit und ohne einbauten." Diss. Universität Dortmund, 1987.

Krishna, R. "A scale-up strategy for a commercial scale bubble column slurry reactor for Fischer-Tropsch synthesis." Oil & Gas Science and Technology 55 (2000): 359 - 393.

Kubie, J. "Bubble induced heat transfer in two phase gas-liquid flow." International Journal of Heat and Mass Transfer 18.4 (1975): 537 - 551.

Kulkarni, A.V., and Joshi, J.B. "Estimation of hydrodynamic and heat transfer characteristics of bubble column by analysis of wall pressure measurements and CFD simulations." Chemical Engineering Research and Design 84.7 A (2006): 601 - 609.

Kumar, S., Kusakabe, K., and Fan, L.S. "Heat transfer in three-phase fluidization and bubble-columns with high gas holdups." AIChE Journal 39.8 (1993a): 1399 - 1405.

Kumar, S., Kusakabe, K., and Fan, L.S. "Heat transfer in three-phase fluidized beds containing low-density particles." Chemical Engineering Science 48.13 (1993b): 2407 - 2418.

Kumar, S., and Fan, L.S. "Heat-transfer characteristics in viscous gas-liquid and gas-liquid-solid systems." AIChE Journal 40.5 (1994): 745 - 755.

Kumar, S., Kusakabe, K., Raghunathan, K., and Fan, L.S. "Mechanism of heat transfer in bubbly liquid and liquid-solid systems: single bubble injection." AIChE Journal 38.5 (1992): 733 - 741.

Kurpiers, P., Steiff, A., and Weinspach, P.M. "Heat transfer and scale-up in stirred single- and multiphase reactors with immersed heating elements." German Chemical Engineering 8.5 (1985a): 267 - 271.

Kurpiers, P., Steiff, A., and Weinspach, P.M. "Heat transfer in stirred multiphase reactors." German Chemical Engineering 8.1 (1985b): 48 - 57.

Lewis, D.A., Field, R.W., Xavier, A.M., and Edwards, D. "Heat transfer in bubble columns." Transactions of the Institution of Chemical Engineers 60.1 (1982): 40 - 47.

Li, H., and Prakash, A. "Heat transfer and hydrodynamics in a three-phase slurry bubble column." Industrial Engineering Chemistry and Research 36 (1997): 4688 - 4694.

Li, H., and Prakash, A. "Analysis of bubble dynamics and local hydrodynamics based on instantaneous heat transfer measurements in a slurry bubble column." Chemical Engineering Science 54 (1999): 5265 - 5271.

Li, H., and Prakash, A. "Analysis of flow patterns in bubble and slurry bubble columns based on local heat transfer measurements." Chemical Engineering Journal 86 (2002): 269 - 276.

Li, H., Prakash, A., Margaritis, A., and Bergougnou, M.A. "Effects of micro-sized particles on hydrodynamics and local heat transfer in a slurry bubble column." Powder Technology 133 (2003): 171 - 184.

Li, H., and Prakash, A. "Survey of heat transfer mechanisms in a slurry bubble column." The Canadian Journal of Chemical Engineering 79.5 (2001): 717 - 725.

Lin, T.J., and Fan, L.S. "Heat transfer and bubble characteristics from a nozzle in high-pressure bubble columns." Chemical Engineering Science 54 (1999): 4853 - 4859.

Lin, T.J., and Hung-Tzu, C. "Effects of macroscopic hydrodynamics on heat transfer in a three-phase fluidized bed." Catalysis Today 79-80 (2003): 159 - 167.

Lin, T.J., and Wang, S.P. "Effects of macroscopic hydrodynamics on heat transfer in bubble columns." Chemical Engineering Science 56 (2001): 1143 - 1149.

Luo, X., Jiang, P., and Fan, L.S. "High-pressure three-phase fluidization: hydrodynamics and heat transfer." AIChE Journal 43.10 (1997): 2432 - 2445.

Magiliotou, M., Chen, Y.M., and Fan, L.S. "Bed-immersed object heat transfer in a three-phase fluidized bed." AIChE Journal 34.6 (1988): 1043 - 1047.

Maretto, C., and Krishna, R. "Modelling of a bubble column slurry reactor for Fischer-Tropsch synthesis." Catalysis Today 52 (1999): 279 - 289.

Mersmann, A. "Zum wärmeübergang zwischen dispersen zeiphasensystemen und senkrechten heizflächen im erdschwerefeld. (On Heat Transfer Between Disperse Two-Phase Systems and Vertical Heating Surfaces in the Gravity Field.)." Verfahrenstechnik 10.10 (1976): 641 - 645.

Mersmann, A. "Heat transfer in bubble columns." International Chemical Engineering 17.3 (1977): 385 - 388.

Michael, R., and Reichert, K.H. "Heat transfer of polyethylene-hydrocarbon dispersions in bubble column reactors." The Canadian Journal of Chemical Engineering 59.October (1981): 602 - 605.

Muroyama, K., Okumichi, S., Goto, Y., Yamamoto, Y., and Saito, S. "Heat transfer from immersed vertical cylinders in gas-liquid and gas-liquid-solid fluidized beds." Chemical Engineering and Technology 24.8 (2001): 835 - 842.

Muroyama, K., Kato, T., Masuda, T., and Kinoshita, S. "Vertical cylinder-to-slurry heat transfer in a gas-slurry transport bed." The Canadian Journal of Chemical Engineering 81.June-August (2003): 426 - 432.

Napp, W., and Hammer, H. "Zur chemischen reacktionstechnik von blasensäulen-reaktoren: stoff- und wärmeübergang von einer festen wand an eine begaste flüssigkeit oder suspension." Chemie Ingenieur Technik 55.8 (1983): 634 - 635.

Nigam, K.D.P., and Schumpe, A. Three-Phase Sparged Reactors. Amsterdam: Overseas Publishers Association B.V., 1996.

Nishikawa, M., Kato, H., and Hashimoto, K. "Heat transfer in aerated tower filled with non-Newtonian liquid." Industrial & Engineering Chemistry, Process Design and Development 16.1 (1977): 133 - 137.

Nore, O., Briens, C., Margaritis, A., and Wild, G. "Hydrodynamics, gas-liquid mass transfer and particle-liquid heat and mass transfer in a three-phase fluidized bed for biochemical process applications." Chemical Engineering Science 47.13-14 (1992): 3573 - 3580.

Ozbelge, T.A. "Heat transfer enhancement in turbulent upward flows of liquid-solid suspensions through vertical annuli." International Journal of Heat and Mass Transfer 44 (2001): 3373 - 3379.

Pandit, A.B., and Joshi, J.B. "Three phase sparged reactors - some design aspects." Reviews in Chemical Engineering 2.1 (1984): 1 - 84.

Pandit, A.B., and Joshi, J.B. "Mass and heat transfer characteristics of three phase sparged reactors." Chemical Engineering Research & Design 64.2 (1986): 125 - 157.

Pauli, D. "Heat transfer in bubble columns." Chemische Technik Berlin DDR 1949 44.4 (1988): 157 - 160.

Prakash, A., Margaritis, A., Li, H., and Bergougnou, M.A. "Hydrodynamics and local heat transfer measurements in a bubble column with suspension of yeast." Biochemical Engineering Journal 9 (2001): 155 - 163.

Quiroz, I., Herrera, I., and Gonzalez-Mendizabal, D. "Experimental study on convective coefficients in a slurry bubble column." International Communications in Heat and Mass Transfer 30.6 (2003): 775 - 786.

Saberian-Broudjenni, M., Wild, G., Midoux, N., and Charpentier, J.C. "Contribution a l'etude du transfert de chaleur a la paroi dans les reacteurs a lit fluidise gaz-liquide-solide a faible vitesse de liquide." The Canadian Journal of Chemical Engineering 63.4 (1985): 553 - 564.

Saxena, S.C. "Bubble column reactors and Fischer-Tropsch synthesis." Catalysis Reviews 37.2 (1995): 227 - 309.

Saxena, S.C., and Chen, Z.D. "Hydrodynamics and heat transfer of baffled and unbaffled slurry bubble columns." Reviews in Chemical Engineering 10.3,4 (1994): 195 - 400.

Saxena, S.C., and Patel, B.B. "Heat transfer and hydrodynamic investigations in a baffled bubble column: air-water-glass bead system." Chemical Engineering Communications 98 (1990a): 65 - 88.

Saxena, S.C., and Patel, B.B. "Heat transfer from a tube bundle in a slurry bubble column involving fine powders." Powder Technology 61.2 (1990b): 207 - 210.

Saxena, S.C., and Patel, B.B. "Heat transfer investigations in a bubble column with immersed probes of different diameters." International Communications in Heat and Mass Transfer 18.4 (1991): 467 - 478.

Saxena, S.C., and Rao, N.S. "Heat transfer and gas holdup in a two-phase bubble-column. Air-water system. Review and new data." Experimental and Thermal Fluid Science 4.2 (1991): 139 - 151.

Saxena, S.C. and Rao, N.S. "Heat transfer from immersed surfaces in three-phase slurry reactors." 3rd UK National Conference incorporating 1st European

Conference on Thermal Sciences, Sep 16-18 1992, Birmingham, Engl: Publ by Inst of Chemical Engineers, Rugby, Engl, 1992. 691-697.

Saxena, S.C., and Rao, N.S. "Estimation of gas holdup in a slurry bubble column with internals: nitrogen-Therminol-magnetite system." Powder Technology 75 (1993): 153 - 158.

Saxena, S.C., Rao, N.S., and Patel, B.B. "Heat transfer and hydrodynamic investigations in two- and three-phase systems in a baffled bubble column." Heat Transfer, Proceedings of the International Heat Transfer Conference (1990a): 407 - 412.

Saxena, S.C., Rao, N.S., and Saxena, A.C. "Heat transfer and gas-holdup in a bubble column: air-water-glass bead system." Chemical Engineering Communications 96 (1990b): 31 - 55.

Saxena, S.C., Rao, N.S., and Saxena, A.C. "Heat transfer from a cylindrical probe immersed in a three-phase slurry bubble column." Powder Technology 44 (1990c): 141 - 156.

Saxena, S.C., Rao, N.S., and Saxena, A.C. "Heat transfer and holdup studies in a three-phase slurry bubble column with internals." Fluidization and Fluid-Particle Systems, Chicago, 11 November 1990a. New York: AIChE (1991a): 101-110.

Saxena, S.C., Rao, N.S., and Saxena, A.C. "Heat transfer and gas holdup studies in a bubble column: air-water-sand system." The Canadian Journal of Chemical Engineering 70.February (1992e): 33 - 41.

Saxena, S.C., Rao, N.S., and Yousuf, M. "Heat transfer and hydrodynamic investigations conducted in a bubble column with powders of small particles and a viscous liquid." Chemical Engineering Journal 47 (1991b): 91 - 103.

Saxena, S.C., Rao, N.S., and Yousuf, M. "Hydrodynamic and heat transfer investigations conducted in a bubble column with fine powders and a viscous liquid." Powder Technology 67 (1991c): 265 - 275.

Saxena, S.C., and Vadivel, R. "Heat transfer from a tube bundle in a bubble column." International Communications in Heat and Mass Transfer 15.5 (1988): 657 - 667.

Saxena, S.C., Vadivel, R., and Saxena, A.C. "Gas holdup and heat transfer from immersed surfaces in two- and three-phase systems in bubble columns." Chemical Engineering Communications 85 (1989a): 63 - 83.

Saxena, S.C., Vadivel, R., and Saxena, A.C. "Hydrodynamics and heat transfer characteristics of bubble columns involving fine powders." Powder Technology 59 (1989b): 25 - 35.

Saxena, S.C., Verma, A.K., Vadivel, R., and Saxena, A.C. "Heat transfer from a cylindrical probe in a slurry bubble column." International Communications in Heat and Mass Transfer 16.2 (1989c): 267 - 281.

Schluter, S., Steiff, A., and Weinspach, P.M. "Heat transfer in two- and three-phase bubble column reactors with internals." Chemical Engineering and Processing 34 (1995): 157 - 172.

Shaykhutdinov, A.G., Bakirov, N.V., and Usmanov, A.G. "Determination and mathematical correlation of heat transfer coefficient under conditions of bubble flow, cellular, and turbulent foam." International Chemical Engineering 11.4 (1971): 641 - 645.

Steiff, A., and Weinspach, P.M. "Heat transfer in stirred and non-stirred gas-liquid reactors." German Chemical Engineering 1.3 (1978): 150 - 161.

Stynberg, A., and Dry, M. Fischer-Tropsch Technology. New York: Elsevier, 2004.

Suh, I.S., and Deckwer, W.D. "Unified correlation of heat transfer coefficients in three-phase fluidized beds." Chemical Engineering Science 44.6 (1989): 1455 - 1458.

Suh, I.S., Jin, G.T., and Kim, S.D. "Heat transfer coefficients in three phase fluidized beds." International Journal of Multiphase Flow 11.2 (1985): 255 - 259.

Tarat, E.Ya., Khoze, A., and Sharov, Yu.I. "Heat transfer from single surfaces in a foam layer." International Chemical Engineering 10.2 (1970): 237 - 240.

Thimmapuram, P.R., Rao, N.S., and Saxena, S.C. "Heat transfer from immersed tubes in a baffled slurry bubble column." Chemical Engineering Communications 120 (1993b): 27 - 43.

Verma, A.K. "Heat transfer mechanism in bubble columns." Chemical Engineering Journal and the Biochemical Engineering Journal 42.3 (1989): 205 - 208.

Vitankar, V.S., Dhotre, M.T., and Joshi, J.B. "A low Reynolds number k-epsilon model for the prediction of flow pattern and pressure drop in bubble column reactors." Chemical Engineering Science 57 (2002): 3235 - 3250.

Westermeyer Benz, H. Wärmeübergang und Gasgehalt in zwei- und dreiphasig betriebenen Blasensäulenreaktoren mit längseingebauten Rohren. Düsseldorf: VDI-Verlag, 1992.

Wu, C., Al-Dahhan, M.H., and Prakash, A. "Heat transfer coefficients in a high-pressure bubble column." Chemical Engineering Science 62.1-2 (2007): 140 - 147.

Yang, G.Q., Luo, X., and Fan, L.S. "Heat-transfer characteristics in slurry bubble columns at elevated pressures and temperatures." Industrial Engineering Chemistry and Research 39 (2000): 2568 - 2577.

Zaidi, A., Deckwer, W.D., Mrani, A., and Benchekchou, B. "Hydrodynamics and heat transfer in three-phase fluidized beds with highly viscous pseudoplastic solutions." Chemical Engineering Science 45.8 (1990): 2235 - 2238.

Zaidi, A.J., Bourziza, H., and Echihabi, L. "Wärmeübergang und effektives schergefälle in blasensäulen-bioreaktoren mit xanthan-lösungen." Chemie Ingenieur Technik 59.9 (1987): 748 - 749.

Zehner, P. "Transfer of momentum, mass, and heat in bubble columns. Impuls- stoff- und wärmetransport in blasensäulen." Chemie Ingenieur Technik 54.3 (1982): 248 - 251.

Zehner, P. "Momentum, mass and heat transfer in bubble columns. Part 1. Flow model of the bubble column and liquid velocities." International Chemical Engineering 26.1 (1986a): 22 - 28.

Zehner, P. "Momentum, mass and heat transfer in bubble columns. Part 2. Axial blending and heat transfer." International Chemical Engineering 26.1 (1986b): 29 - 35.